USGS
OFR 69-326
copy 1.

Zohdy, A.R. copy 1

GEOPHYSICAL SURVEYS FOR GROUNDWATER AT

WHITE SANDS MISSILE RANGE, NEW MEXICO

by

Adel A. R. Zohdy
Dallas B. Jackson
Robert E. Mattick
Donald L. Peterson

UNITED STATES DEPARTMENT OF THE INTERIOR

GEOLOGICAL SURVEY

GEOPHYSICAL SURVEYS FOR GROUND WATER AT WHITE SANDS MISSILE RANGE, NEW MEXICO

By Adel A. R. Zohdy, Dallas B. Jackson,

Robert E. Mattick, and Donald L. Peterson

Open-file report

1969

Work done in cooperation with the

White Sands Missile Range, New Mexico

This report has not been edited or reviewed for conformity to Geological Survey standards.

U. S. GEOLOGICAL SURVEY
Released to open files
August 14, 1969

Contents

Illustrations

Illustrations
continued

Table

INTRODUCTION

In February and March 1966, and April and May 1967, the U.S. Geological Survey, in cooperation with the White Sands Missile Range, made geophysical surveys (seismic, gravity and resistivity) in support of ground-water investigations in the vicinity of White Sands Missile Range (WSMR), New Mexico. This report is concerned with the results obtained from the analysis and interpretation of the seismic refraction, the gravity measurements, and the resistivity vertical electrical soundings.

The primary objective of the seismic refraction profiles and the gravity measurements was the delineation of the bedrock configuration.

The objective of the resistivity soundings was the delineation of the fresh water-salt water interface and determination of the depth to bedrock, wherever possible.

Four seismic refraction lines were shot along reversed profiles (varying in length from 4 to 9 miles), 230 gravity stations were occupied, and eighty-five resistivity soundings were made using the Schlumberger electrode configuration (with maximum electrode spacings ($\frac{AB}{2}$) varying from 1400 feet to 10,000 feet). Figure 1 shows the location of the four seismic profiles and the areas investigated by the gravity measurements and by the electrical soundings.

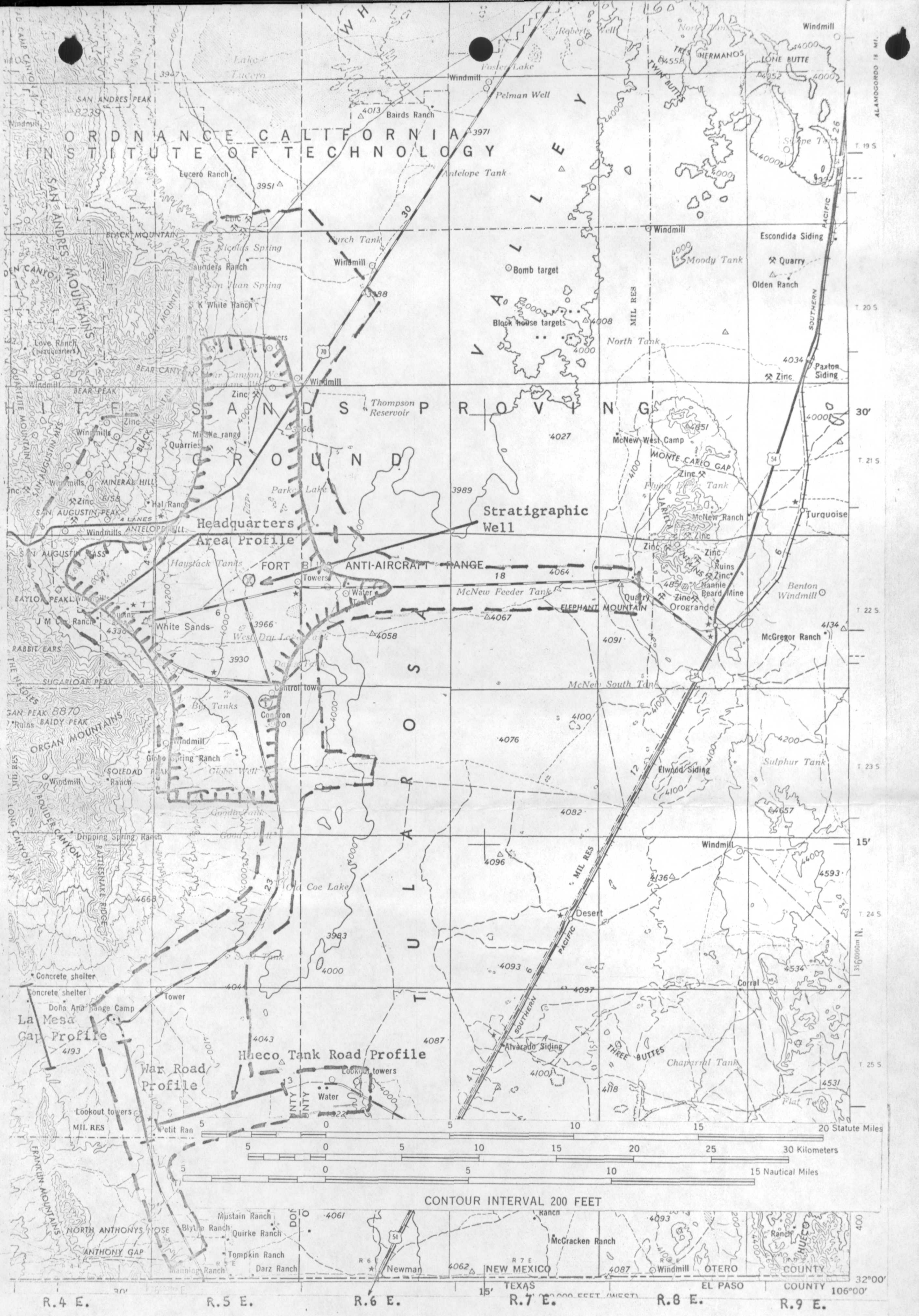

Figure 1. Location map of resistivity (hachured outline), seismic (solid lines), and gravity (dashed outline) surveys, White Sands, New Mexico.

FIELD PROCEDURES

The seismic refraction measurements were made using one recording unit which recorded the output of 12 vertical seismometers that were evenly spaced at 650 foot intervals along a 7150 foot cable. The scheme used in shooting a profile (4 to 9 miles in length) was as follows: The cable was laid at one end of the profile and the output from a dynamite charge exploded one at a time at each end of the profile was recorded. The cable was then moved 7150 feet along the profile and the previous shotpoints at each end of the profile were reshot. This procedure of reshooting at the same shotpoints and moving the cable was continued until the entire distance along a profile was covered. In addition, intermediate shots at about 7150 foot intervals were used to record lateral velocity changes occurring the valley fill material. The dynamite charges varied from 50 to 400 pounds and were loaded in dug holes at a depth of about 14 feet.

The gravity observations were made with two Worden gravimeters having calibration constants of about 0.5 mgal (milligals) per dial division. The 230 gravity stations were established during a period of 8 days. Readings were made at a base station at morning, mid-day, and evening.

The conventional Schlumberger (AMNB) electrode configuration was used for making the resistivity soundings. This sounding procedure is commonly referred to as vertical electrical sounding (VES) or simply electrical sounding (ES) (Kalenov, 1957; Kunetz, 1966). To make an electrical sounding, four electrodes A, M, N, and B are driven into the ground along a straight line such that the distance between the current electrodes (AB) is at least five times the distance between the potential electrodes $\overline{MN}$ i.e. $\overline{AB} \geq 5\ \overline{MN}$. A measurement of the apparent resistivity is computed from the formula:

$$\bar{\rho} = \pi \frac{(AB/2)^2 - (MN/2)^2}{MN} \frac{\Delta V}{I} \tag{1}$$

where (AB/2) and (MN/2) are half the distances between the current electrodes and the potential electrodes, respectively, ΔV is the potential difference between the electrodes M and N, and I is the electric current. Although the electrode spacings (AB/2) and (MN/2) are measured in feet, the apparent resistivity is expressed in ohm-m through multiplication of equation (1) by a proper factor. The current electrode spacing $\frac{AB}{2}$ is increased at a logarithmic rate, while the spacing $\frac{MN}{2}$ is held constant, until the ratio $\frac{AB}{MN} \geq 10$. The maximum value of the ratio $\frac{AB}{MN}$ depends on the magnitude of the signal ΔV. At some value of $\frac{AB}{MN} \geq 10$, the spacing $\frac{AB}{2}$ is held constant while the spacing $\frac{MN}{2}$ is increased so that $\frac{AB}{MN} = 5$ and the measurement is repeated. The expansion of the spacing $\frac{AB}{2}$ is then resumed. The value of the apparent resistivity is plotted as a function of the current electrode spacing $\frac{AB}{2}$ on a set of bilogarithmic coordinates and the result is a VES curve. VES curves obtained in the field are always composed of a few segments, each of which corresponds to a given value of $\frac{MN}{2}$ = constant. The discontinuities at the end of one segment and the beginning of the next segment (at $\frac{AB}{2}$ = constant) are caused by the variation in probing depth as a function of the ratio $\frac{AB}{MN}$ (Deppermann, 1954). On some VES curves the discontinuities are complicated because of lateral heterogenieties in the ground.

The minimum electrode spacing (AB/2) used in the present survey was 10 feet and the maximum was 10,000 feet. The VES curves obtained in this survey are given in an appendix to this report.

The resistivity equipment consisted of a 2.5 kilowatt generator (for power supply), a pulser (for stepping up the impressed voltage and regulating the current), a potentiometric chart recorder (for recording the potential difference), and more than 20,000 feet of cable for connecting the electrical equipment to the electrodes which were made of stainless steel rods (2 feet in length, 3/4 of an inch in diameter). The maximum intensity of electric current put into the ground was about 1.2 amperes and the smallest potential difference measured was about 0.01 millivolts.

QUALITY OF RESULTS

AND METHODS OF INTERPRETATION

Most of the seismograms obtained were of good quality with the first arrivals easily identifiable on most of the records. No attempt was made to determine second and later arrivals. The travel times from shot point to the seismometers were picked to the nearest 0.002 second.

Travel time curves were constructed for each of the four profiles and velocities were determined by visual fitting of straight line segments to the travel time data. In most cases the ground elevation along a profile remained relatively constant and no elevation corrections were necessary. The first arrival times for all the profiles show a time intercept varying from about 0.03 to 0.07 second. This intercept time can be explained by the presence of a thin layer of low velocity weathered material (weathering layer).

Conventional seismic interpretation methods were used in calculating the depths and dips of the various refracting horizons. For the La Mesa Gap profile, where the valley fill material overlying the bedrock is relatively thin, the method of Hawkins (1961) was used. For the remaining profiles, where the depths to basement are of the order of several thousands of feet and the overlying material consists of multiple refracting horizons, the method of Slotnick (1950) was used for depth determination. Final interpretation was checked by ray path analysis.

The observed gravity values are referenced to two gravity base stations at WSMR established by the U.S. Geological Survey which are, in turn, referenced to the airport base station at El Paso, Texas (Behrendt and Woollard, 1961). An assumed density of 2.67 gm/cc was used in making the Bouguer correction. Theoretical gravity was computed from the international formula. The terrain effect was computed using the U.S. Coast and Geodetic Survey system (Swick, 1942) for stations within or marginal to the mountains. For other stations the terrain effect is negligible.

Most of the VES curves were of good quality and were interpretable in terms of earth models comprised of horizontally stratified media. Only a few sounding curves (less than 10 percent of the total) were distorted by the presence of strong lateral heterogeneities in the geologic section, or by electrical malfunctions in the equipment (current leakage from damaged insulation on the current cables (Zohdy, 1968 -b. Geologically meaningful interpretations of the distorted sounding curves depended on the nature of the distortions (Chastenet de Gery and Kunetz, 1956; Dakhnov, 1953).

The interpretation of the VES curves obtained in the field was made in three steps. First, a qualitative examination was made to determine, in an approximate manner, the variation of the resistivity as a function of depth and geographic location. This first step of interpretation involved the construction of apparent resistivity maps, apparent resistivity sections, and the transformation of a few VES curves into differential sounding curves (Rabinovich, 1965). Second, the first quantitative step of interpretation was made by matching the observed VES curves to theoretically computed ones using the three-layer albums published by the Compagnie Générale de Géophysique (1963) and by Orellana and Mooney (1966). The auxiliary point method (Kalenov, 1957; Zohdy, 1965) and the H-A auxiliary curve (Zohdy, 1968-a) were used to complete the interpretation of field VES curves which reflected the presence of six and seven layers in many parts of the survey area. Third, the second step of the quantitative interpretation was made by computing theoretical multilayer VES curves by means of a 360/65 IBM digital computer for all the field VES curves on the basis of their graphical interpretation with the auxiliary point method and the three-layer master curves. It was found that the accuracy of the auxiliary point method for certain multilayer VES curves is unsatisfactory and the geoelectrical models had to be readjusted and the VES curves recalculated by the computer in order to obtain a satisfactory fit between the observed and the calculated VES curve. The computer program is based on the work done by Mooney, Orellana, Pickett and Tornheim (1966) and was made available to the Geological Survey through the courtesy of Chevron Oil Co.

RELATIONSHIP BETWEEN MEASURED GEOPHYSICAL PARAMETERS AND HYDROGEOLOGY

The three geophysical methods used in this survey, seismic, gravity, and resistivity, depend on the presence of contrasts in the physical parameters of seismic velocity (feet/sec), density (gm/cc), and electrical resistivity (ohm-m), respectively. It is generally hoped, in any geophysical investigation , that layers of different physical properties correspond to layers of different lithologic characteristics and/or geologic ages. However, this may not always be the case. Layers of different lithologies may be characterized by similar velocities, densities, or resistivities, whereas different physical parameters may be found within a lithologically uniform layer thus dividing it into two or more layers. The reason for this is that lithology constitutes only one factor upon which the physical parameters may depend. Other factors affecting the magnitudes of the physical parameters include the degree of cementation and/or compaction, quality of the ground water, etc.

The geoelectric section in the White Sands area may be described as follows: (1) near-surface alluvium of variable resistivity (8-500 ohm-m) including gypsiferous layers of very high resistivities, (2) clean sand and gravel probably saturated with ground water of excellent quality (200 ohm-m), (3) sand and gravel with some clay layers probably saturated with potable fresh water (30-45 ohm-m), (4) sedimentary rocks probably saturated with fresh to brackish water (9-22 ohm-m), (5) non-potable, saline water-saturated sedimentary rocks (3.5-5 ohm-m), (6) highly mineralized water-saturated sedimentary rocks (0.5-1 ohm-m), (7) non-water bearing, crystalline rocks or dense limestone of practically "infinite" resistivity.

The lower the resistivity of a geoelectric layer, the higher the probability for the existence of clay intercalations and/or water of inferior quality (mineralized water). The fact that in certain areas the true resistivity was found to be less than 1 ohm-m indicates that in these areas the degree of salinity of the water is extremely high (several thousand parts per million of dissolved solids). Neither the gravity nor the seismic methods can furnish information on the approximate quality of the ground water. However, the seismic refraction method in certain areas might determine the depth to the water table whereas resistivity may fail to do so.

NEW MEXICO-TEXAS
LA MESA QUADRANGLE
15-MINUTE SERIES

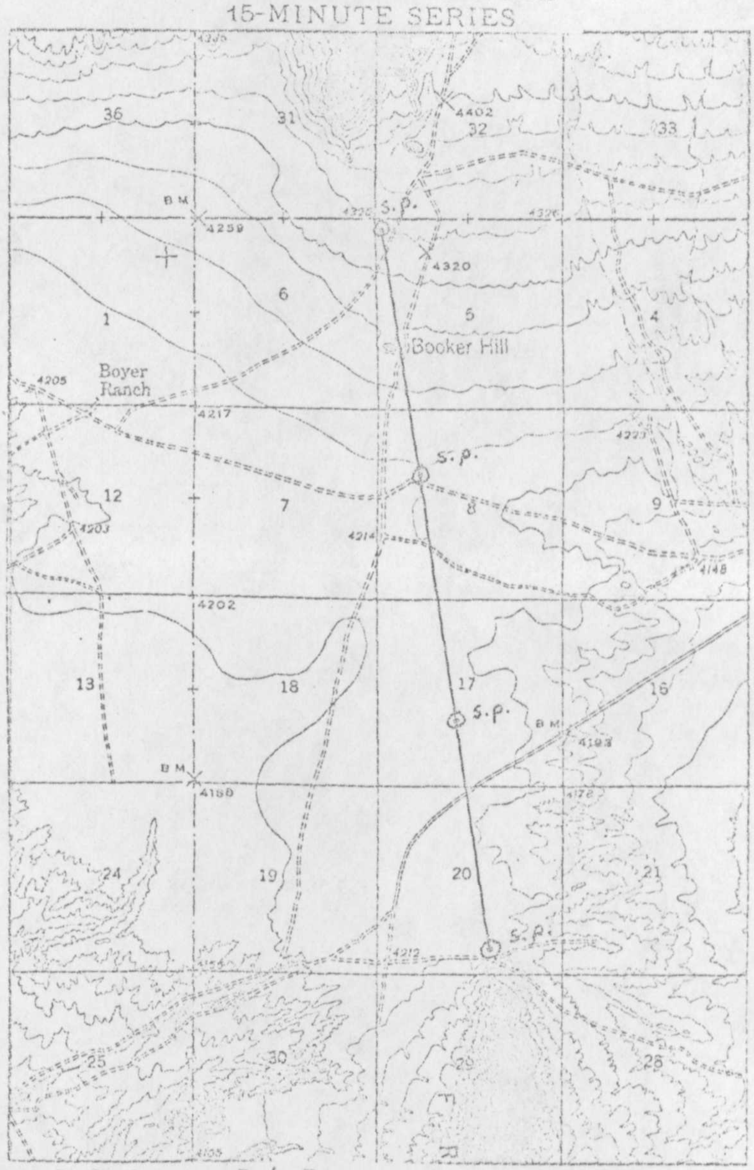

T.24 S.

T.25 S.

R.3 E. R.4 E.

Figure 2a. Map showing location of Seismic refraction profile across La Mesa Gap. SP, shotpoint.

0 1 2 miles

RESULTS OF SEISMIC REFRACTION PROFILES

Three seismic refraction profiles were shot to the south and southeast of the Organ Mountains where only a few gravity stations were occupied and no resistivity soundings were made. These profiles are designated as: (1) La Mesa Gap profile, (2) War Road profile, and (3) Hueco Tanks Road profile.

A fourth seismic profile was shot north of the Organ Mountains, near the Headquarters area where gravity measurements and resistivity soundings were made.

(1) <u>LA MESA GAP PROFILE</u>

This profile extends across the gap between the Franklin Mountains, to the south, and the Organ Mountains to the north, and is approximately 21,000 feet in length (Figure 2a). At the southern shot hole, located about 300 feet north of an outcrop of Paleozoic limestone at the base of the Franklin Mountains, numerous limestone boulders were encountered. The northernmost shot hole was located about 2200 feet south of an outcrop of Paleozoic limestone located at the base of the Organ Mountains (Dane and Bachman, 1965).

The curve representing the apparent velocity of the direct waves through the surface sediments is poorly defined as a result of the relatively large spacing between geophones (650 feet) in comparison to the calculated depths to basement rock. However, by assuming a velocity of 2000 ft/sec for the near-surface, unsaturated sediments to a depth of about 150 feet (a representative velocity in other areas in the vicinity of WSMR) and a velocity of 5500 ft/sec for the sediments below 150 feet, the calculated depths to basement rock are in good agreement with projected depths obtained from two available well logs (personal communication, W. Balance, U.S.G.S.).

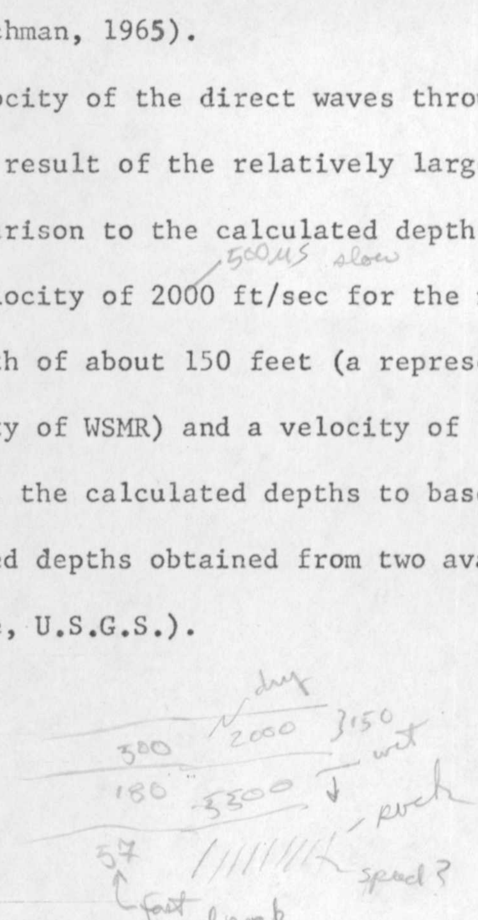

Along the northern half of the profile the sediments were calculated to be relatively thin (less than 500 feet) (Figure 2b). Near the north central part of the profile, in the vicinity of Booker Hill, a well defined offset appears on both segments of the reversed traveltime curves. The offset is recorded on two geophones and represents a time difference of about 0.040 seconds. This offset is interpreted as indicating an upthrown block of Paleozoic limestone which crops out at Booker Hill (Dane and Bachman, 1965). The faults are shown as vertical because no information as to the actual dip could be gained from the available data.

The largest calcuated depths to bedrock are recorded near the south-central part of the profile, at the center of a seismically well-defined, fault-bounded trough. The thickness of the sedimentary rocks at the center of the trough is calculated to be about 1000 feet. Although the faults to the north and south of the trough are well defined on the travel time curves with significant offsets, the actual dip of the faults cannot be determined. There is good agreement in the apparent velocities measured in opposite directions along the northern half of the profile, which leads to an accurate estimation of the true velocity of the bedrock (17,500 feet/sec). Along the southern half of the profile, however, a true bedrock velocity is difficult to determine due to the steeply dipping sides of the trough.

(2) WAR ROAD AND HUECO TANKS ROAD PROFILES

These profiles, located at the intersection of War Road and Hueco Tanks Road, 6 miles north of the Texas-New Mexico border (Figures 3a and 4a), were shot almost "end to end", at right angles to one another. The War Road profile extends north for a distance of about 21,000 feet along War Road to a point 1.4 miles south of Dona Ana Target Range Camp.

The Hueco Tanks Road profile extends eastward along Hueco Tanks Road for a distance of about 28,000 feet. The two profiles are somewhat similar and will be discussed together.

Bedrock.--Reference to the computed cross-sections (Figures 3b and 4b) shows the bedrock dipping both to the NNW (12^{o}) and ENE (20^{o}) from the intersection of the War Road and the Hueco Tanks Road. Examination of the gravity data (Figure 7) in this area shows a relatively steep gradient to the northeast of the War Road-Hueco Road Intersection. Also, there is a suggestion that the gravity contours, which further south parallel the Franklin Mountains, tend to gently curve around the road intersection. This suggests that a buried nose of the Franklin Mountains extends to about the intersection of War Road and Hueco Tanks Road.

Figure 3b shows that along War Road the bedrock surface dips northward and reaches a maximum depth of 4400 feet at the northern end of the profile. On the other hand, figure 4b shows that along Hueco Tanks Road the bedrock dips eastward and the maximum depth to the bedrock surface is 7800 feet at the eastern end of the profile.

Overlying sedimentary rocks.--Reference to figure 3b and 4b shows that the overlying sedimentary rocks along the War Road and Hueco Road profiles consist of four and five velocity horizons, respectively, as computed from the seismic data. The velocities of these sediments vary from about 2000 to 8500 feet/sec on the former profile and from about 2000 to 11,100 feet/sec on the latter profile. Although the lithologic characteristics of these layers cannot be determined without further information, the interface between the 2000 feet/sec horizon and the 6600 feet/sec horizon at a computed depth of about 300 feet probably represents the top of the water table. P-wave velocities of 2000 and 6600 feet/sec are not unusual for dry and water-saturated sands, respectively.

The traveltime curve for the War Road profile suggests that near the northern end of the profile a high velocity layer (11,000 to 13,000 feet/sec) possibly overlies the bedrock. A westward projection of the Hueco Tanks Road profile which intersects the south end of the War Road profile suggests that perhaps 1,000 feet of the 11,000 feet/sec layer is present above the bedrock near the southern end of the War Road profile. Therefore, it is not unreasonable to assume that a thin layer of the 11,000 feet/sec sediments, occurring as a "blind zone", is present along the War Road profile and that the basement depths calculated along this profile should be increased by 10 to 15 percent.

The phenomenon of a blind zone directly above the high velocity bedrock surface is not unusual in seismic refraction work. This blind zone effect would result if the 11,000 feet/sec layer were thin thereby causing the compressional waves which refract from the top of the 11,000 feet/sec layer to arrive later than the refracted waves from the basement surface.

(3) <u>HEADQUARTERS AREA PROFILE</u>

This profile (Figure 5a) can be divided into two sections. One leg of the profile extends in a southwest-northeast direction across the reentrant area south of Highway 70. The second leg extends due east from a point about 3 miles east of Antelope Hill for a distance of 28,000 feet.

<u>Bedrock</u>.-- The computed cross-section (Figure 5b) shows that

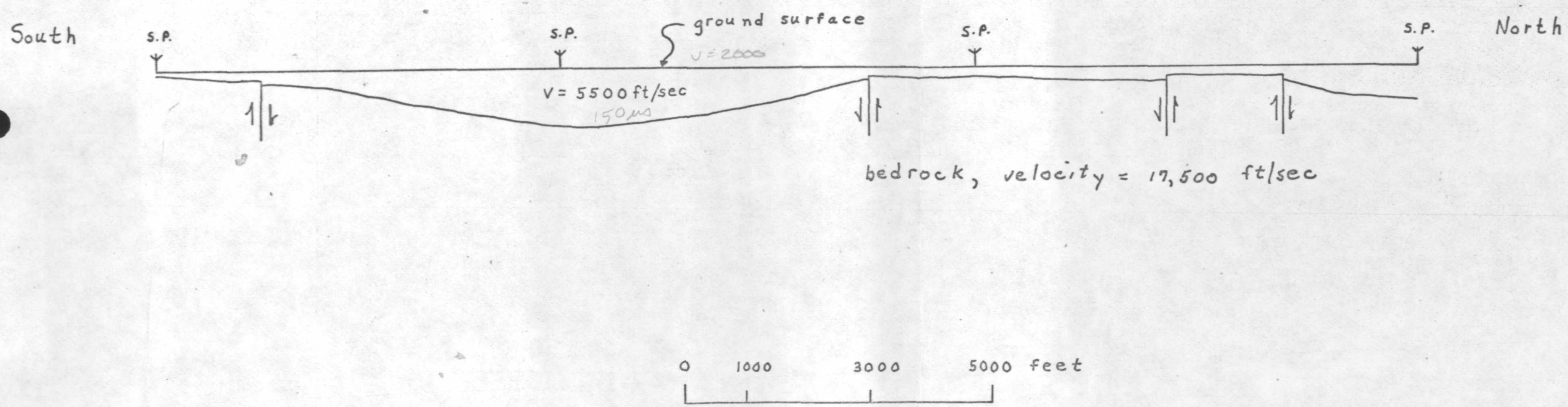

Figure 2b. Seismic refraction profile across La Mesa Gap. SP, shotpoint

Figure 3a. Map Showing Location of Seismic Refraction Profile Along War Road, New Mexico. SP, shotpoint.

0 1 2 miles

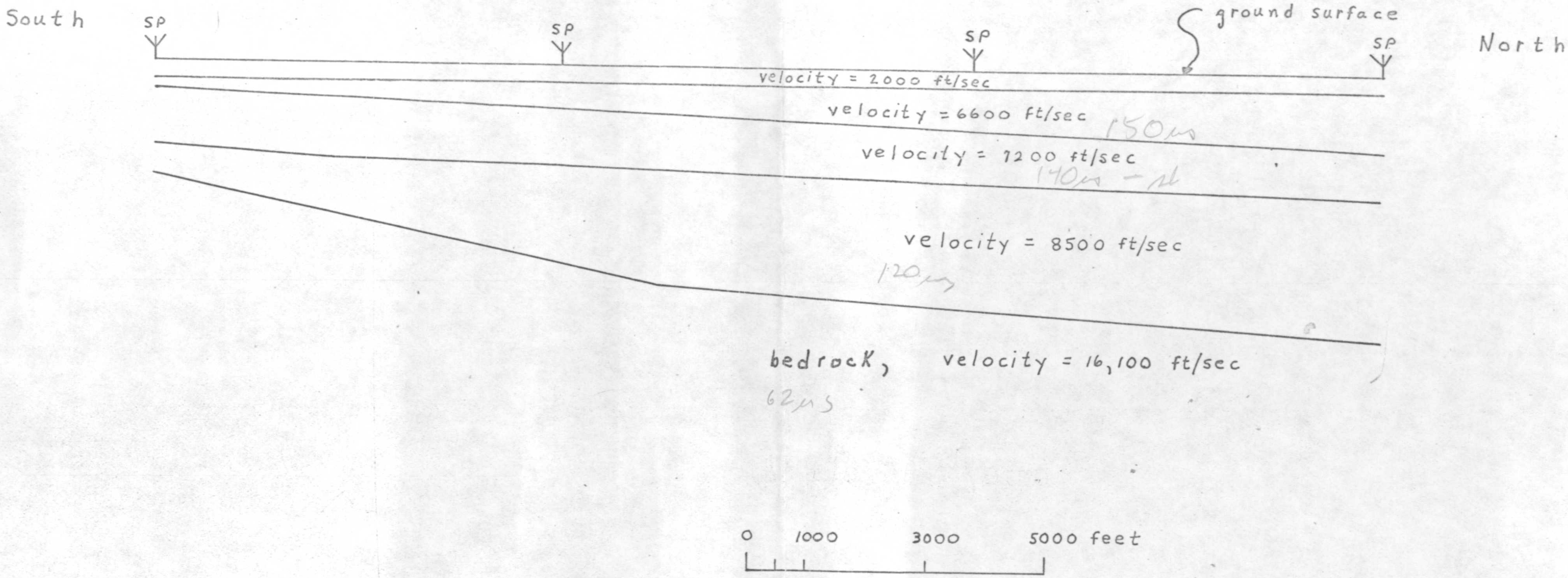

Figure 3b. Seismic refraction profile along War Road, New Mexico. SP, shotpoint

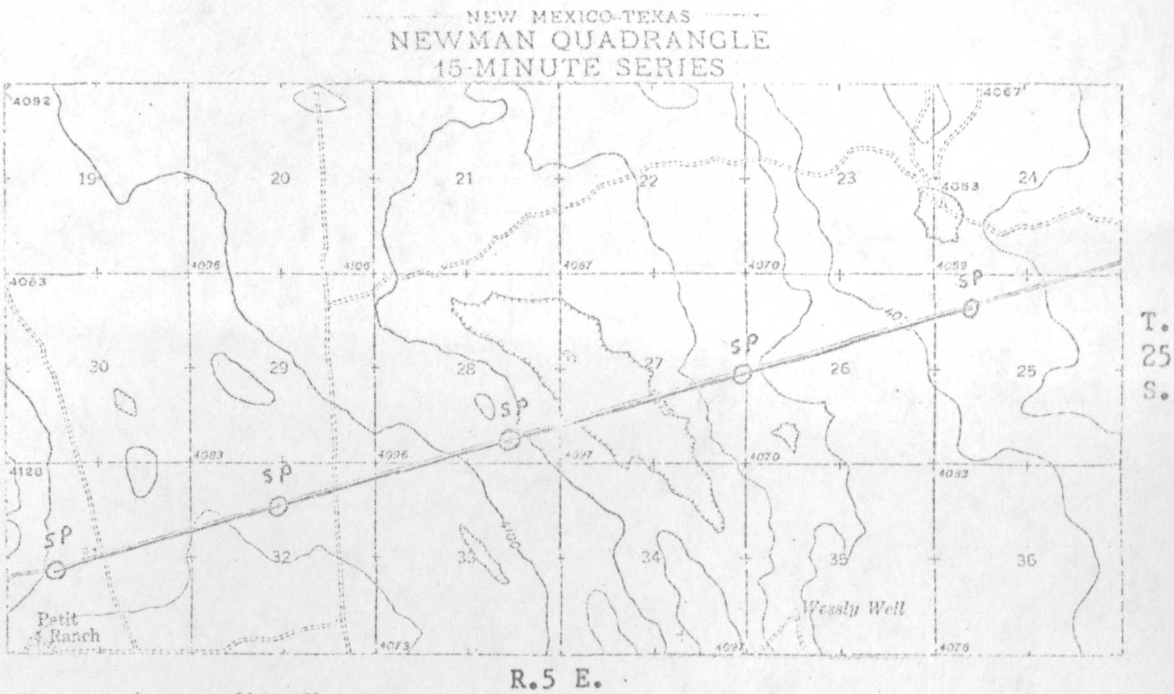

Figure 4a. Map Showing Location of Seismic Refraction Profile Along Hueco Tanks Road, New Mexico. SP, shotpoint.

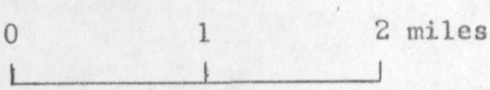

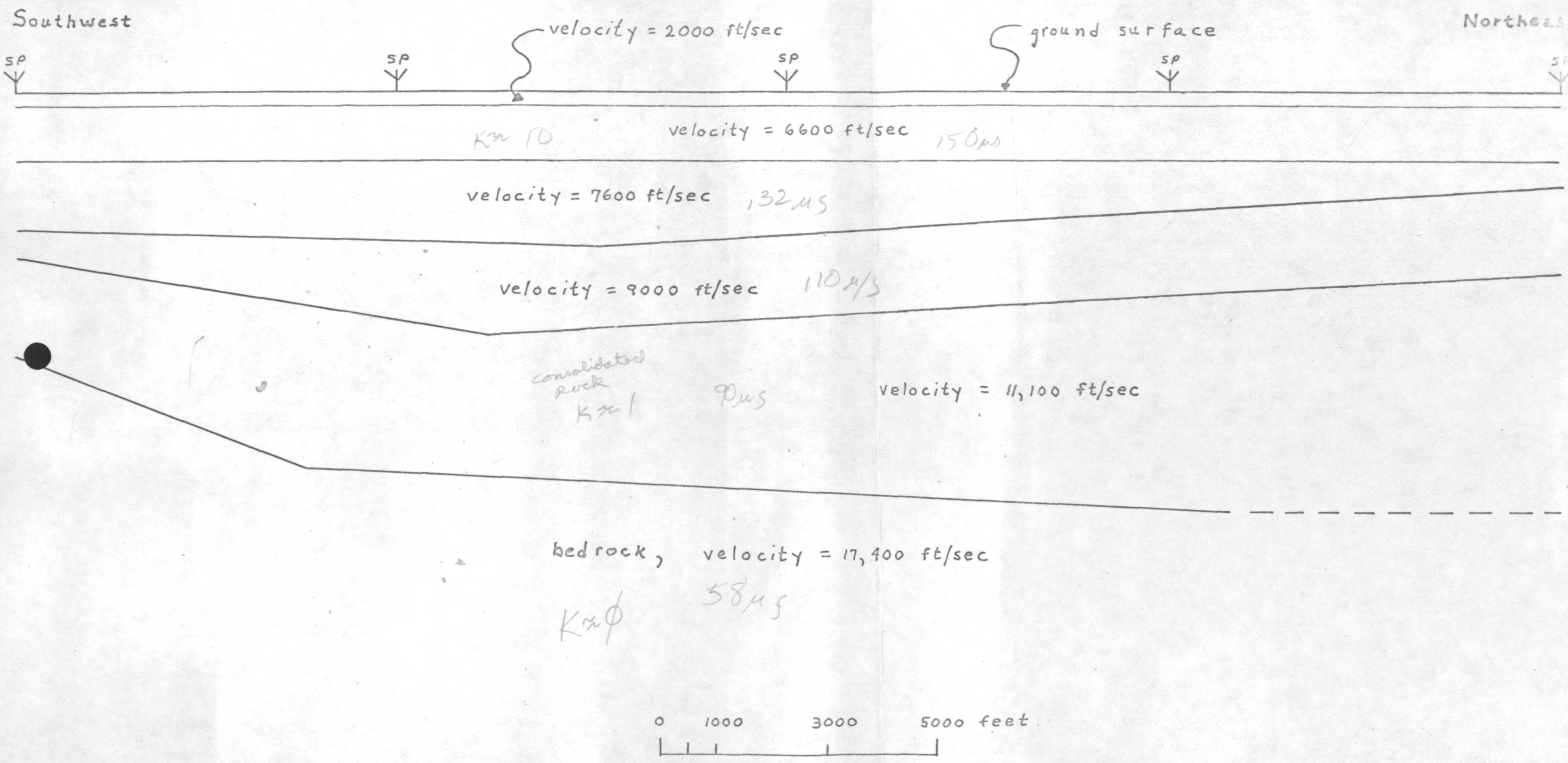

Figure 4b. Seismic refraction profile along Hueco Tanks Road, New Mexico. SP, shotpoint

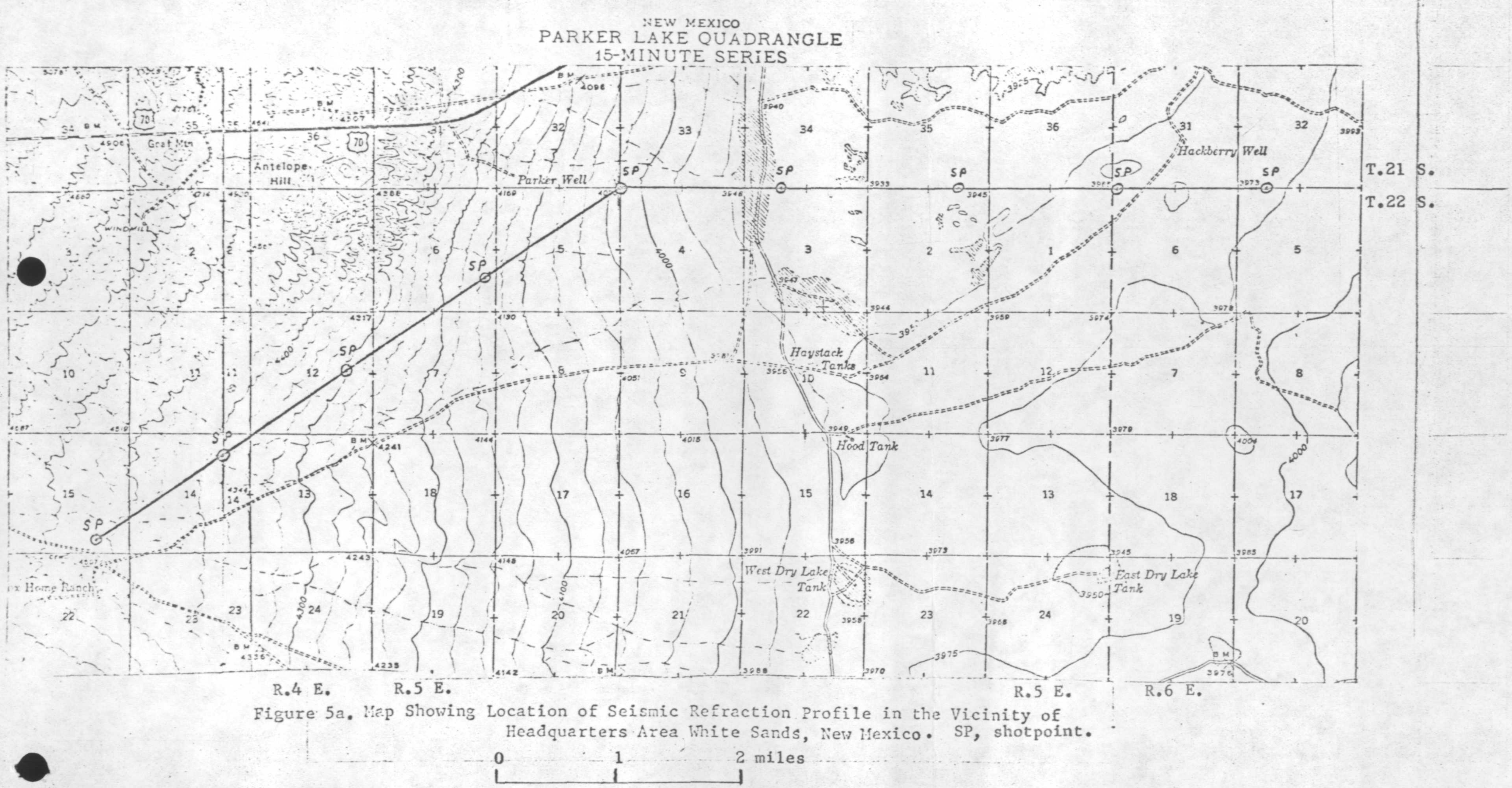

Figure 5a. Map Showing Location of Seismic Refraction Profile in the Vicinity of Headquarters Area White Sands, New Mexico. SP, shotpoint.

Figure 5b. Seismic refraction profile in the vicinity of Headquarters Area, White Sands, New Mexico. SP, shotpoint

at the southwestern end of the profile near the Cox Home Ranch, the bedrock is calculated to be close to the surface and dipping to the northeast at about 17 degrees. This dip continues for a distance of about 5000 feet where, at a point southwest of the second shotpoint, the dip angle decreases. About 3.5 miles due east of Antelope Hill the bedrock surface was computed to be relatively flat and at a calculated depth of about 5500 feet beneath the ground surface.

The results of two test wells drilled to bedrock near the line of profile in the reentrant area were in general agreement with the seismic-refraction results. Test well T-8 (drilled after completion of seismic work) located about 1/2 mile north of the second shotpoint penetrated igneous rock (personal communication, James Cooper, USGS)at a depth of about 1790 feet; whereas, at the second shotpoint, the depth to bedrock as calculated from the seismic data is about 2000 feet. Since the gravity map (figure 9) indicates that T-8 is located updip from the second shotpoint, the depth to bedrock according to T-8 and the calculated seismic depth are in agreement with an error of less than 10 percent.

The results from test well T-6, which was drilled prior to the seismic work, are not as encouraging; according to the drilling log, bedrock was penetrated at a depth of about 490 feet. During field work the location of T-6 could not be found, but the well is believed to be located approximately on or near the seismic line and about 2000 feet northeast of the southwesternmost shotpoint. Since the bedrock dips steeply in this area as confirmed by the seismic results (figure 5b) and the gravity data (figure 9), an error estimation would depend on a more precise location of T-6.

At the turning point near the center of the profile the traveltime curve indicates an increase of dip (figure 5b); this is attributed to the change in direction of the line of profile (the seismic data reflects only apparent dip parallel to the direction of traverse).

Overlying sedimentary rocks.--The curve representing the the apparent velocity of the first arriving waves through the overlying sedimentary rocks is sharp and clearly defined. Along the southwest-northeast trending leg of the profile a large decrease in seismic velocity is noted from southwest to northeast. Along the east-west trending leg of the profile, the sedimentary rocks display no lateral variations in velocity; instead a significant increase in velocity with depth is observed.

As shown on the computed seismic cross-section (figure 5b) the velocity of seismic waves through the sedimentary rocks decreases from about 8700 ft/sec, near the Cox Home Ranch, to about 6500 feet/sec near the turning point on the profile. This large lateral velocity decrease can probably be attributed to the combination of two effects: (1) a northeasterly reduction in particle size and (2) a northeasterly increase in porosity accompanying an improvement in sorting.

Along the eastern half of the profile three distinct velocity horizons in the sedimentary rocks were identified with the following average velocities: 6600 feet/sec, 7200 feet/sec, and 9000 feet/sec. These calculated velocities are comparable with velocities obtained from the sonic log (figure 6) of the deep stratigraphic test well located east of WSMR Headquarters area approximately 2 miles south and 3 miles west of the eastern end of the seismic profile. The average velocities according to the sonic log are as follows: 6600 ft/sec to a depth of about 1400 feet, 7400 ft/sec from 1400 feet to about 2800 feet, 8500 ft/sec from 2800 feet to about 3600 feet and a velocity of about 11,100 ft/sec from 3600 feet to a depth of about 5100 feet. Below 5100 feet the velocity gradually increases to about 15,200 ft/sec.

These results suggest that along the seismic profile the velocity of the sedimentary rocks below a depth of approximately 4000 feet is about 11,000 ft/sec rather than the 9,000 ft/sec as computed from the seismic data (see page 13 for an explanation of a blind zone effect). Consequently, the computed depths to bedrock along the eastern half of the profile in Figure 5b should probably be increased by about 10 to 15 percent. It is interesting to note that a layer having a velocity of 11,000 ft/sec is present on the Hueco Tanks profile.

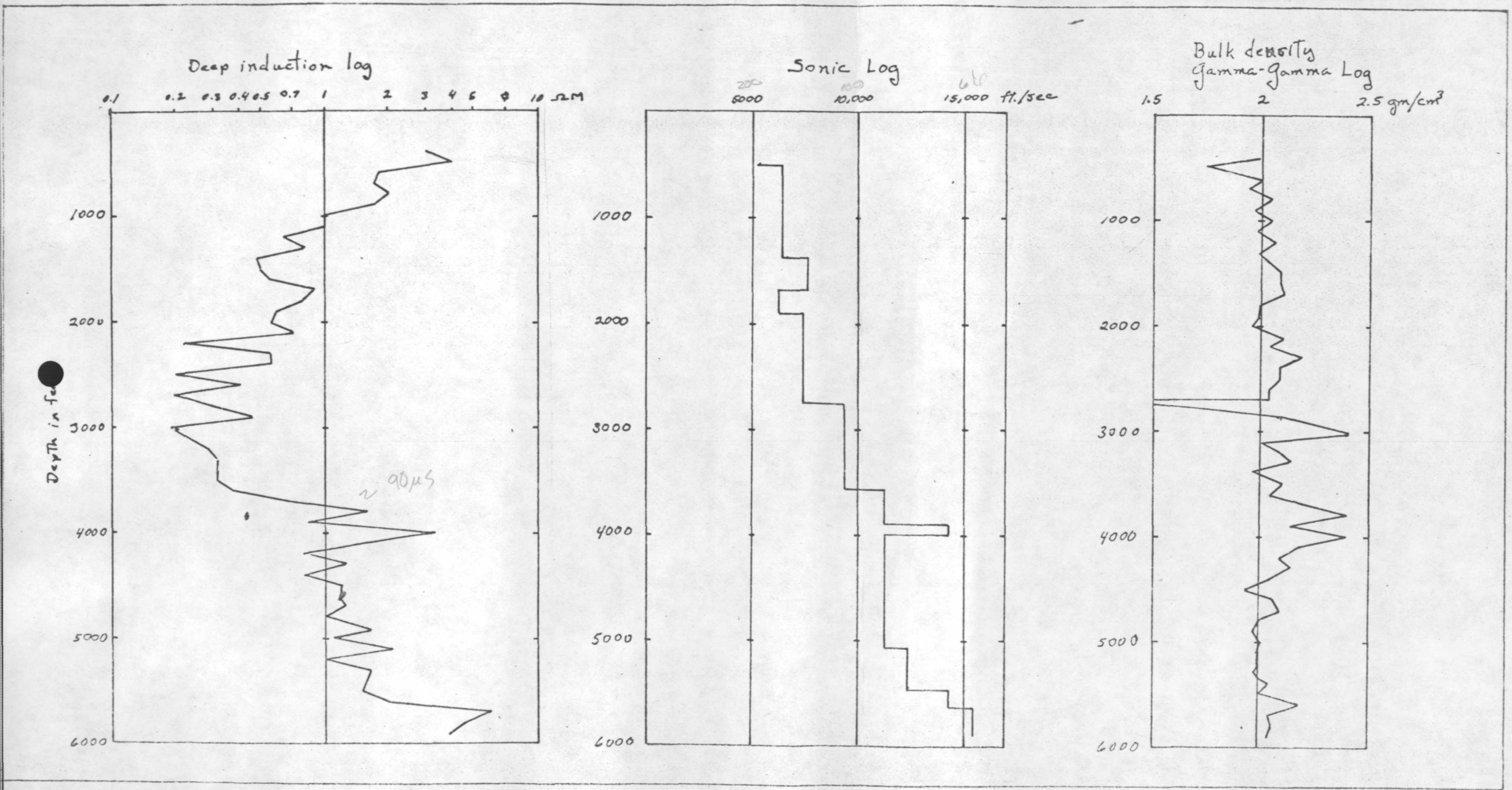

Figure 6. Deep induction, sonic, and bulk density logs of the Stratigraphic Well, White Sands, New Mexico.

GRAVITY RESULTS

Figure 7 is the complete Bouguer anomaly map. The gravity data are plotted on the 1:250,000 scale map of the Las Cruces AMS sheet enlarged to a scale of 1:125,000. The location and the Bouguer anomaly value for each station are shown on the map.

The dominant feature on the map is an elongate gravity low which trends in a north-south direction about 4 miles east of Headquarters area. This low is assumed to be produced by relatively low density Cenozoic sedimentary rocks overlying a high density basement (Tertiary intrusive-Precambrian?). Four gravity stations along the New Mexico-Texas state line show that this low terminates a few miles north of the state line, which indicates that the depth to bedrock in that area is shallower than at the Headquarters area. This conclusion does not however agree with the seismic results along Hueco Tanks Road which indicate that the depth to bedrock (7800 feet) is deeper in the south of the survey area than in the north. Furthermore, according to the seismic and electrical sounding data (Mattick, 1967; Zohdy, 1966), 3 miles south of the New Mexico-Texas border, the depth to bedrock is about 9000 feet. These depths indicate that the bedrock surface probably continues to deepen toward the south which does not agree with the observed gravity data. The following explanations are offered as possible solutions. A thick section of Cenozoic sediments may continue southward into Texas through the southern zone of higher gravity values where the termination of the gravity low may be produced by a southward increase of a regional gravity gradient. Bouguer anomaly values on or near bedrock along the western edge of the map show a southward increase of approximately 1.5-1.8 milligals per mile. If this regional gravity gradient is removed from the map the gravity low would extend southward into Texas with approximately the same amplitude as shown 4 miles east of the Headquarters area. Another explanation is that the Cenozoic sedimentary rocks shown in the southern area of the map have a higher density than sedimentary rocks to the north. Seismic measurements indicate the presence of a thick section of rocks with higher velocity in the south than in the north. If this is true the higher density sedimentary rocks would give rise to a smaller anomaly.

The gravity low is flanked on the west by steep gravity gradients which, in general, coincide with the eastern front of the Organ and San Andres Mountains. These steep gravity gradients are interpreted as indicating a high angle fault or series of faults.

To the east of the gravity gradient is less steep. About 9 miles west of the southern end of the Jarilla Mountains the gravity data indicate a depression in the pre-Cenozoic bedrock surface. More gravity data are needed to the north and to the south of the gravity profile in that area to determine the extent of this depression.

A two-dimensional profile (figure 8) was constructed along profile A-A' (figure 7) Antelope Hill to the Jarilla Mountains. The model computed on the basis of the residual anomaly shows the generalized configuration of the top of the pre-Cenozoic bedrock and the thickness of the Cenozoic sedimentary rocks. In making the analysis it was assumed that a 0.5 gm/cc density contrast exists between the Cenozoic sedimentary rocks and pre-Cenozoic bedrock. This contrast was chosen as it has been used successfully in similar areas of the southern Basin and Range province. A regional gravity gradient, increasing eastward at approximately 0.45 milligal per mile, was removed to facilitate the analysis. The model shows the thickness of Cenozoic sedimentary rocks to be about 6000 feet in the deepest part of the basin.

Figure 9 is a Bouguer anomaly map of the reentrant areas south and north of Highway 70. The map is con- toured at 2-milligal interval. The steep gravity gradient trending in a north-south direction is interpreted as a high angle fault or series of faults. This steep gradient trend is interrupted in the southern reentrant area by a western extension of low gravity values. Consequently, the nature of faulting is not clear across the mouth of the southern reentrant area. The fault zone is however quite clearly defined by the steep gradient across the mouth of the northern, and smaller of the two reentrant areas. The gravity data indicate that the northern reentrant area contains very thin deposits of Cenozoic sedimentary rocks in contrast to the southern reentrant area.

The gravity field in the southern reentrant area is distorted by the local gravity field associated with the Organ batholith and speculation on the depth to bedrock, especially in the southern reentrant area, is unreliable without better gravity control, geologic, and/or geophysical information. However, an approximate bedrock map based on the results of the resistivity soundings, the seismic refraction and the gravity data is given in a following section.

RESULTS OF THE RESISTIVITY SOUNDINGS

A total of 85 vertical electrical soundings was made in the White Sands Missile Range area, east of the San Andres and the Organ Mountains. The location of these soundings is shown in Figure 10. The results of the interpretation of all the soundings are given in Table 1 in the appendix.

APPARENT RESISTIVITY MAP:

Several apparent resistivity maps and apparent resistivity sections were prepared during the qualitative stage of the interpretation of the sounding data. As mentioned earlier, the value of such maps and sections is to familiarize the interpreter with the general horizontal and vertical distribution of the resistivity in the area. However, the contours on an apparent resistivity map, or section, may or may not be closely related to the actual distribution of the true resistivities at a given depth. Therefore, in the final analysis these maps and sections should be considered to be strictly qualitative in character. The apparent resistivity map obtained by contouring the apparent resistivity values (obtained from the VES curves), at the electrode spacing $\frac{AB}{2} = 1000$ feet, is shown in Figure 11. The contoured values of apparent resistivity do not represent the true resistivity at a depth of 1000 feet. Consequently, the contours only reflect the approximate areal distribution of the average resistivity of a section which is generally less than 1000 feet and greater than about 200 feet in depth.

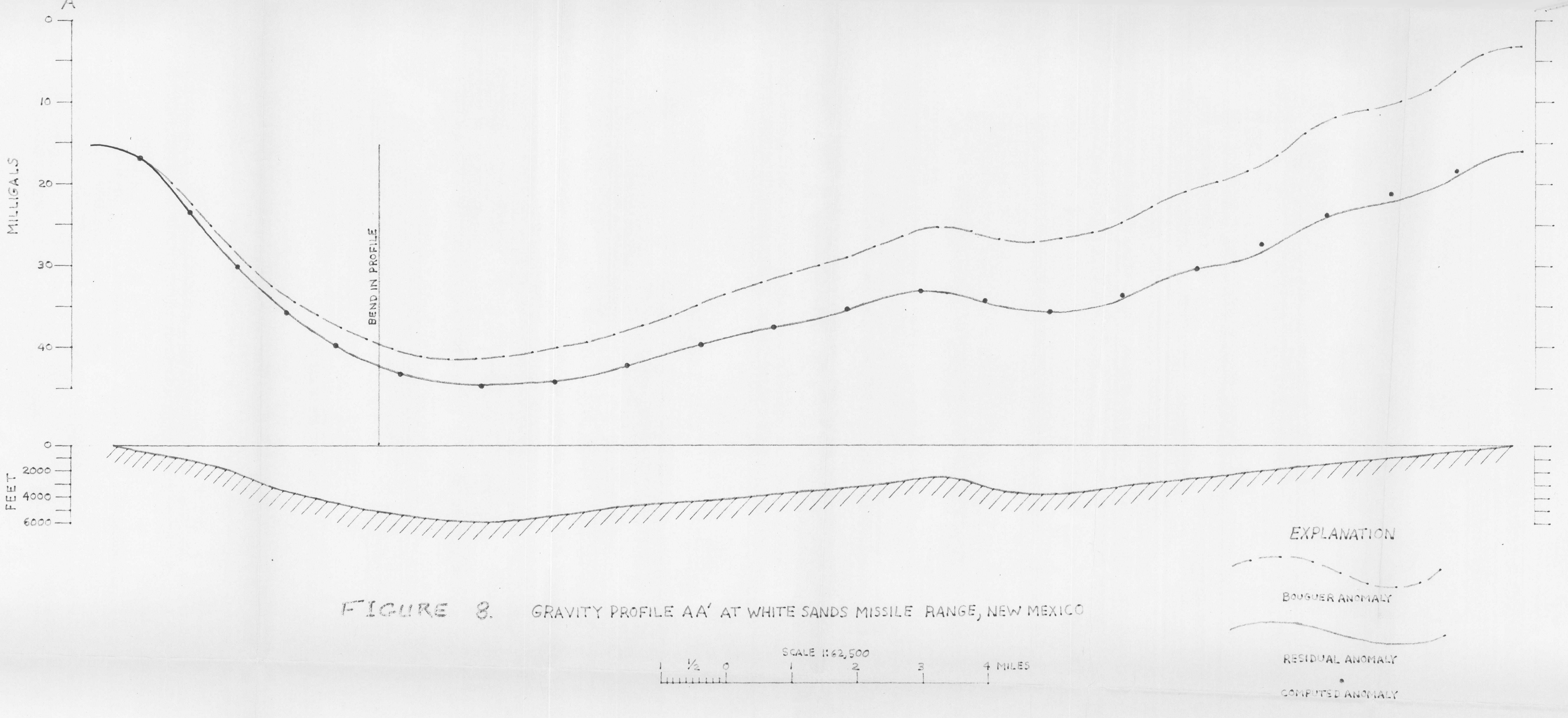

FIGURE 8. GRAVITY PROFILE AA' AT WHITE SANDS MISSILE RANGE, NEW MEXICO

ASSUMED DENSITY CONTRAST EQUALS 0.5 G PER CC.

LOCATION OF PROFILE SHOWN ON FIGURE 7

FIGURE 9

COMPLETE BOUGUER ANOMALY MAP IN THE VICINITY OF HEADQUARTERS AREA, WSMR, NEW MEXICO.

1 ½ 0 1 2 3 4

CONTOUR INTERVAL = 2 MILLIGALS

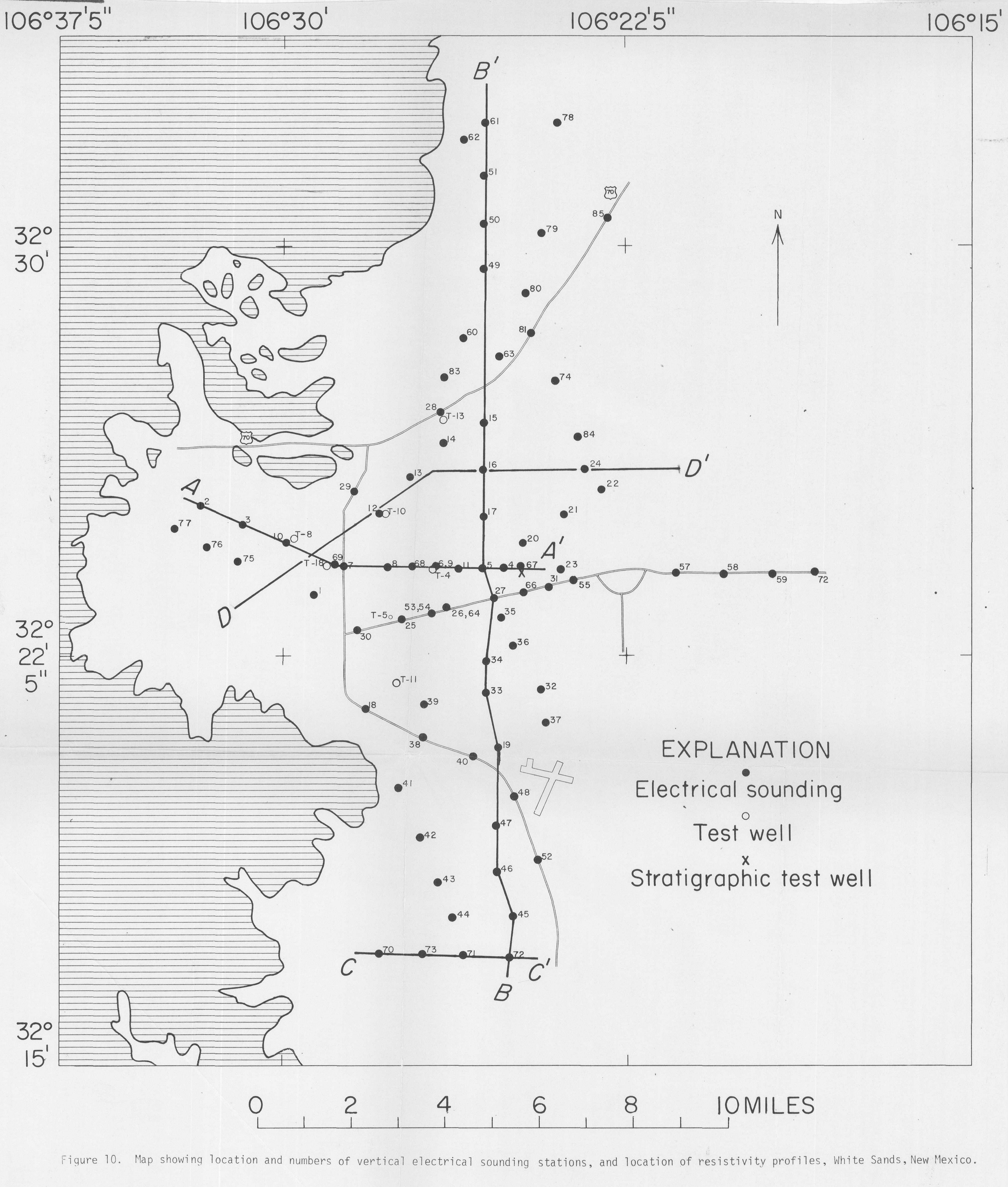

Figure 10. Map showing location and numbers of vertical electrical sounding stations, and location of resistivity profiles, White Sands, New Mexico.

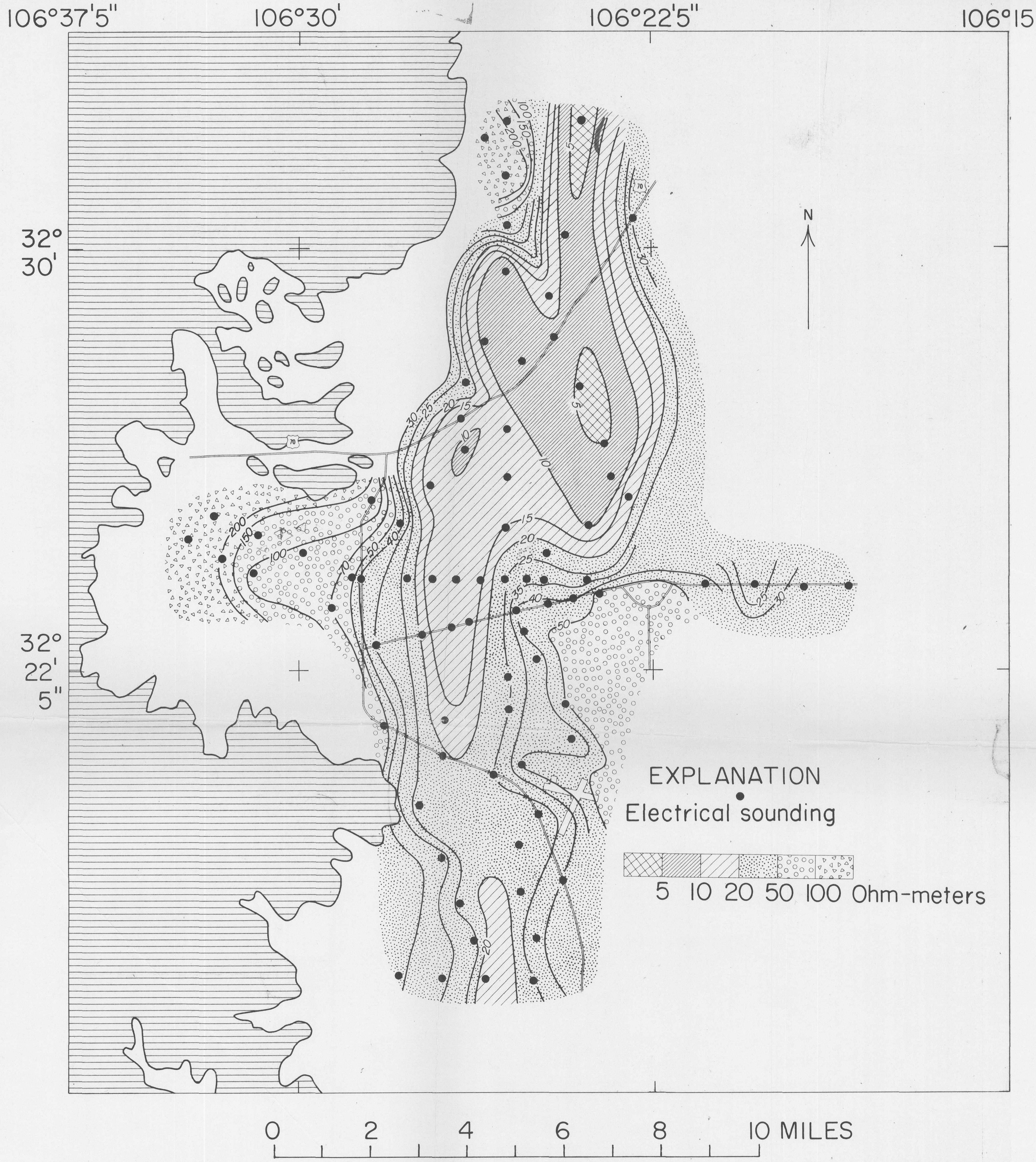

Figure 11. Apparent resistivity map for electrode Spacing $\frac{AB}{2}$ = 1000 feet, White Sands, New Mexico

High apparent resistivity values ($\geq$ 50 ohm-m) are observed near the western boundaries of the studied area (east of the Organ and San Andres Mountains), especially in the reentrant areas as well as on the alluvial fan deposits near Bear Canyon. These high resistivity values are the result of two possible effects: (1) presence of relatively clean sand and gravel probably saturated with fresh water, and (2) relative shallowness (< 700 feet) of the crystalline bedrock. In the reentrant areas both effects contribute to the high apparent resistivities, whereas on the Bear Canyon alluvial fan the high apparent resistivity values result totally from the presence of a thick section of alluvium saturated with fresh water.

The areas north of Nike Avenue are characterized by very low apparent resistivities (< 15 ohm-m) in comparison to the areas south of Nike Avenue (> 15 ohm-m). The apparent resistivity contour of 15 ohm-m may be considered to outline the boundaries of the area where drilling for fresh water is not recommended. The relatively high apparent resistivity values observed near the eastern boundaries of the survey area (~ 40 ohm-m) are probably related to the presence of gypsum and anhydrite layers in the section.

Figure 12. Geoelectric section along profile AA', White Sands, New Mexico.

Numbers in layers indicate true resistivities.

HEADQUARTERS EAST-WEST PROFILE (AA')

The location of this profile is shown in Figure 10. The cross section is shown in Figure 12, and is based on the interpretation of 12 VES curves and three test wells. There are six major geoelectric layers in this section. (1) Near surface deposits of variable resistivity of 74 to 175 ohm-m, (2) a layer of intermediate resistivity of 30-40 ohm-m, probably representing fresh water saturated sand and gravel, (3) a conductive layer of 8-15 ohm-m, probably representing sedimentary rocks saturated with brackish water, and/or sedimentary rocks containing large amounts of clayey deposits, (4) a more conductive layer of 4-5 ohm-m which, more likely, is saturated with saline water, (5) a layer of extremely low resistivity of less than or equal to 1 ohm-m which is definitely saturated with highly mineralized water in addition to the presence of a high clay or shale content, and (6) basement rocks whose resistivity is practically infinite with respect to the overlying sedimentary rocks.

The basement configuration along this profile has been changed from a previous interpretation based on the data obtained in 1966. The depth to the basement at VES 69 and 7 has been increased and a layer of resistivity of about 10 ohm-m has been introduced after the interpretation of VES 69. The data for VES 69 had not been obtained at the time when the first interpretation was made. In fact, as a result of the interpretation of VES 69, 7, 8, and 68 it was found that the depth to basement must be increased and that a gradual decrease in resistivity (from 35 to 10 to 5 to 1 ohm-m) from west to east exists. It is interesting to note that a similar decrease in seismic refraction velocity was observed from west to east. In combination, the decrease in resistivity and velocity indicates an increase in porosity; however the decrease in resistivity is so significant that the increase in porosity must be accompanied by an increase in salinity.

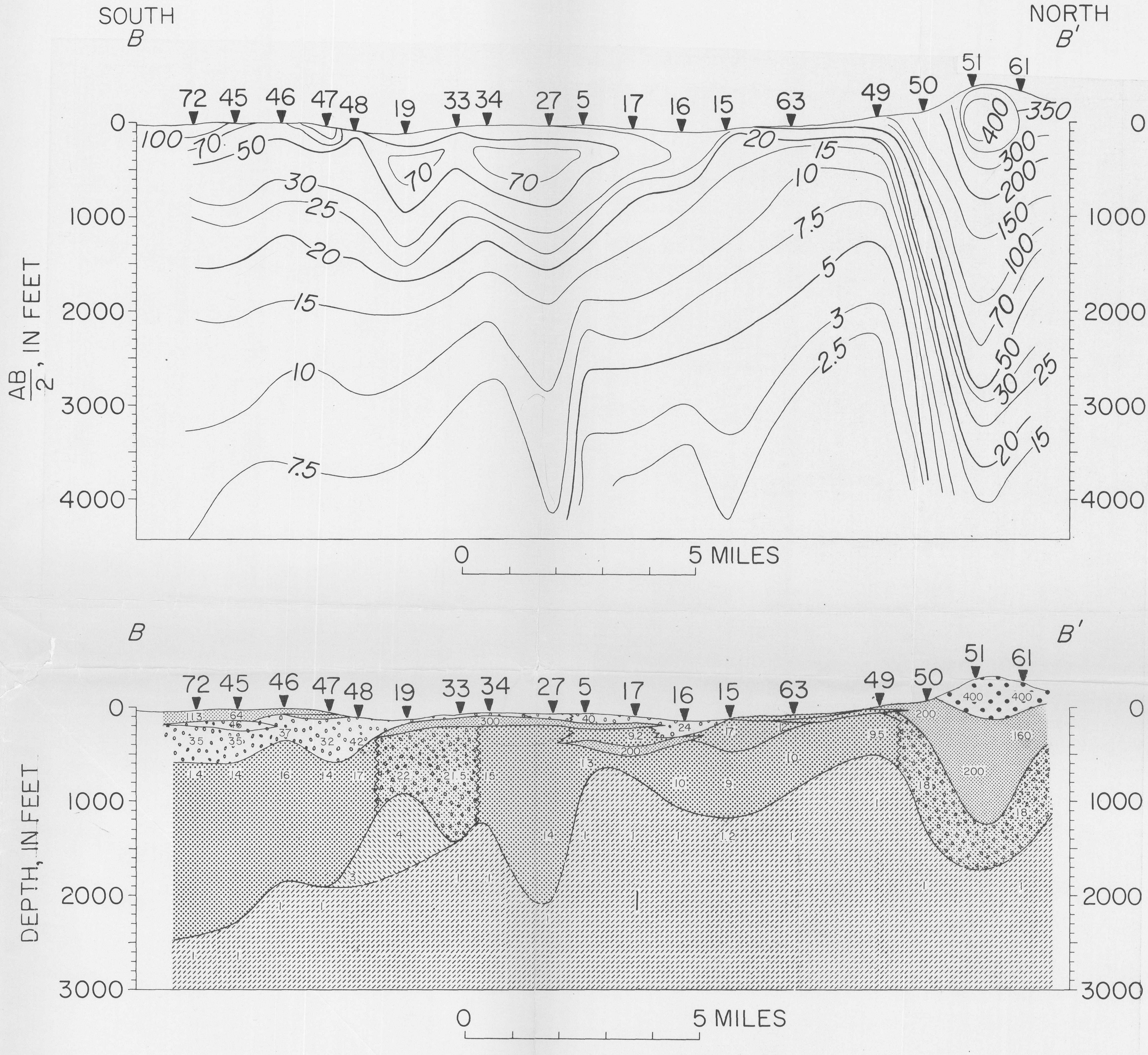

Figure 13 a) Apparent resistivity section along profile BB', White Sands, New Mexico. Numbers on contours indicate apparent resistivities.

b) Geoelectronic section along profile BB'. Vertical exaggeration X10.56. White Sands, New Mexico. Numbers in layers indicate true resistivities.

Figure 14.--Geoelectric section along profile BB'. No vertical exaggeration.

All the VES curves along this profile were interpreted by matching the observed VES curves to theoretically computed ones.

HEADQUARTERS NORTH-SOUTH PROFILE (BB')

The profile BB' is approximately 19 miles in length and approximately parallels the Organ and San Andres Mountains. The cross-section along this profile is based on the interpretation of 18 vertical electrical soundings. Two representations of this cross section are shown in Figure 13 and 14. The apparent resistivity section (figure 13a) was prepared by plotting and contouring the apparent resistivity values as a function of the electrode spacing, AB/2, for each VES station along the cross-section. The analogy between the form of the apparent resistivity contours in Figure 13a and the distribution of the layers according to the quantitative interpretation in Figure 13b is remarkable.

The same quantitative interpretation shown in Figure 13b is shown without vertical exaggeration in Figure 14. The interpretation of the VES curves obtained along this profile indicates that there is a continuous sedimentary layer saturated with highly saline water (< 1 ohm-m) at the bottom of the section. Excellent possibilities for tapping ground water aquifers exist near the north end of the profile between VES 50 and 61. There is strong geophysical and geological evidence for a lens of fresh water (160 to 200 ohm-m) of about 1000 feet maximum thickness floating over a ground water body of potable but average quality (18 ohm-m) which, in turn, overlies highly mineralized non-potable water (1 ohm-m or less). It is recommended that a borehole be drilled on the alluvial fan east of Bear Canyon near VES 51, or to the north of it, to tap and evaluate this ground water lens. It should however be noted that to the east of this area near Highway 70, it seems (according to VES 78,79, and 85) that the eastward lateral extent of the fresh water lens is very limited and ground water of very inferior quality prevails at shallow depths.

Interpretation of the VES curves from stations 49 to 27 indicates that this part of the section is characterized by ground water of rather inferior quality and/or sedimentary rocks of low permeability. This inference is based on the low resistivity values (9-10 ohm-m) of the sedimentary rocks below the water table in that area. Furthermore the interface between the "fresh" and highly mineralized water in that part of the section is relatively shallow.

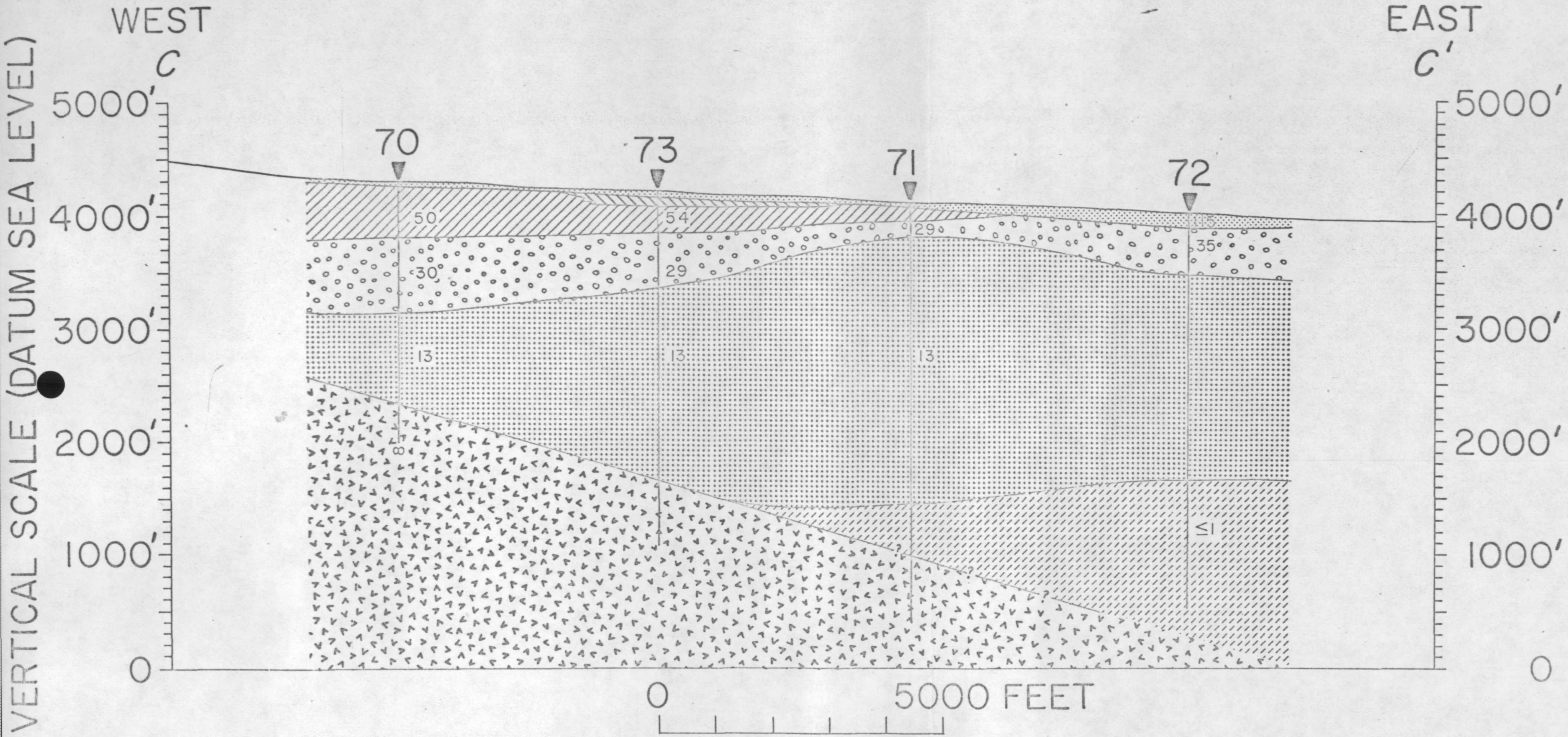

Figure 15. Geoelectric section along profile CC'. Vertical exaggeration X2. White Sands, New Mexico.

To the south of Nike Avenue, from VES 34 to VES 48 there probably exists a zone for potential ground water development. This zone has a resistivity of about 22 ohm-m which indicates the presence of either coarser sedimentary deposits and better permeability and/or ground water of better quality than that present to the north or to the south.

The southern part of the section between VES 47 and 72 is mainly characterized by a layer of great thickness (about 1500 feet) and intermediate resistivity 14-16 ohm-m. This layer is underlain by the highly mineralized ground water layer ($\leq$ 1 ohm-m) and is overlain by a layer (35 ohm-m) which probably is saturated with ground water of better quality than that saturating the layer of 14-16 ohm-m.

EAST-WEST PROFILE (CC')

This profile is approximately 3.5 miles in length and located between Globe Well and Goodin Tank (Figure 10). The cross section CC' (figure 15) is based on the interpretation of four electrical sounding curves: VES 70, 71, 72, and 73. According to the interpretation of the four VES curves, there are two layers that are of hydrogeologic significance. These are the layers of 29-35 ohm-m, and the layer of 13-14 ohm-m. If the 29-35 ohm-m layer is saturated with water then it will represent water of good quality. On the other hand, the 13-14 ohm-m layer is probably saturated with ground water of acceptable to poor quality.

No quantitative estimate in terms of parts per million dissolved solids can be given from the resistivity data alone. The 13 ohm-m layer should not be overlooked as a potential fresh-water reservoir of substantial thickness consisting of several aquifers saturated with fresh water but separated from one another by clayey aquicludes.

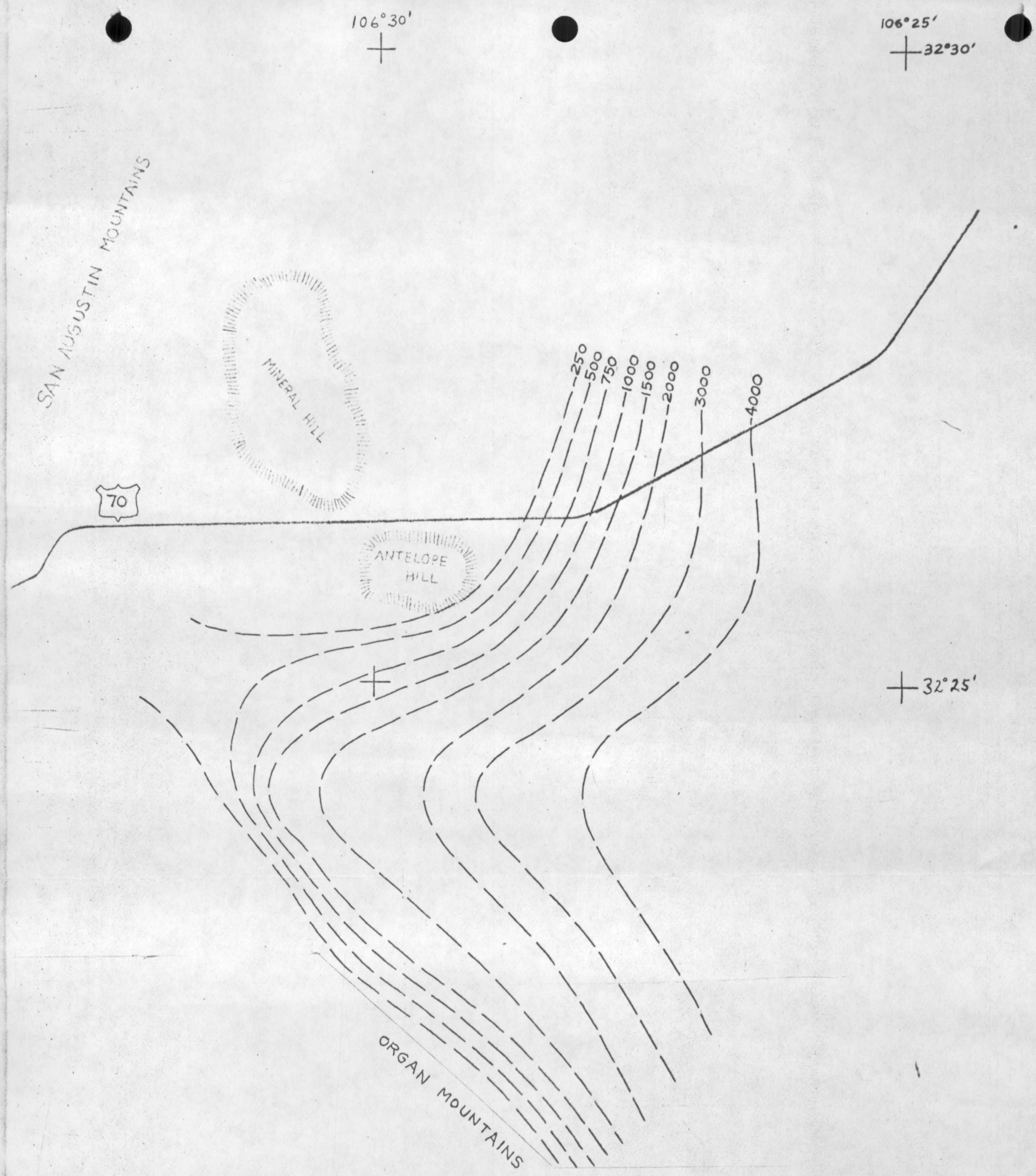

FIGURE 16.

APPROXIMATE THICKNESS, IN FEET, OF THE BOLSON DEPOSITS IN THE HEADQUARTERS AREA, WHITE SANDS MISSILE RANGE, NEW MEXICO

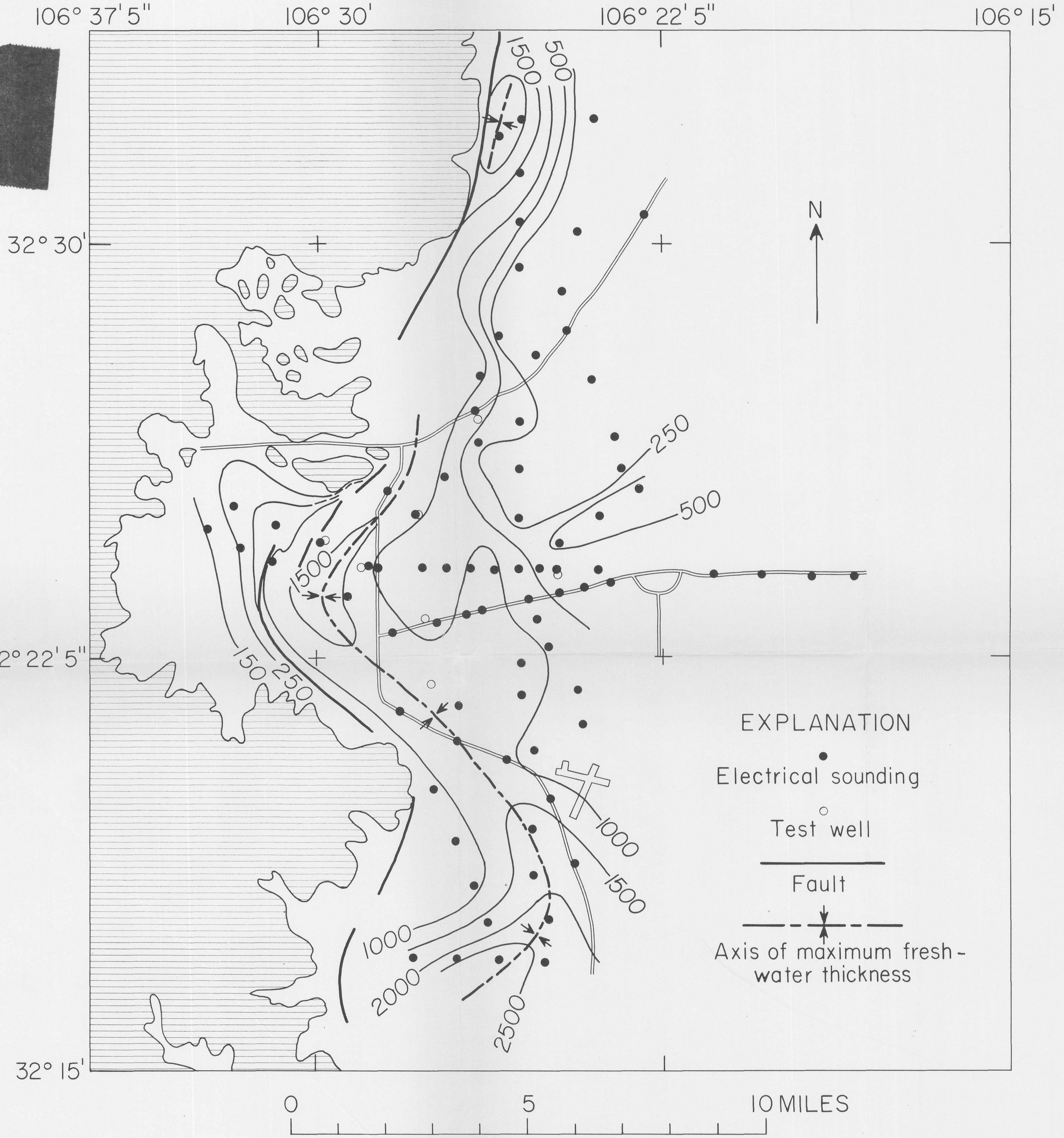

Figure 17. Map showing isobaths of the lower surface of fresh water aquifer, WSMR. Datum is land surface. Line pattern is Paleozoic rocks.

BEDROCK MAPS

Two isobath (equal-depth) maps were prepared. The first map (figure 16) shows the approximate thickness of bolson deposits in the reentrant area south of Highway 70. The map was constructed on the basis of the interpretation of 17 electrical soundings, the seismic profile and the gravity data. Geologic information from a few test wells in the area was also used. However, only three wells (T-6, T-8, and T-9) are believed to have penetrated the bedrock at depths varying from about 480 to 1800 feet. No attempt was made to define the faults that are present in this area. Consequently the map should be considered only as a generalized contour map on the pre-Cenozoic bedrock.

The second isobath map (figure 17) is based on the results of the electrical prospecting in the entire area. The depth contours on this map represent the depth to either the impervious bedrock (resistivity $\rightarrow \infty$) or to sedimentary rocks saturated with highly mineralized waters (resistivity less than 10 ohm-m). Therefore, the contours represent the maximum depth of interest for fresh ground-water exploration. However, above the contoured horizon, in some areas, there are thick layers of 12-14 ohm-m which may represent sand and gravel aquifers with substantial amounts of clays and they may thus be of low permeability. The locations of major faults as inferred from the electrical soundings and the geologic map of New Mexico (Dane and Bachman, 1965) are shown on the map. The dashed line on the map represents the axis of the thickest section of fresh-water saturated sedimentary rocks.

According to the interpretation of VES 62, the fault bounding the east side of the San Andres Mountains, near Bear Canyon, must be steeply dipping ($\geq$ 60 degrees) because no evidence of the bedrock was obtained on the curve of VES (62) although the electrode spacing was expanded to $\frac{AB}{2}$ = 4000 feet. Similarly the fault bounding the Organ Mountains near VES 41 must also be steeply dipping since no evidence of high resistivity rocks was observed on the curve of VES 41 even at $\frac{AB}{2}$ = 4000 feet.

CONCLUSIONS

The use of seismic, gravity and resistivity measurements in the White Sands Missile Range area has been very effective in contributing to the knowledge of the hydrogeology of the area. All three methods augmented one another in determining the depth to the impervious bedrock. The most promising areas for supplies of fresh ground water were delineated on the basis of the resistivity measurements. These areas were found to be in the Bear Canyon alluvial fan, in the reentrant area south of Highway 70, and in the area east of Soledad Peak and west of Globe Well and Goodin Tank. In general, potable water is found in a belt zone at the foot of the San Andres and Organ Mountains.

The water-saturated sedimentary rocks have resistivities varying from 200 ohm-meters to less than 1 ohm-meter. Layers having resistivities of less than 10 ohm-meters are considered to be saturated with brackish to highly mineralized water. There are layers having resistivities between 10 and 15 ohm-m which are difficult to classify in terms of the quality of their water content. These layers may contain brackish water and therefore should be considered before the 1 ohm-m layers in future desalinization programs. On the other hand, the 10 to 15 ohm-m layers may be comprised of several sand aquifers separated from one another by numerous clay beds.

ACKNOWLEDGMENTS

The authors thank Chevron Oil Company for making the computer program for calculating theoretical Schlumberger curves available to the U.S. Geological Survey. They also thank George Van Trump of the U.S. Geological Survey for modifying the computer program in accordance with their needs.

REFERENCES

Behrendt, J. C., and Wollard, G. P., 1961, An evaluation of the gravity control network in North America: Geophysics, v. 26, pp. 57-76.

Chastenet de Gery, C. J., and Kunetz, G., 1956, Potential and apparent resistivity over dipping beds: Geophysics, v. 21, no. 3, pp. 780-793.

Compagnie Général de Géophysique, 1963, Master curves for electrical sounding: The Hague, European Association of Exploration Geophysicists.

Dakhnov, V. N., 1953, Electrical prospecting for petroleum and natural gas deposits (in Russian): Moscow, Gostoptekhizdat, 497 p.

Dane, C. H., and Bachman, G. O., 1965, Geologic map of New Mexico: U.S. Geological Survey, special maps.

Deppermann, K., 1954, Die Abhangigkeit des scheinbaren Widerstandes vom Sondenabstand bei der Vierpunkt-Methode: Geophysical Prospecting, v. 2, no. 4, pp. 262-273.

Flathe, H., 1963, Five-layer master curves for hydrogeological interpretation of geoelectrical resistivity measurements above a two-story aquifer: Geophysical Prospecting, v. 11, no. 4, pp. 471-508.

Hawkins, L. V., 1961, The reciprocal method of routine shallow seismic refraction investigations: Geophysics, v. 26, pp. 806-819.

Kalenov, E. N., 1957, Interpretation of vertical electrical sounding curves (in Russian): Moscow, Gostoptekhizdat, 472p.

Kunetz, G., 1966, Principles of direct current resistivity prospecting: Berlin-Nikolassee, Gebruder Borntraeger, 103 p.

Mattick, R. E., 1967, A seismic and gravity profile across the Hueco Bolson, Texas: U. S. Geological Survey Prof. Paper 575-D, p. D85-D91.

Mooney, H., Orellana, E., Pickett, H., and Tornheim, L., 1966, A resistivity computation method for layered earth models: Geophysics, v. 31, no. 1, pp. 192-203.

Orellana, E., and Mooney, H., 1966, Master tables and curves for vertical electrical sounding over layered structures: Madrid, Interciencia.

Rabinovich, B. I., 1965, Fundamentals of the method of field difference (in Russian): Prikladnaia Geofizika (Applied Geophysics), v. 43, p. 47-59.

Slotnick, M. M., 1950, A graphical method for the interpretation of refraction profile data: Geophysics, v. 15, pp. 163-180.

Swick, C. H., 1942, Pendulum gravity measurements and isostatic reductions: U. S. Dept. of Commerce Coast and Geodetic Survey, Spec. Publ. No. 232, pp. 67-68.

Zohdy, A.A.R., 1965, The auxiliary point method of electrical sounding interpretation and its relationship to the Dar Zarrouk parameters: Geophysics, v. 30, pp. 644-660.

Zohdy, A.A.R., 1966, Geoelectrical exploration for ground water in the southwestern United States (abstract): Geophysics, v. 31, no. 6, p. 1216.

Zohdy, A.A.R., 1968a, A rapid graphical method for the interpretation of A- and H-type electrical soundings: Geophysics, v. 33, pp. 822-833.

Zohdy, A.A.R., 1968b, The effect of current leakage and electrode spacing errors on resistivity measurements: U.S. Geol. Survey Prof. Paper 600-D, p. D258-D264.

APPENDIX

TABLE 1: LAYER DEPTHS AND RESISTIVITIES ACCORDING TO THE INTERPRETATION OF THE VES CURVES, WHITE SANDS, NEW MEXICO.

VES. No.	Layers								Quality of Theoretical Fit	Remarks
	1	2	3	4	5	6	7	8		
1	5.2* 122+	16 2440	122 170	750 85	open 18				good	
2	24 170	70 45	305 170	∞ ∞					very good	
3	30 250	60 40	210 80	450 175	680 35	∞ ∞			very good	
4	33 15	115 160	360 15	390 150	open < 1.5				satisfactory	noisy field data
5	17 100	100 40	180 210	280 9	360 110	720 13	open < 3		good	
6	11 120	22 24	105 100	300 36	1000 11	5000 2.5	∞ ∞		-	fit by aux. curve method
7	8.5 86	17 17	440 74	720 30	4000 8.3	∞ ∞			very good	rising terminal branch not well developed
8	29 168	88 68	110 300	460 40	4200 4.8	∞ ∞			good	
9	-	-	-	-	-	-	-	-		crossed sounding at VES 6
10	24 150	48 240	510 160	1750 35	∞ ∞				satisfactory	lateral effect on terminal branch
11	50 108	200 34	1100 14	open ~ 1					very good	
12	120 86	360 117	1100 21.2	2400 1.7	∞ ∞				good	

* Depth to the base of the layer in feet

\+ Resistivity of the layer in ohm-m

TABLE 1: LAYER DEPTHS AND RESISTIVITIES ACCORDING TO THE INTERPRETATION OF THE VES CURVES, WHITE SANDS, NEW MEXICO. --Continued

VES. No.	Layers								Quality of Theoretical Fit	Remarks
	1	2	3	4	5	6	7	8		
13	43 45	130 115	600 15	1500 7	4950 2	∞ ∞			good	rising terminal branch undeveloped
14	28 98	90 40	250 21	1100 9.6	open 2				very good	
15	5 70	20 46	350 17	1070 9	3400(?) 1.2	∞ ∞			very good	rising terminal branch undeveloped
16	14 60	205 24	215 250	950 10	3300(?) 1.75	∞ ∞			satisfactory	rising terminal branch undeveloped
17	16 54	64 23	113 160	340 9	400 110	800 12	open 0.8		good	
18	34 143	120 54	680 92	3000? 13	∞ ? ∞ ?				good	rising terminal branch undeveloped
19	3.5 110	10 10.5	14 175	28 10	143 250	680 22	open 4		good	
20	14 8.7	225 44	690 24	open 1.5					satisfactory	
21	2.7 800	15 47.5	42 120	122 35	700 15	open 0.78			good	
22	5.6 165	33 15	117 180	700 16	open ~ 0.8				satisfactory	
23	-	-	-	-	-	-	-	-	no interpretation	extremely noisy
24	10 166	33 70	80 14	205 16	1050 4	open 2			good	

TABLE 1: LAYER DEPTHS AND RESISTIVITIES ACCORDING TO THE INTERPRETATION OF THE VES CURVES, WHITE SANDS, NEW MEXICO. --Continued

VES. No.	Layers								Quality of Theoretical Fit	Remarks
	1	2	3	4	5	6	7	8		
25	23 238	70 30	200 105	870 16	open 1.7				very good	
26	35 170	250 45	1200 16	3400 1.7	∞ ∞				good	
27	6 (?) 200(?)	40 18	120 400	2000(?) 14	open < 1.5				satisfactory	
28	18 56	180 80	750 13	3650 4	∞ ∞				very good	
29	18 78	81 115	128 540	1230 125	3300(?) 31(?)	∞ ? ∞ ?			good	terminal branch descending
30	10.5 180	32 120	107 45	240 135	840 18	open 4.5			good	
31	82 100	210 150	260 15	375 150	1200 8	open < 5			satisfactory	field curvehighly distorted
32	-	-	-	-	-	-	-	-	no interpretation	extremely noisy
33	5.2 250	42 31	125 158	1330 21.5	open ~ 1				good	
34	10 250	60 31	160 158	1230 21.5	open ~ 1				satisfactory	
35	-	-	-	-	-	-	-	-	no interpretation	extremely noisy
36	39 25	122 230	980 20	open < 3					satisfactory	lateral effects on field data

TABLE 1: LAYER DEPTHS AND RESISTIVITIES ACCORDING TO THE INTERPRETATION OF THE VES CURVES, WHITE SANDS, NEW MEXICO. --Continued

VES. No.	Layers								Quality of Theoretical Fit	Remarks
	1	2	3	4	5	6	7	8		
37	4.2 52	25 2.6	220 150	open 4.5						Questionable
38	7 170	14 34	205 100	860 20	open 5.5				good	
39	5.2 700	52 140	170 90	1100 19	open 5				very good	
40	23 28	170 140	1100 21	open 5.3					good	
41	16 72	42 175	75 23	145 120	open 18				very good	
42	14 210	28 21	340 96	1000 17.6	2700 5	∞ ∞			very good	
43	11 146	17 730	120 103	400 48	780 16	4200 ? 8 ?	∞ ∞		very good	terminal branch undeveloped
44	22 460	69 190	240 90	460 40	open 11.3				satisfactory	
45	5.6 170	110 69	220 46	550 35	2250 14	open ~ 1			good	
46	18 400	60 80	330 37	1850 16	open ~ 1				good	
47	25 88	65 220	520 32	1850 14	open ~ 1				good	lateral effects near 100 feet AB/2
48	9 26	18 260	44 16	350 42	1400 17	open 3.3			very good	

TABLE 1: LAYER DEPTHS AND RESISTIVITIES ACCORDING TO THE INTERPRETATION OF THE VES CURVES, WHITE SANDS, NEW MEXICO. --Continued

VES. No.	Layers								Quality of Theoretical Fit	Remarks
	1	2	3	4	5	6	7	8		
49	8 190	32 42	73 75	550 9.5	open ~ 1				satisfactory	
50	11 27	350 200	1400 18	open < 1					satisfactory	
51	10 90	400 460	1500 200	open ~ 1					good	
52	11 56	56 30	180 160	1600 18	open ~ 1				satisfactory	
53	-	-	-	-	-	-	-	-	-	equatorial continuation of VES 52
54	-	-	-	-	-	-	-	-	-	equatorial continuation of VES 52
55	-	-	-	-	-	-	-	-	no interpretation	large lateral effects
56	-	-	-	-	-	-	-	-	no interpretation	large lateral effects
57	5 70	75 14	225 290	1675 4.6	open 0.5				satisfactory	very noisy
58	12 46	25 115	104 240	open (but probably thin filled 70 by saline H_2o)					very questionable	lateral effect from AB/2 = 1000 to end of curve
59	10 17.5	34 44	142 84	155 13.7	240 280	open 1			good	
60	21 48	200 73	1250 7.2	2850 1.5	∞ ∞				satisfactory	rising branch undeveloped

TABLE 1: LAYER DEPTHS AND RESISTIVITIES ACCORDING TO THE INTERPRETATION OF THE VES CURVES, WHITE SANDS, NEW MEXICO.--Continued

ES. No.	Layers 1	2	3	4	5	6	7	8	Quality of Theoretical Fit	Remarks
61	290 400	950 160	1800 18	open 7					satisfactory	
62	10 755	60 300	560 500	open 46					good	very noisy data
63	6 140	34 56	70 31	920 9.7	open 0.9				good	
64	-	-	-	-	-	-	-	-	-	extension of VES 26
65	-	-	-	-	-	-	-	-	-	extension of VES 27
66	9.5 30	320 120	1000 30	open ~ 1					satisfactory	very noisy data
67	12 40	40 27	185 150	300 15	385 185	6600 1.2	∞ ∞		-	fitted by aux. curves method
68	17 65	112 90	520 35	1200 10	4400 3.7	∞ ∞			good	
69	110 125	220 200	440 66	1320 35	4100 10	∞ ∞			good	
70	18 350	500 50	960 30	1950 13	∞ ∞				good	
71	30 385	165 57	300 29	2650 13	3100 1	∞ ? ∞ ?			good	
72	124 112	520 35	2300 14	open ~ 1					very good	

TABLE 1: LAYER DEPTHS AND RESISTIVITIES ACCORDING TO THE INTERPRETATION OF THE VES CURVES, WHITE SANDS, NEW MEXICO.-- Continued

VES. No.	Layers								Quality of Theoretical Fit	Remarks
	1	2	3	4	5	6	7	8		
73	40 260	120 75	380 54	820 29	2550 13	∞ ∞			good	
74	20 25	50 2.2	55 150	95 2.2	105 150	open 2.2			satisfactory	
75	22 197	64 38	1300 76	∞ ∞					very good	
76	10 225	40 92	140 40	250 75	∞ ∞				good	
77	10 145	90 or 165 56	∞ ∞						satisfactory	basement depth uncertain due to lateral effect at AB/2 = 120
78	20 27	85 18	370 7.2	open ~ 0.55					good	
79	14 103	225 19.3	245 108	710 9.6	open ~ 0.55				very good	
80	12 93	68 18.5	128 108	780 11.2	open ~ 0.55				good	
81	18 130	86 13	123 150	200 3.7	243 150	open ~ 0.5			questionable	large lateral effects
82	20 12.5	80 120	140 30	220 280	open ~ 1				satisfactory	distorted beyond. AB/2 = 2000
83	5.6 315	68 61.5	95 525	420 37	1100 12.5	3300 5.2	∞ ∞		very good	rising branch undeveloped
84	10 800	250 11	open 1.7						questionable	curve highly distorted

TABLE 1: LAYER DEPTHS AND RESISTIVITIES ACCORDING TO THE INTERPRETATION OF THE VES CURVES, WHITE SANDS, NEW MEXICO.-- Continued

VES. No.	Layers								Quality of Theoretical Fit	Remarks
	1	2	3	4	5	6	7	8		
85	68 22.5	140 470	138 11	open ~ 0.5					satisfactory	

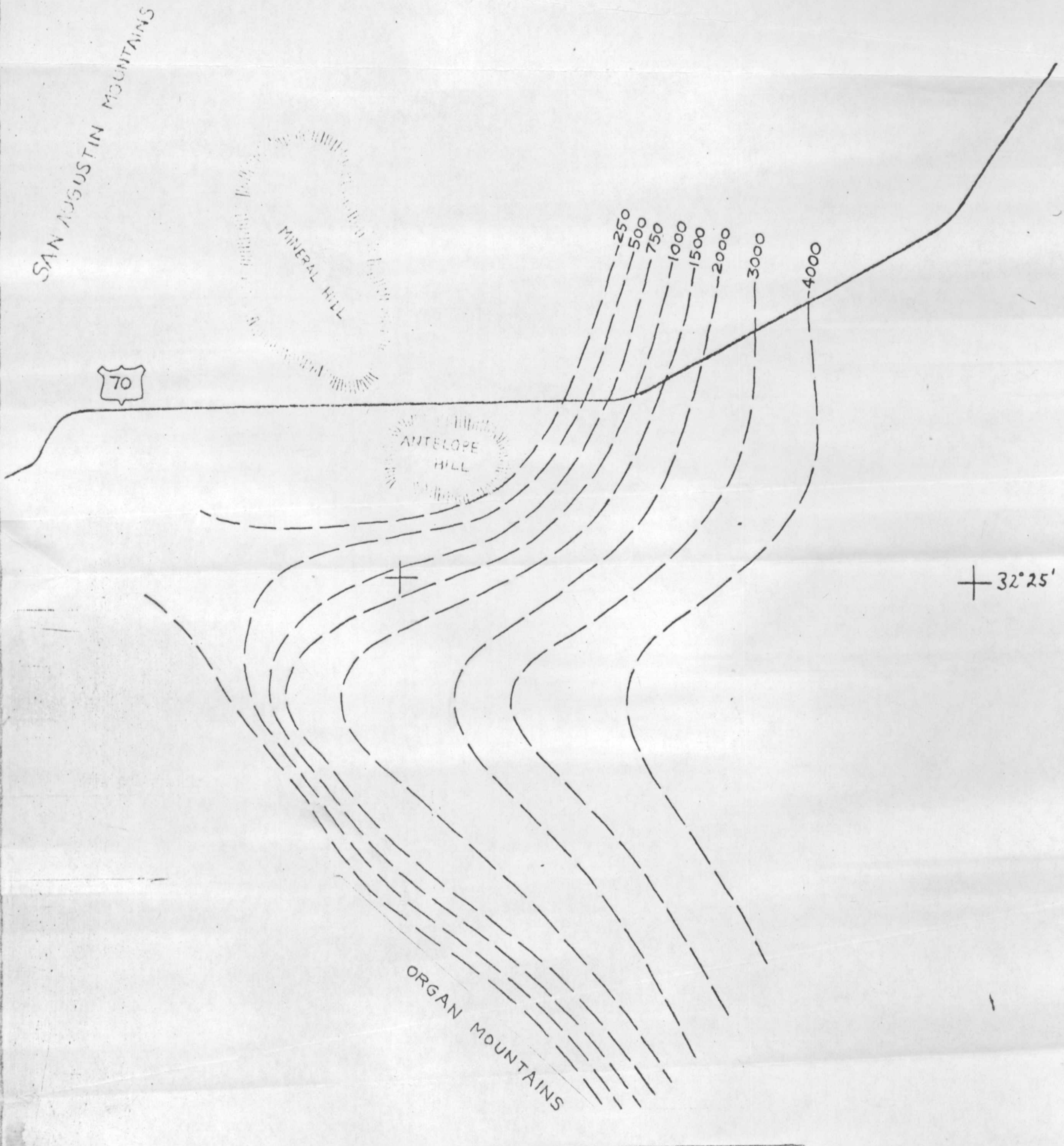

FIGURE 16.

APPROXIMATE THICKNESS, IN FEET, OF THE BOLSON DEPOSITS IN THE HEADQUARTERS AREA, WHITE SANDS MISSILE RANGE, NEW MEXICO

1 ½ 0 1 2 3 4 MILES

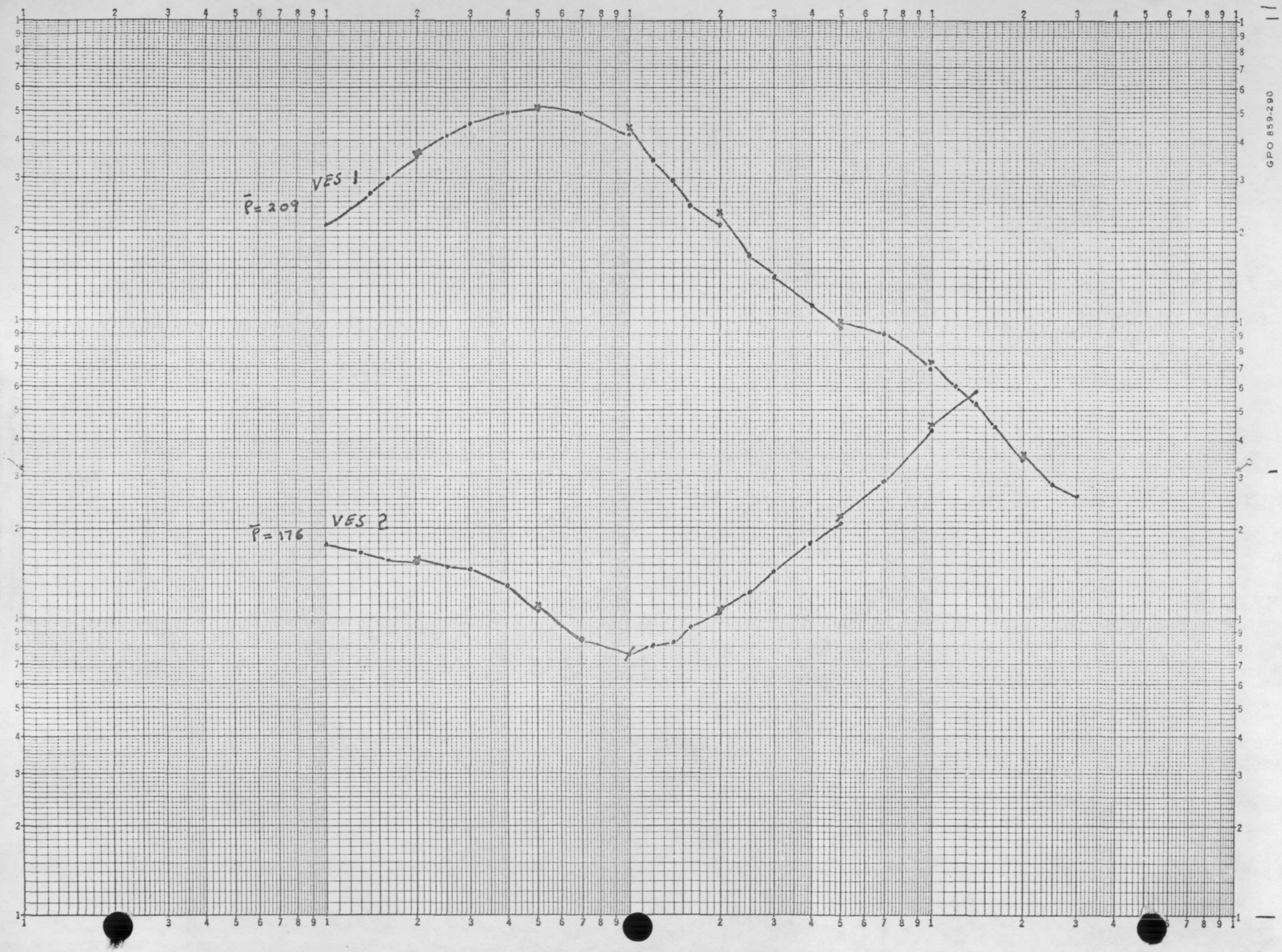

VES 1
ρ̄ = 209
VES 2
ρ̄ = 176
GPO 859-290

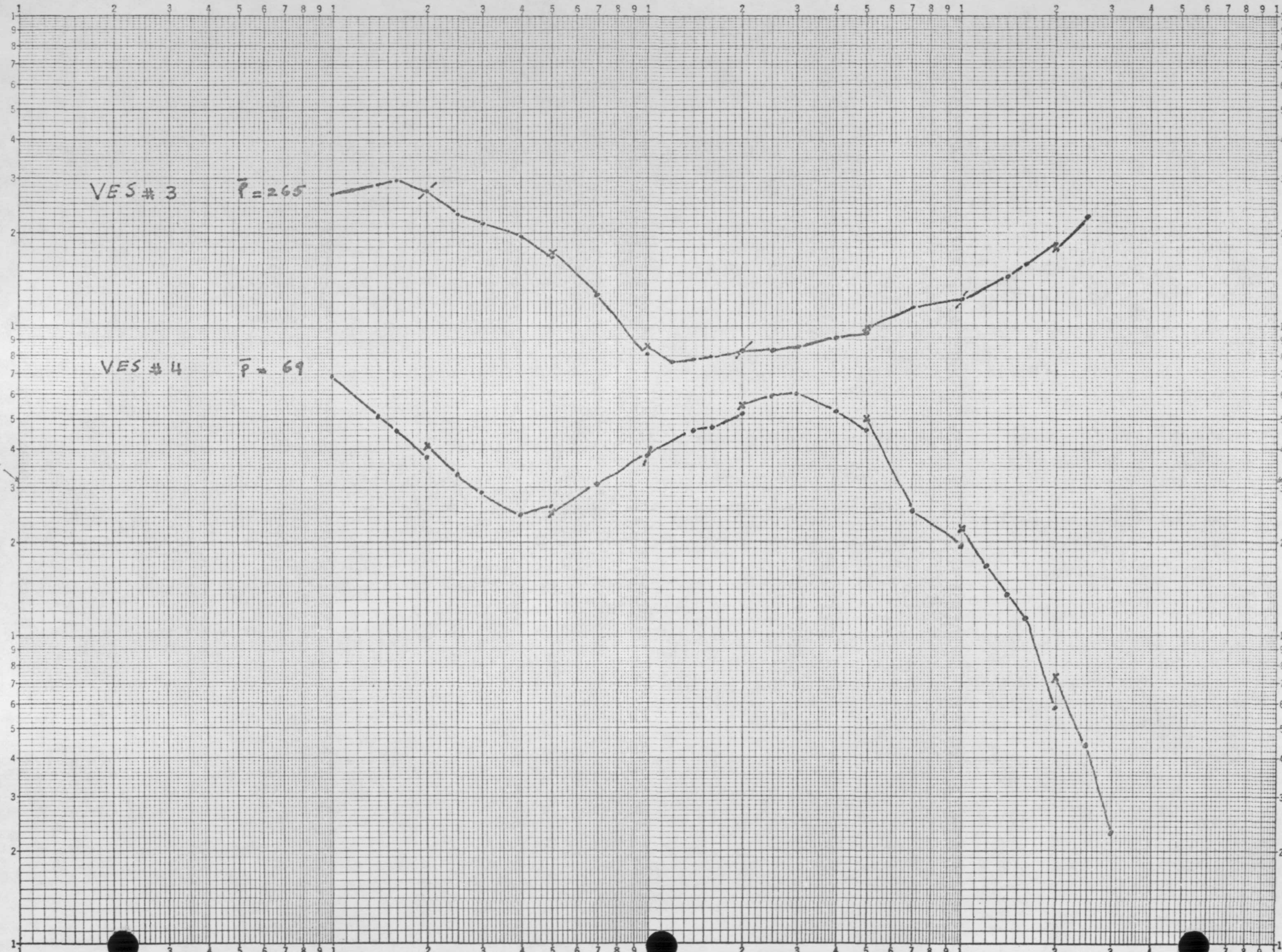
VES # 3
$\bar{\rho}$ = 265
VES # 4
$\bar{\rho}$ = 69
GPO 859-290

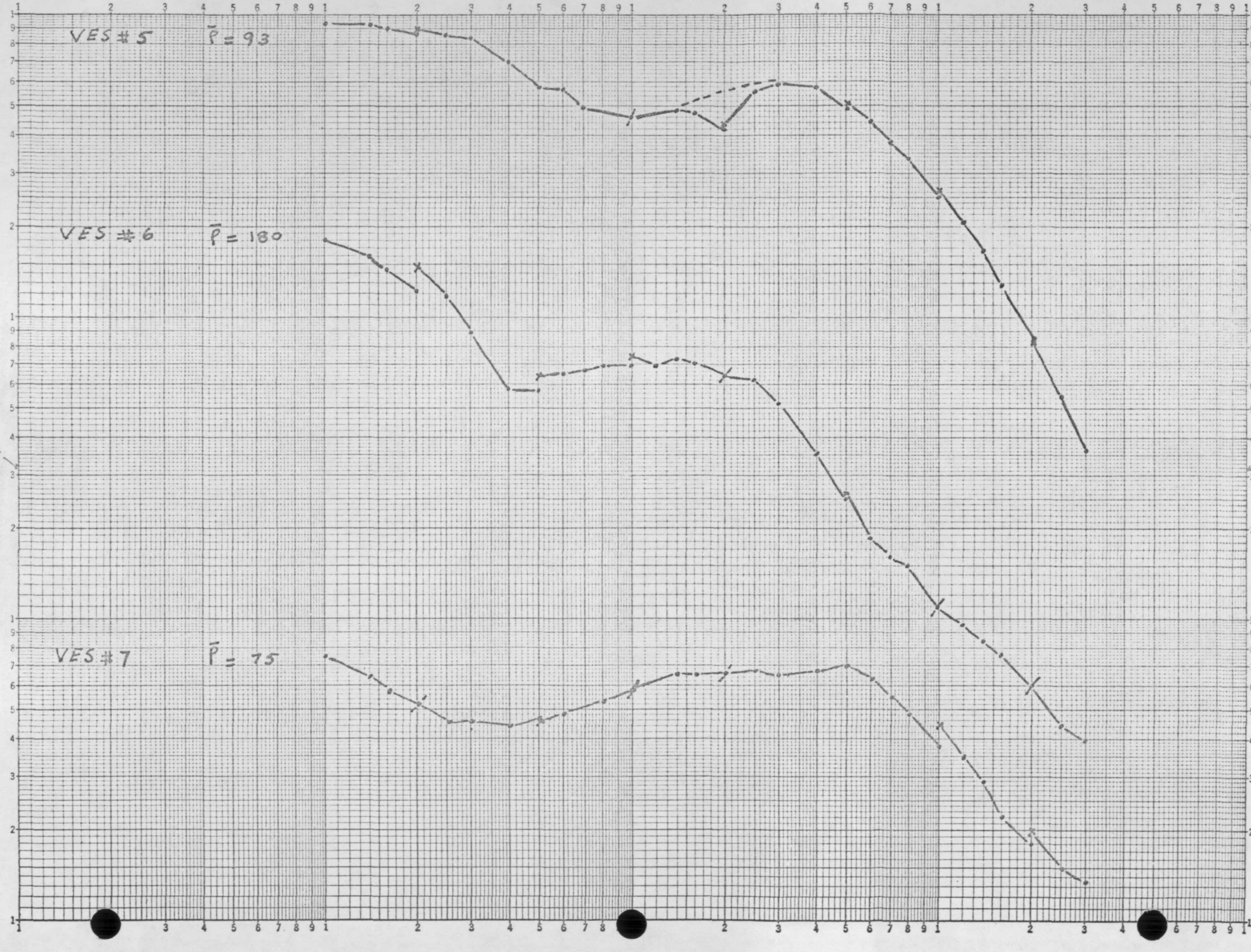
VES #5
ρ̄ = 93
VES #6
ρ̄ = 180
VES #7
ρ̄ = 75
GPO 859-290
13

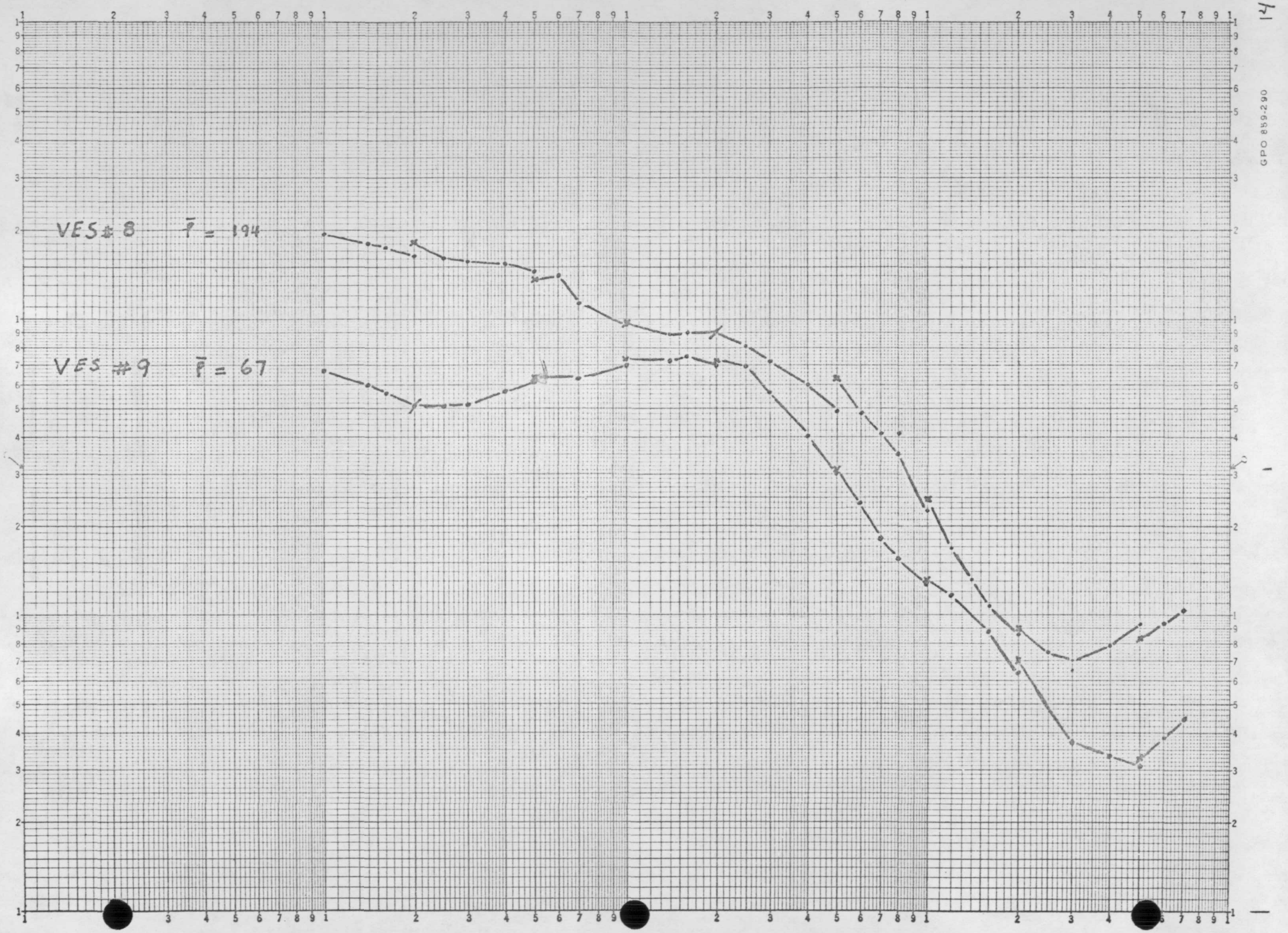
VES # 8 $\bar{\rho}$ = 194
VES #9 $\bar{\rho}$ = 67
GPO 859-290
14

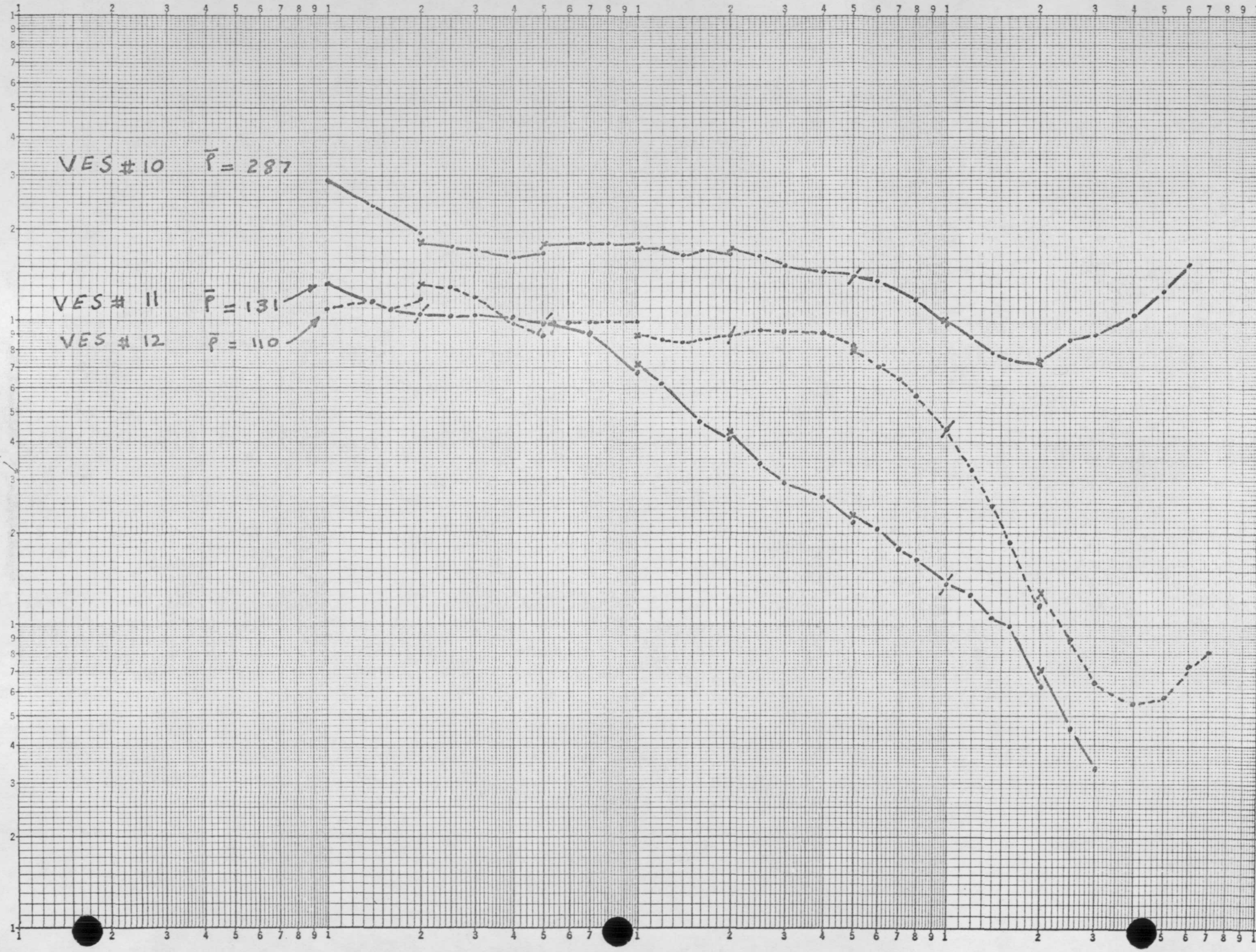

GPO 859-290

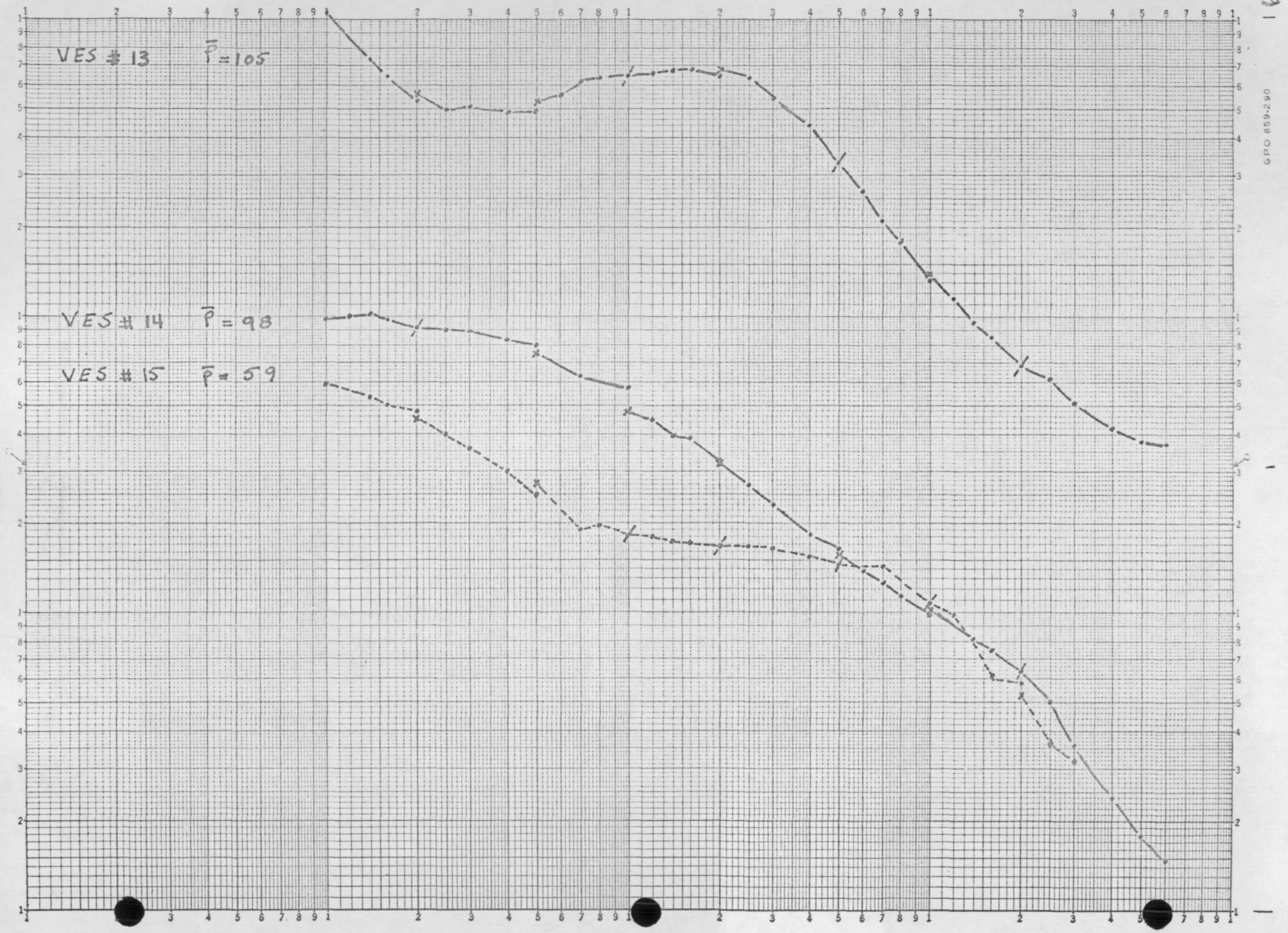

VES # 13 $\bar{\rho}$ = 105
VES # 14 $\bar{\rho}$ = 98
VES # 15 $\bar{\rho}$ = 59
GPO 859-290

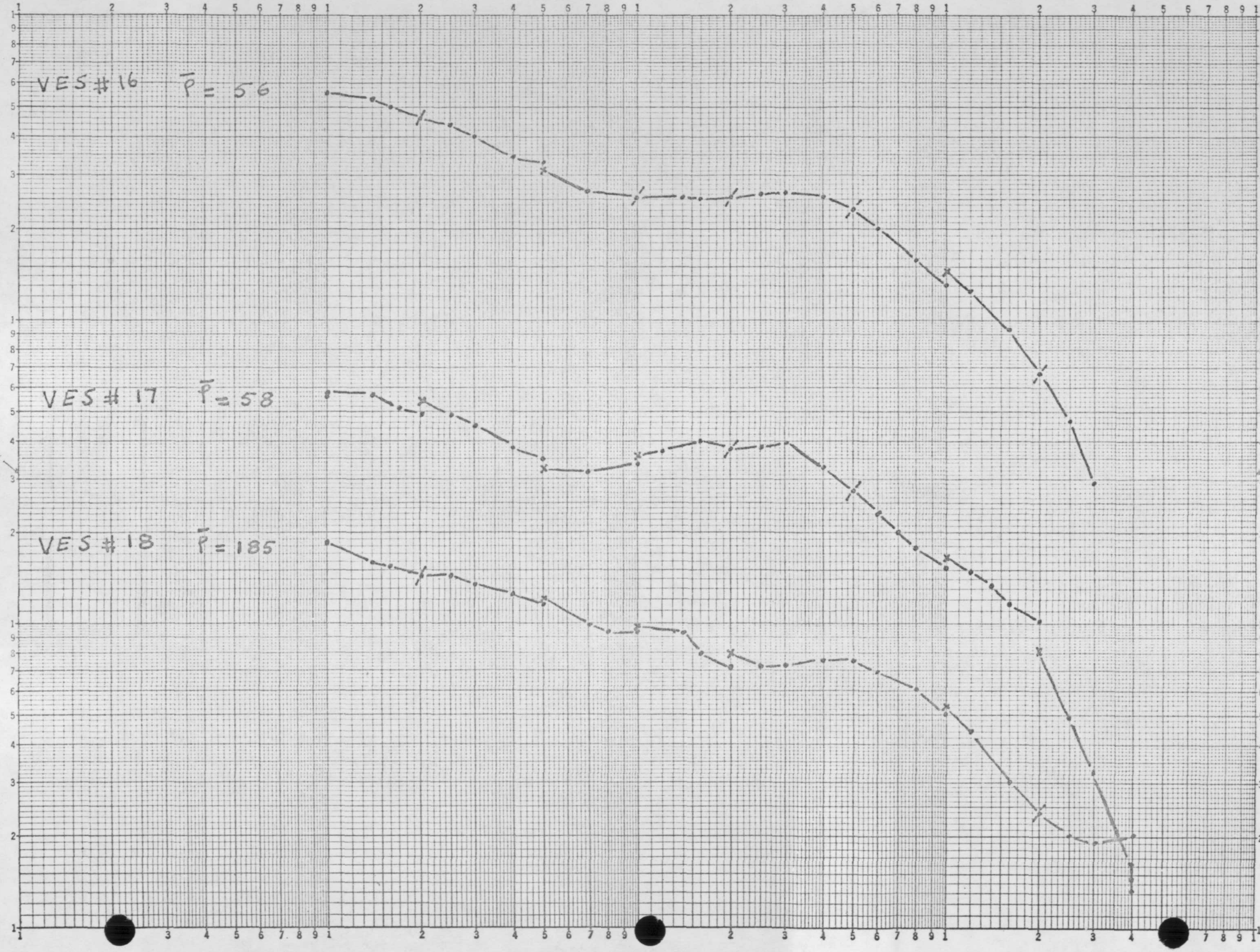
VES # 16 $\bar{\rho}$ = 56
VES # 17 $\bar{\rho}$ = 58
VES # 18 $\bar{\rho}$ = 185

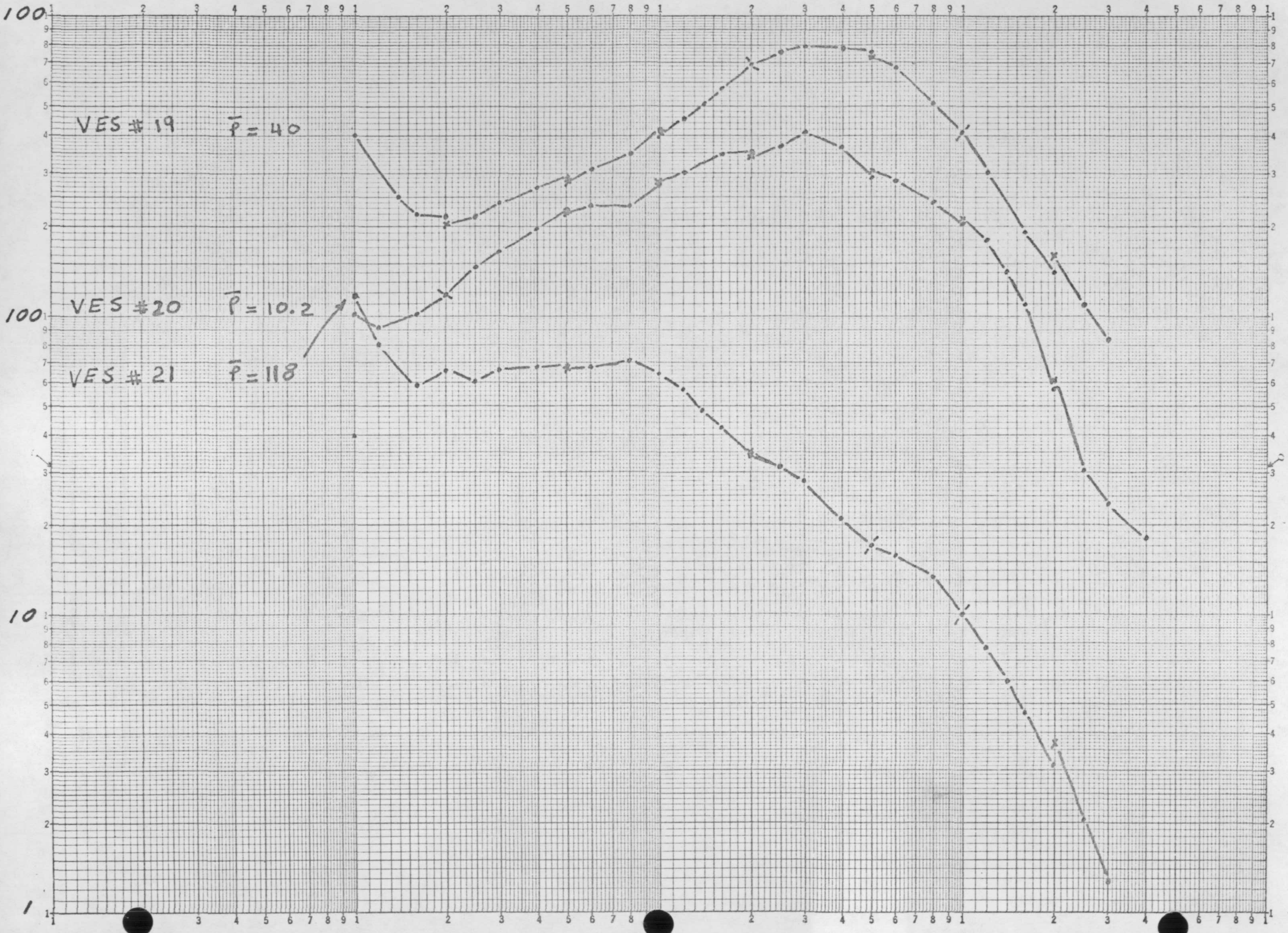
VES # 19 $\bar{\rho}$ = 40
VES # 20 $\bar{\rho}$ = 10.2
VES # 21 $\bar{\rho}$ = 118
100
100
10
1

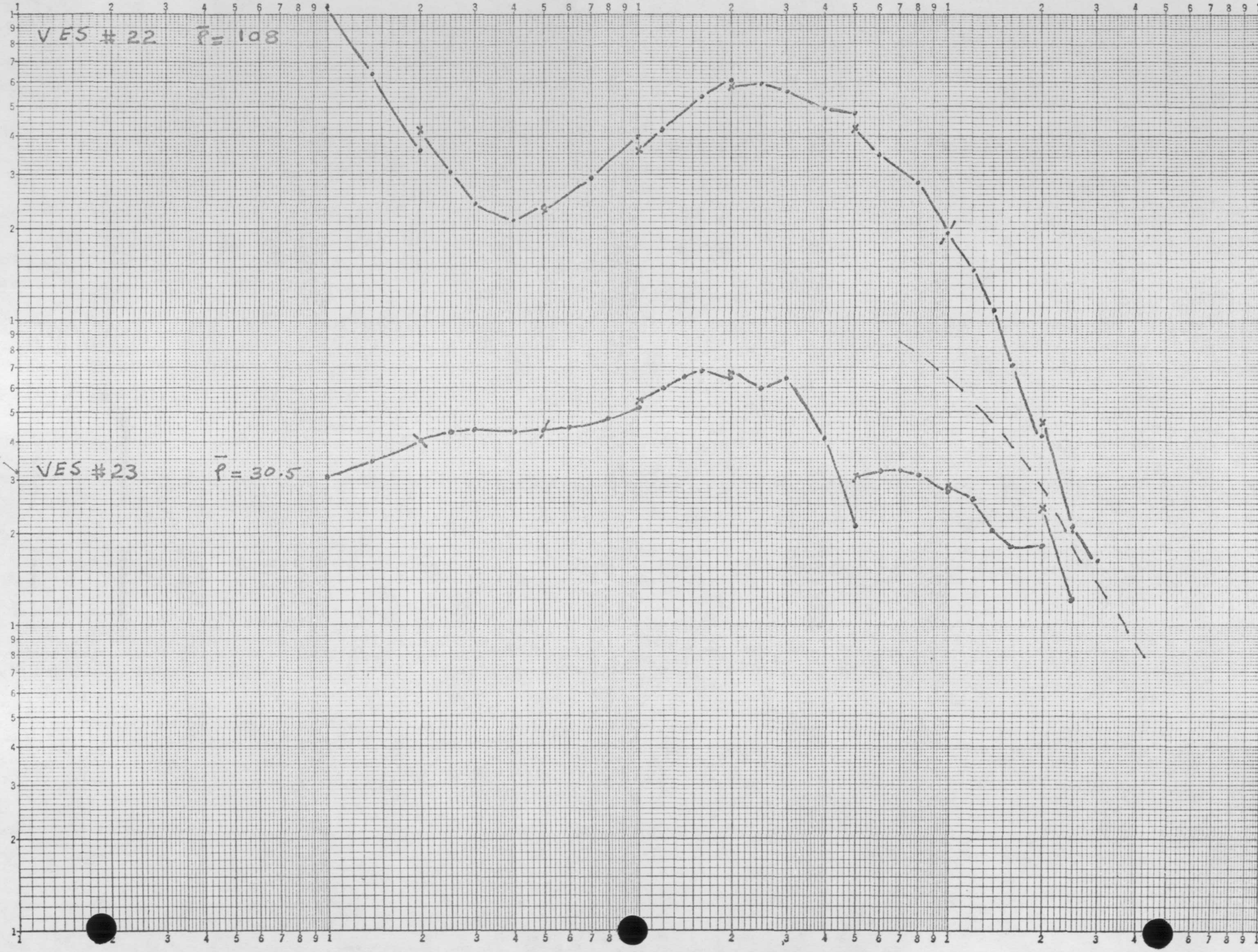

VES # 22 $\bar{\rho}$ = 108
VES # 23 $\bar{\rho}$ = 30.5
GPO 859-290

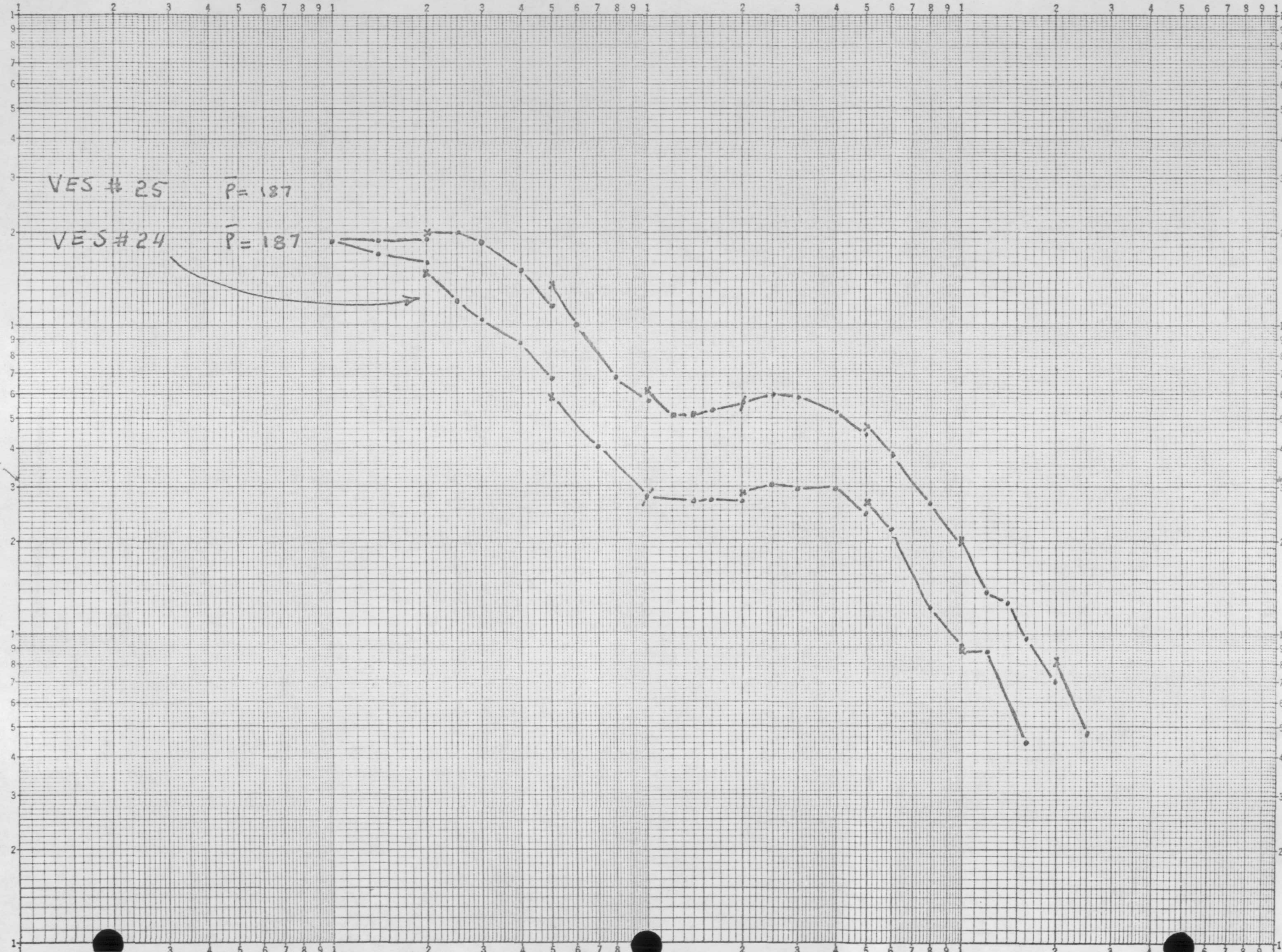
VES # 25 $\bar{\rho}$ = 187
VES #24 $\bar{\rho}$ = 187

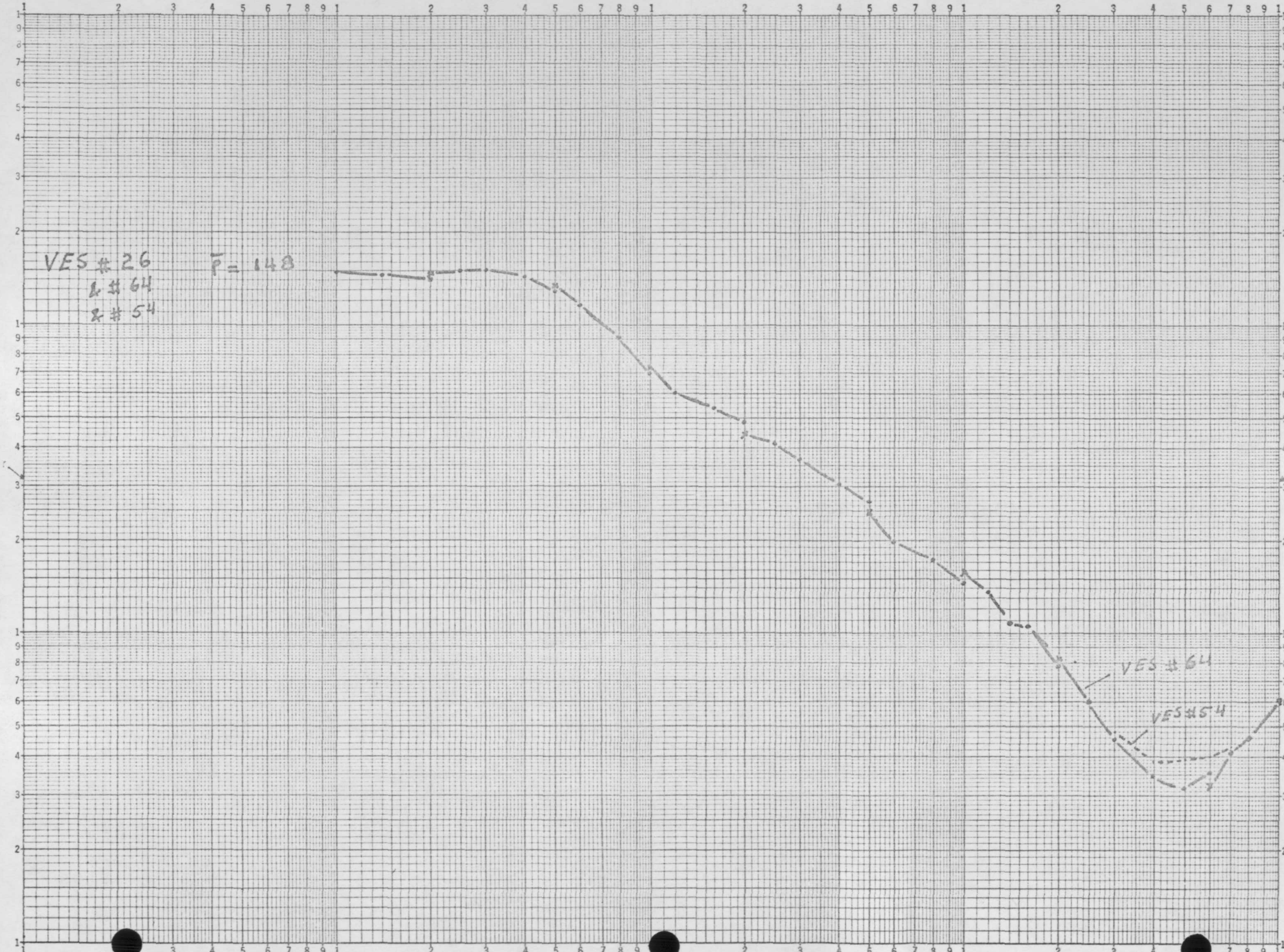

VES # 26
& # 64
& # 54
ρ̄ = 148
VES # 64
VES#54
GPO 859-290

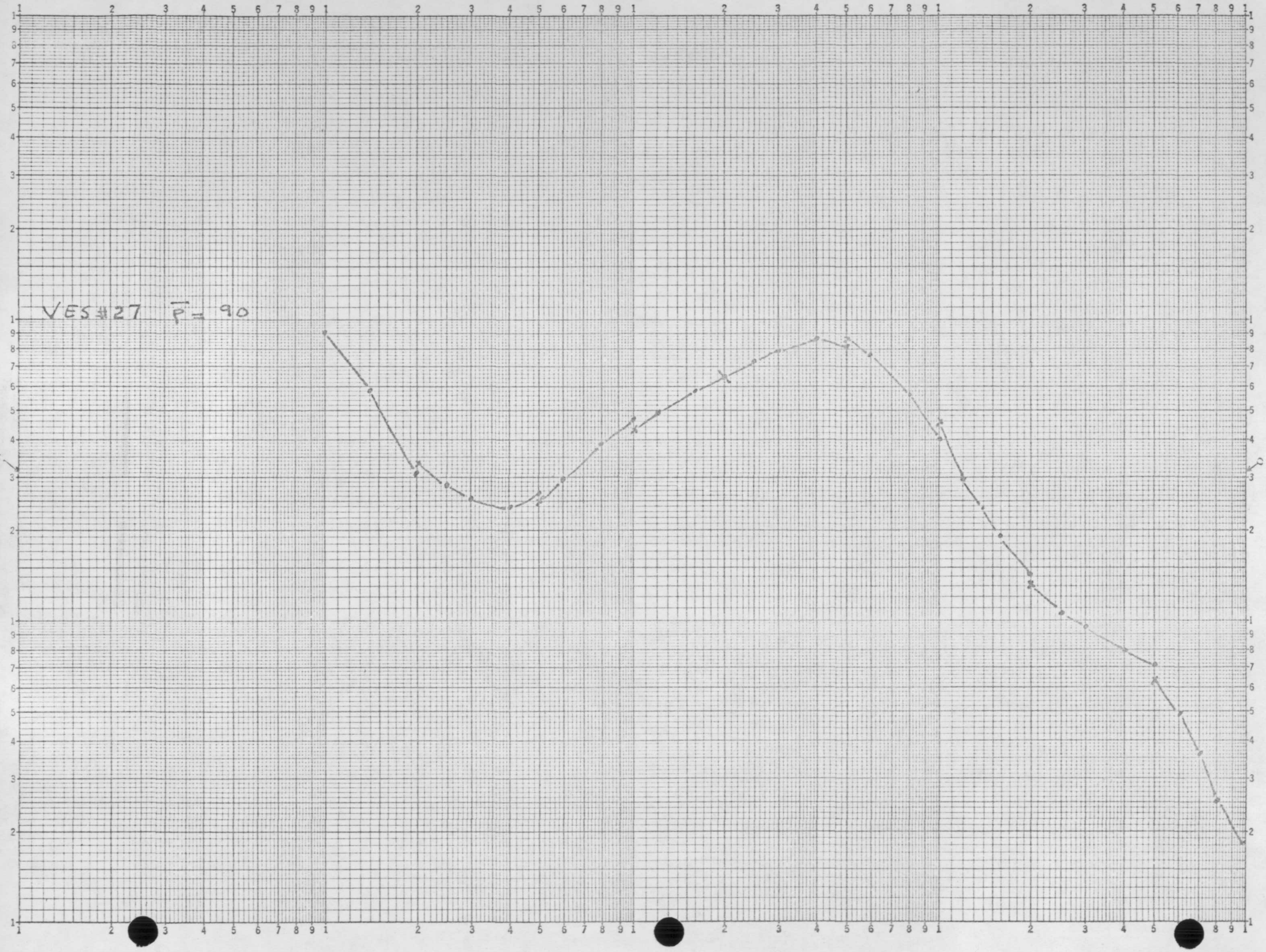
VES #27 ρ̄ = 90

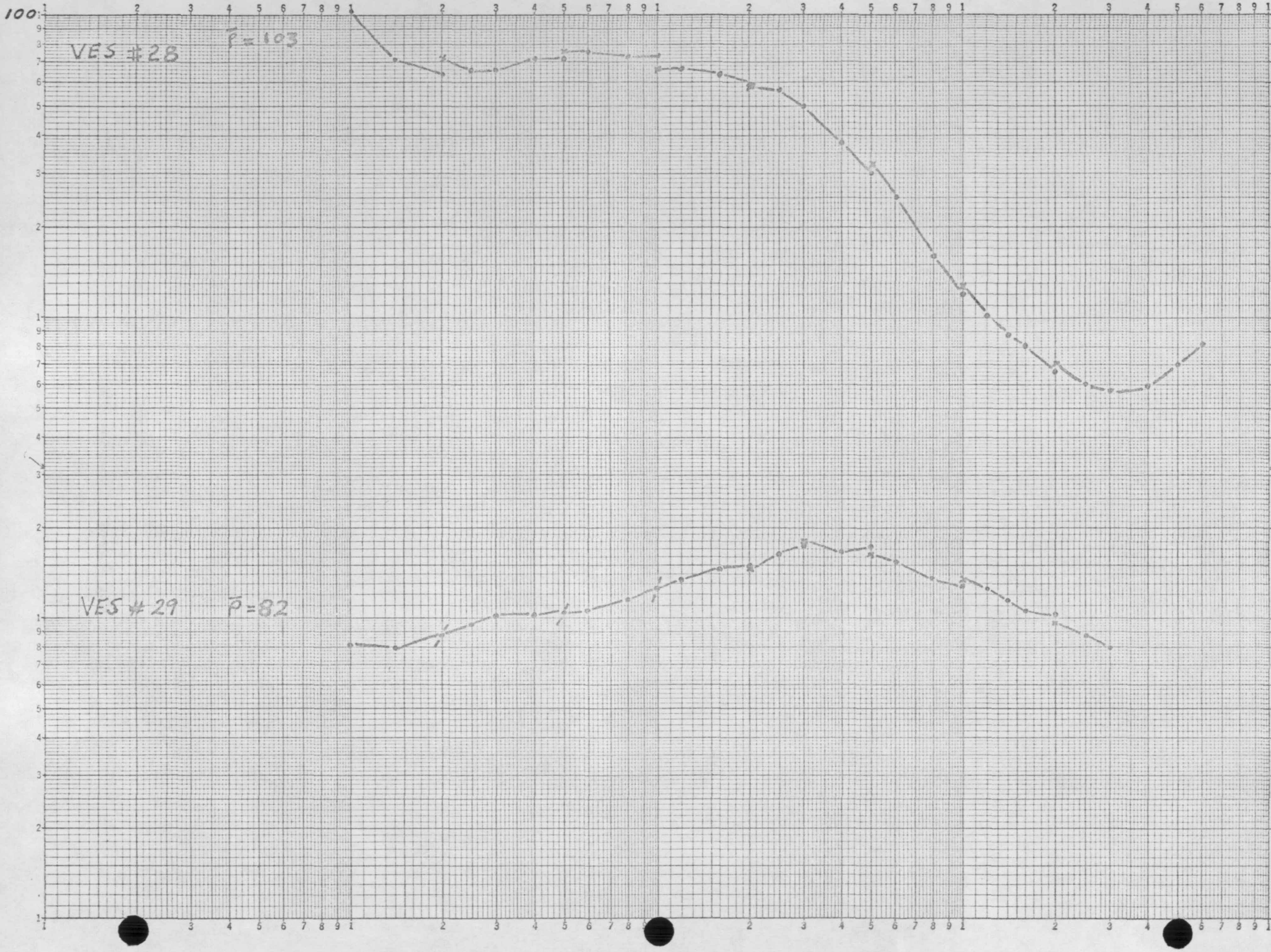
100
VES #28
ρ̄ = 103
VES #29
ρ̄ = 82

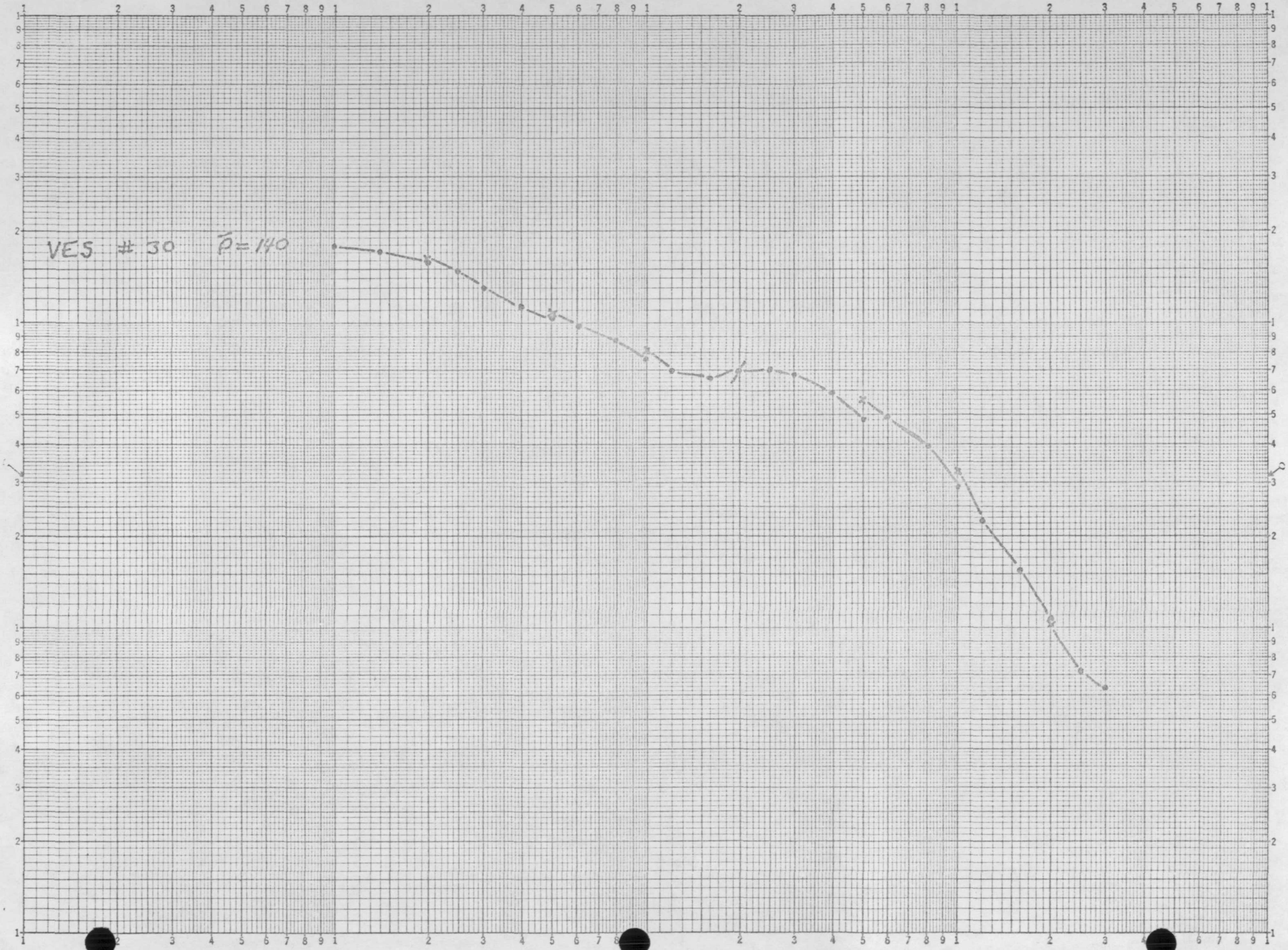
VES # 30 ρ̄=140

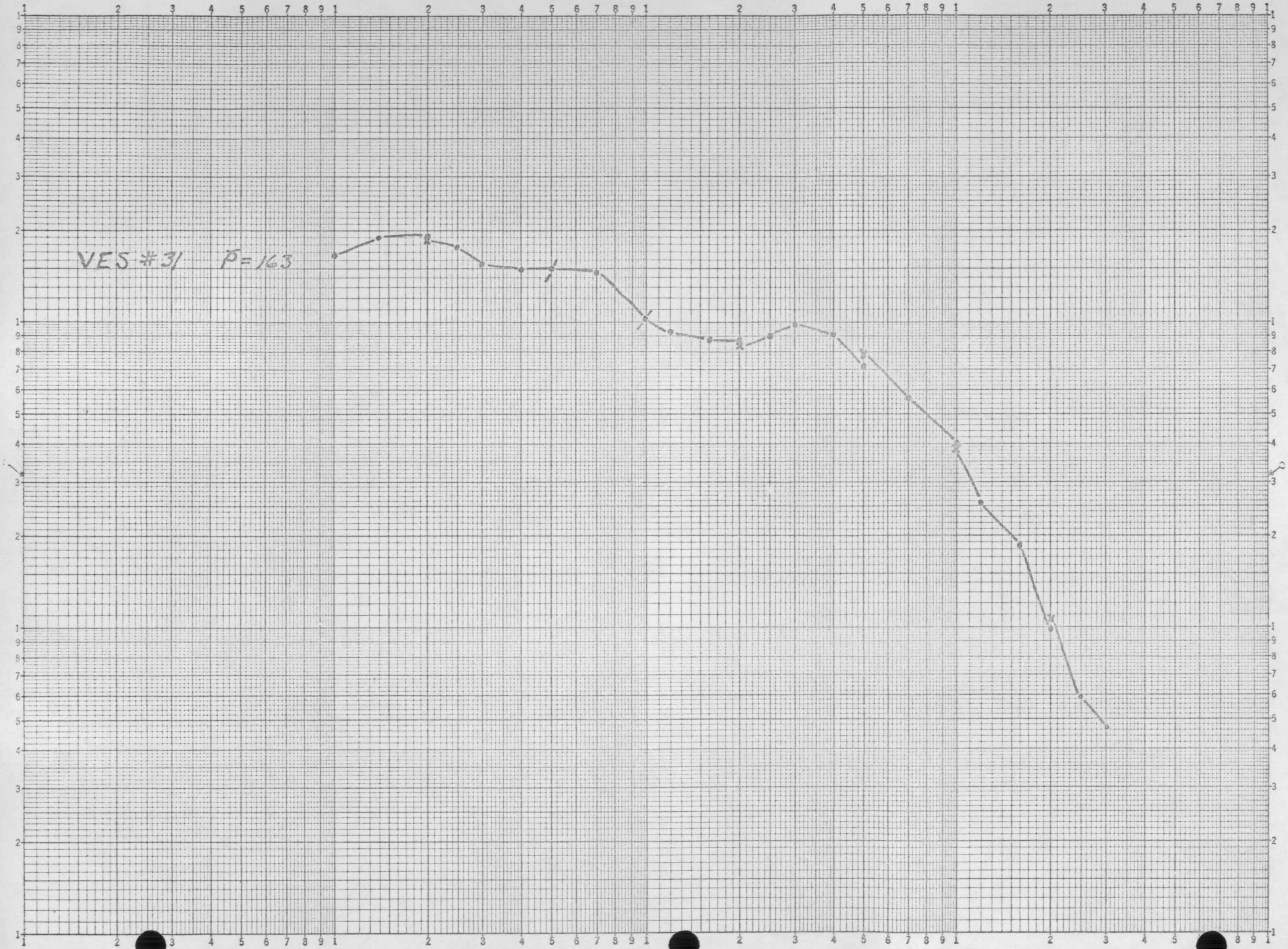
VES #31 $\bar{\rho}$=163

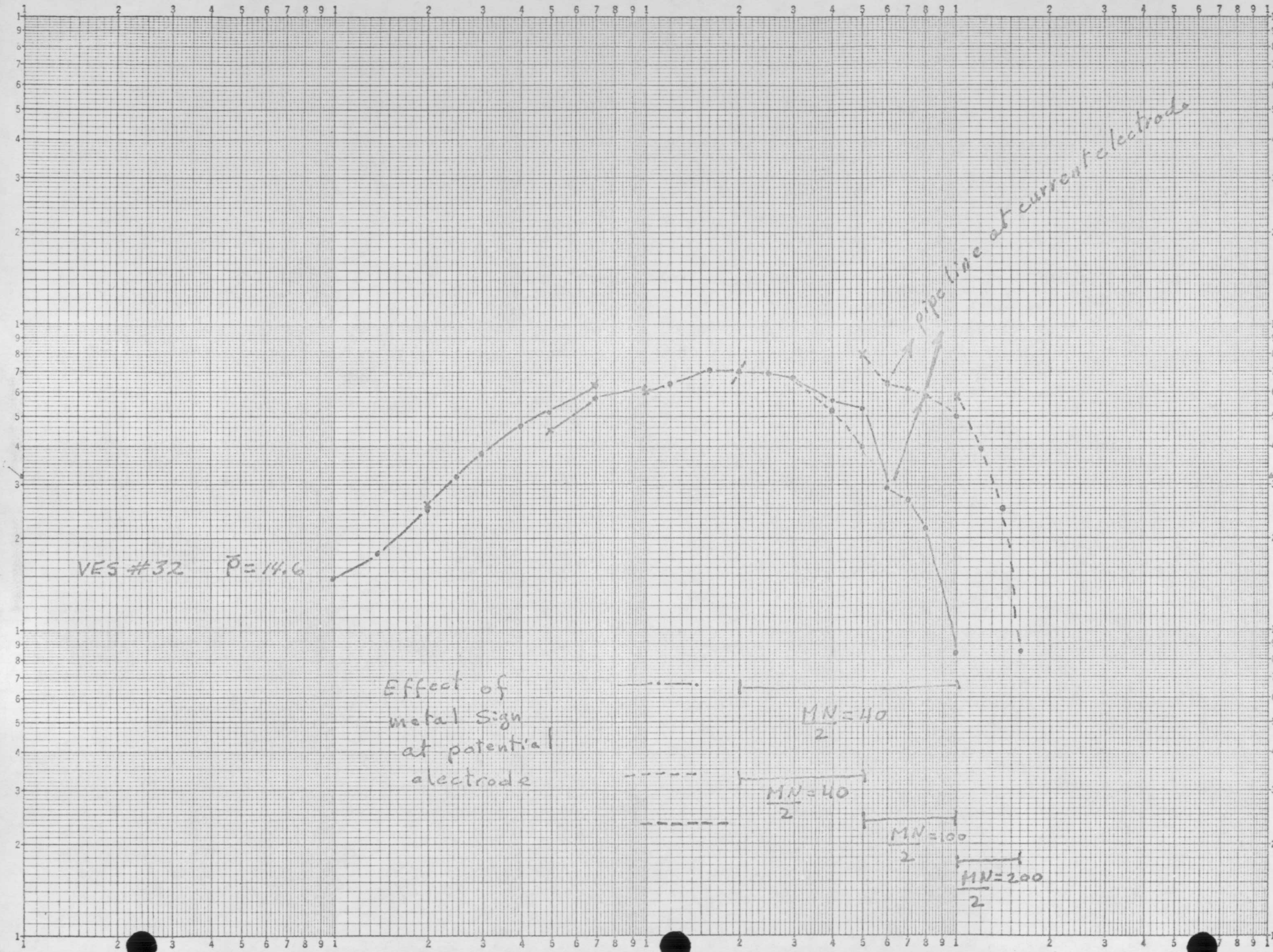

VES #32 ρ̄ = 14.6
pipe line at current electrode
Effect of metal sign at potential electrode
MN/2 = 40
MN/2 = 40
MN/2 = 100
MN/2 = 200

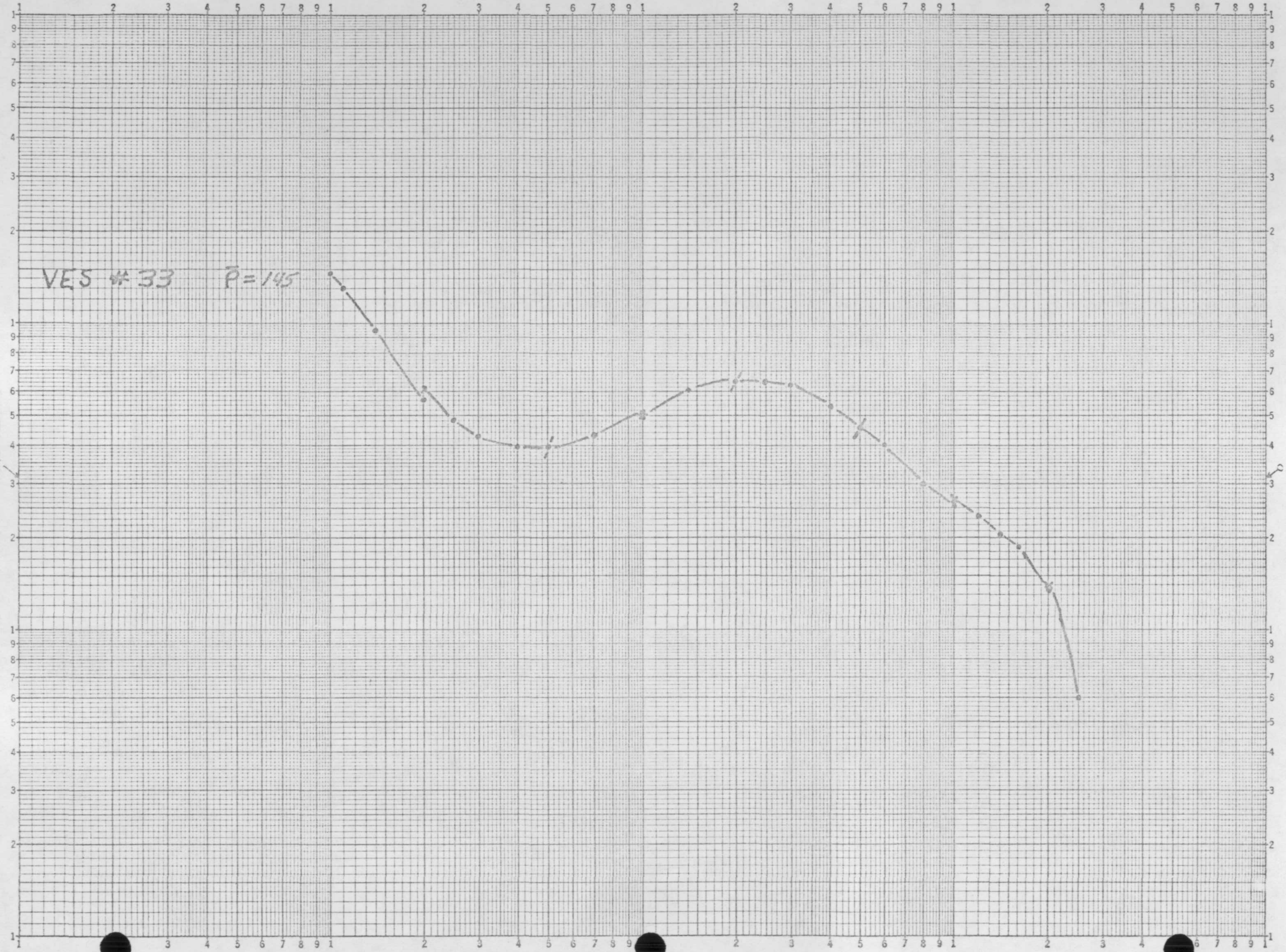

117

GPO 859-290

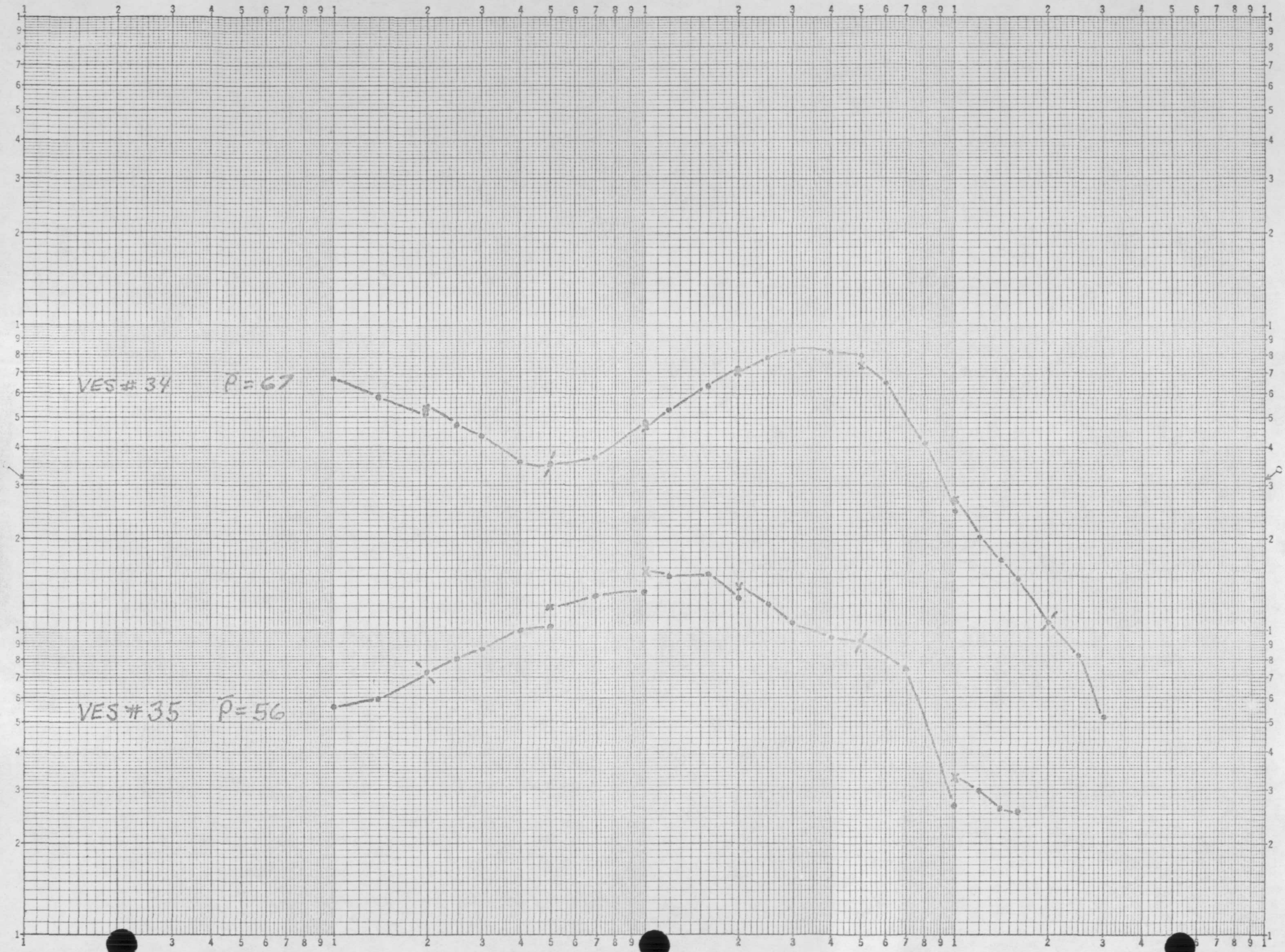
VES # 34 ρ = 67
VES # 35 ρ̄ = 56

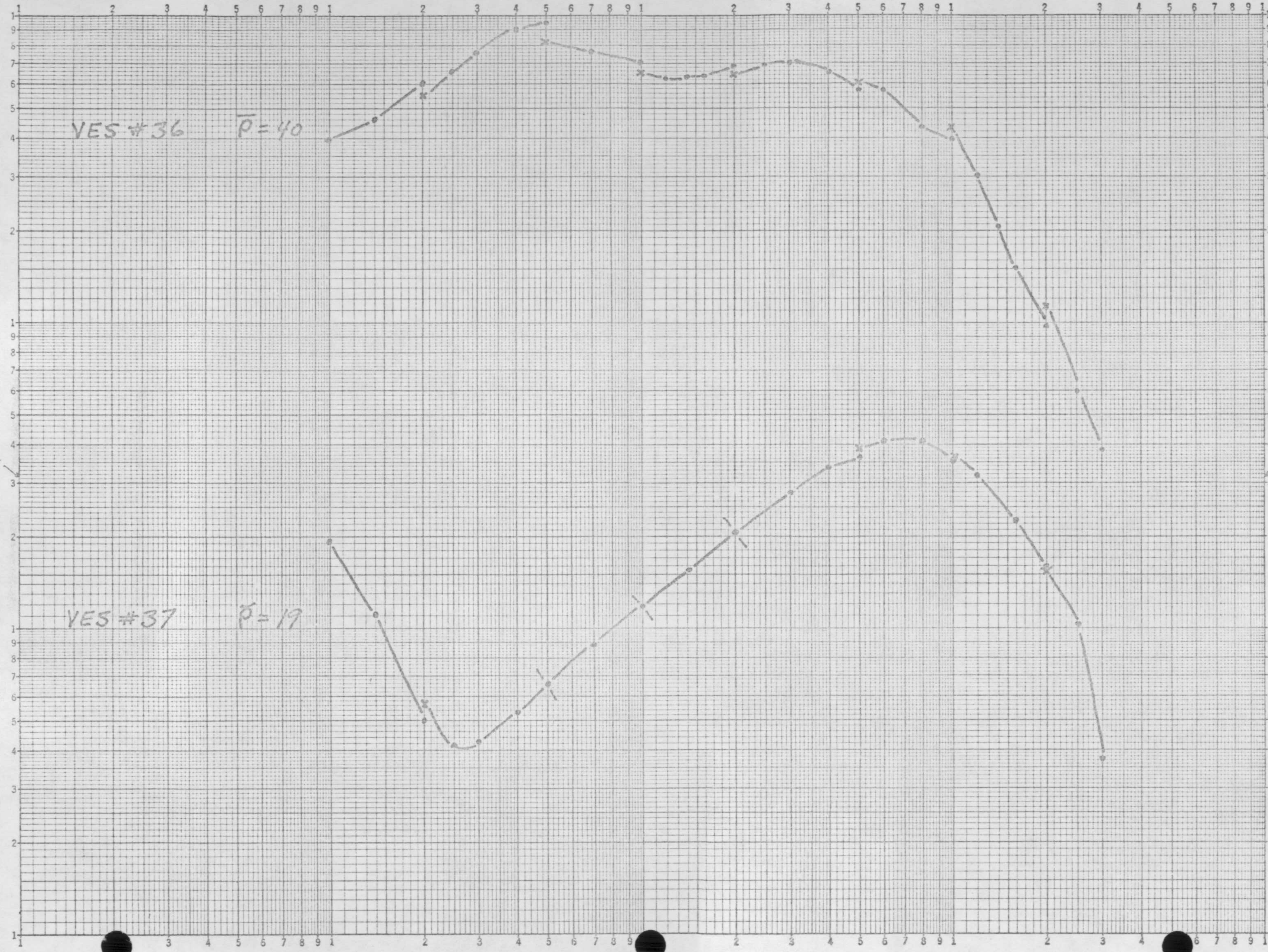

119

12D

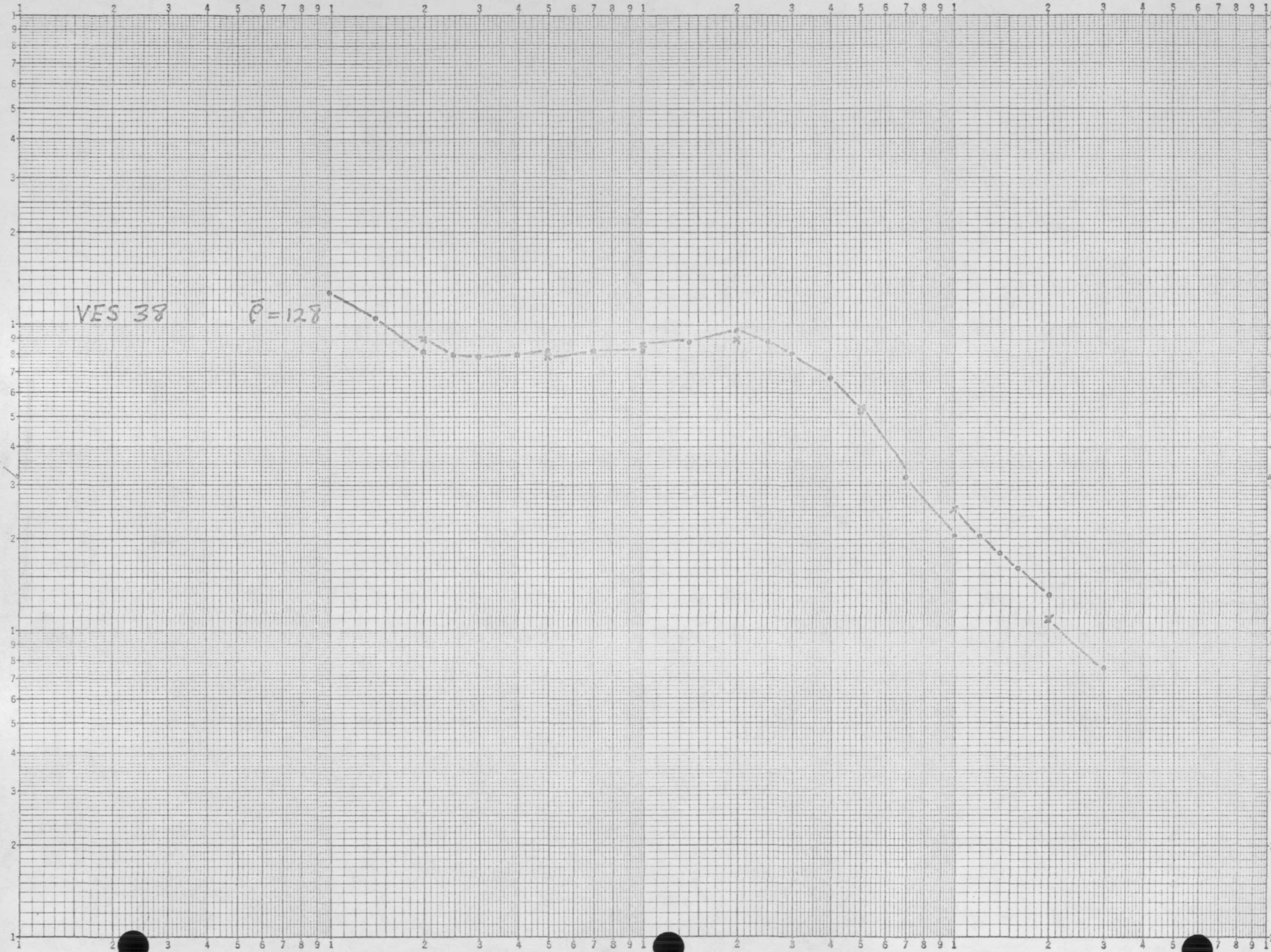

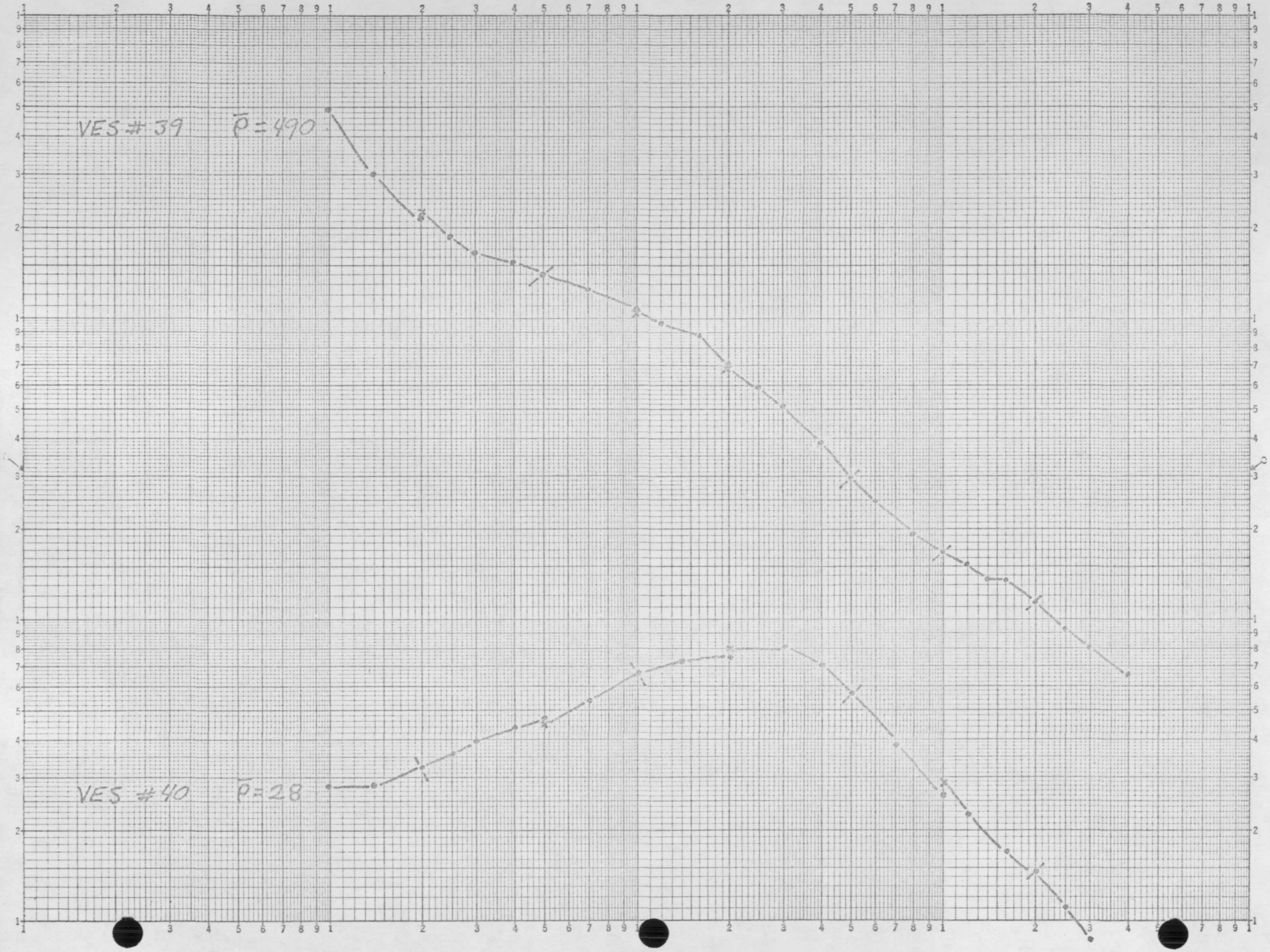
VES # 39 $\bar{\rho}$ = 490
VES # 40 $\bar{\rho}$ = 28
GPO 859-290

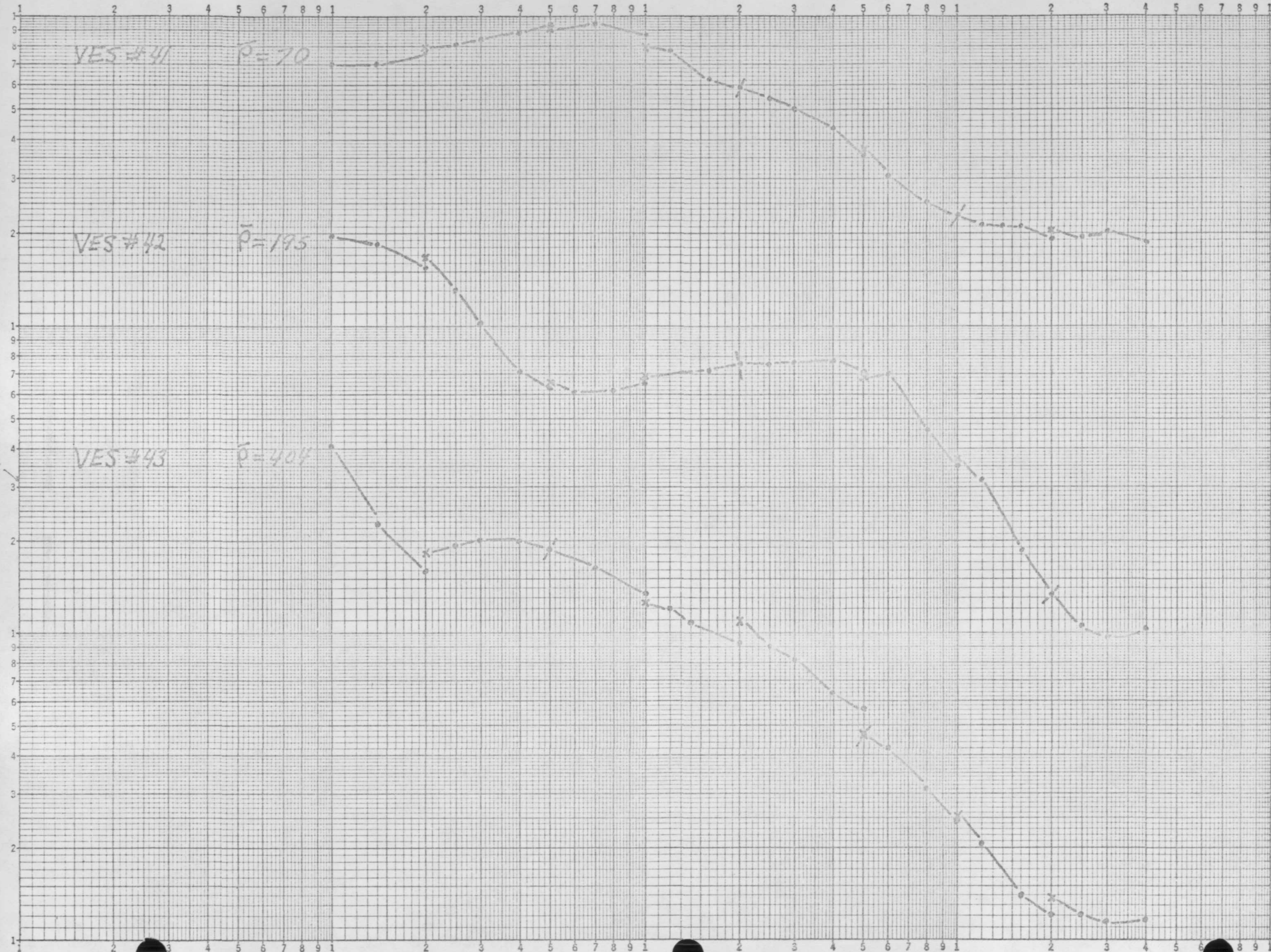
VES #41
ρ̄ = 70
VES #42
ρ̄ = 195
VES #43
ρ̄ = 404

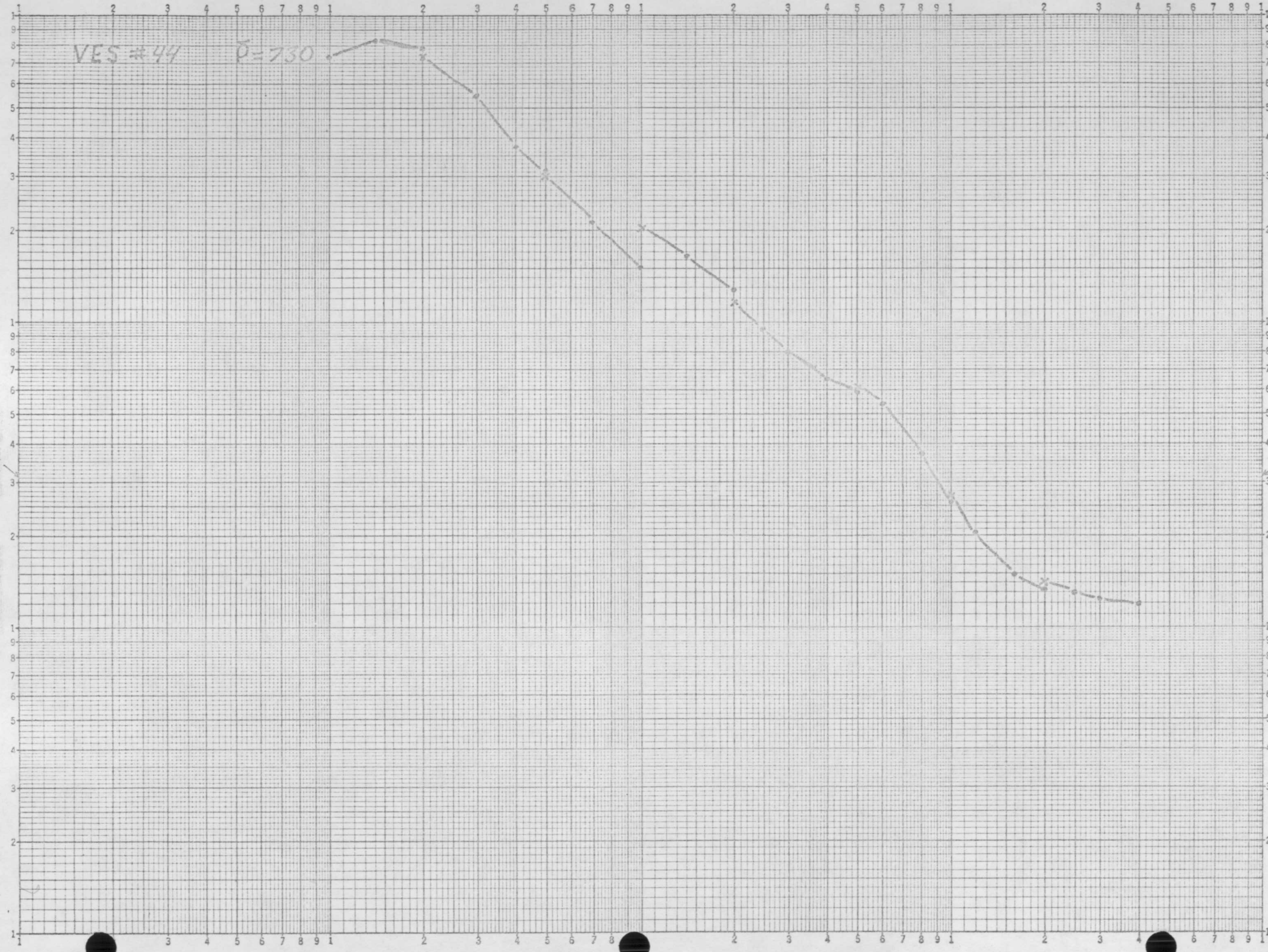
VES #44
ρ̄=730
GPO 859-290
123

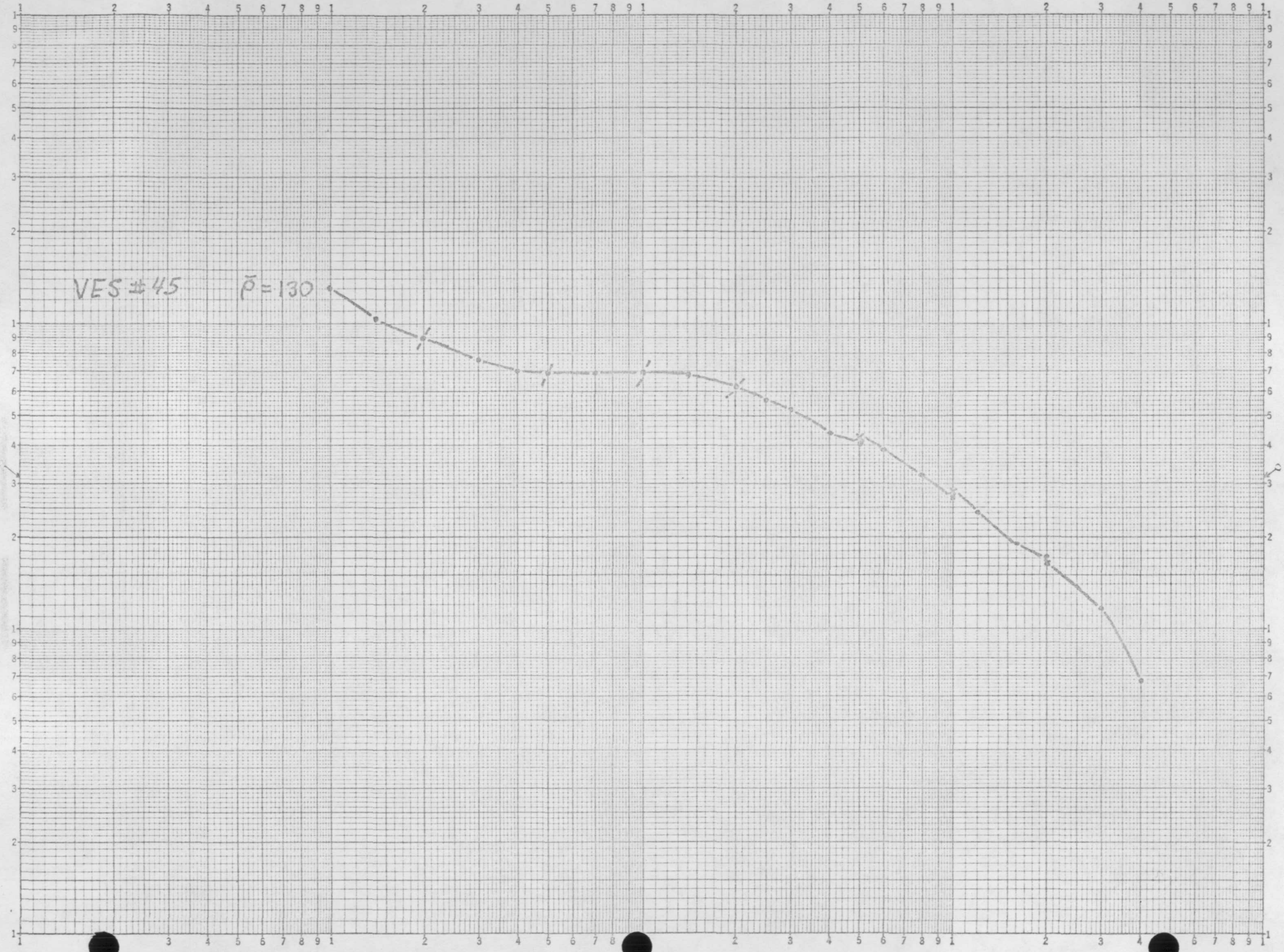

GPO 859-290

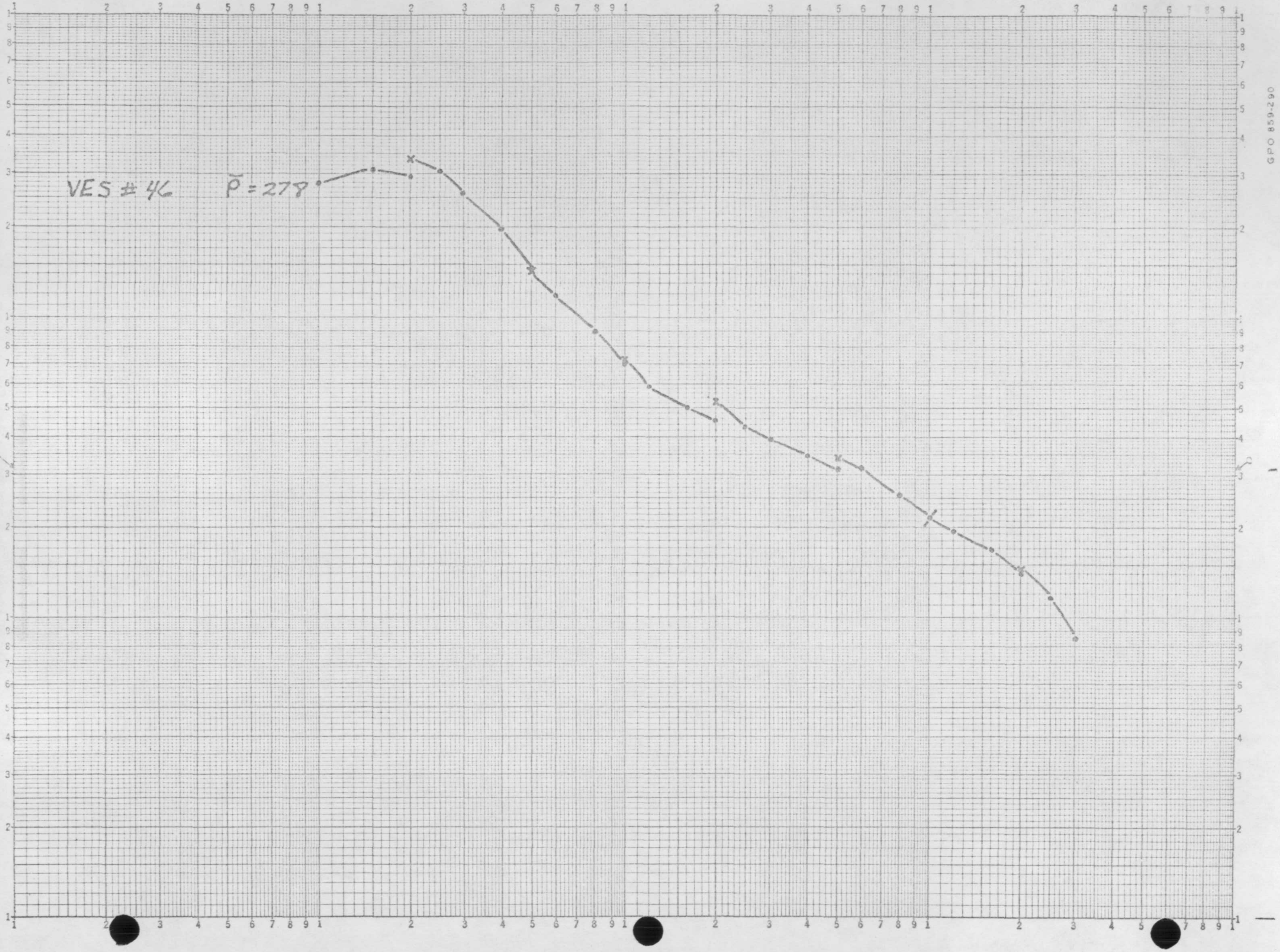
VES # 46
$\tilde{P}$ = 278
GPO 859-290

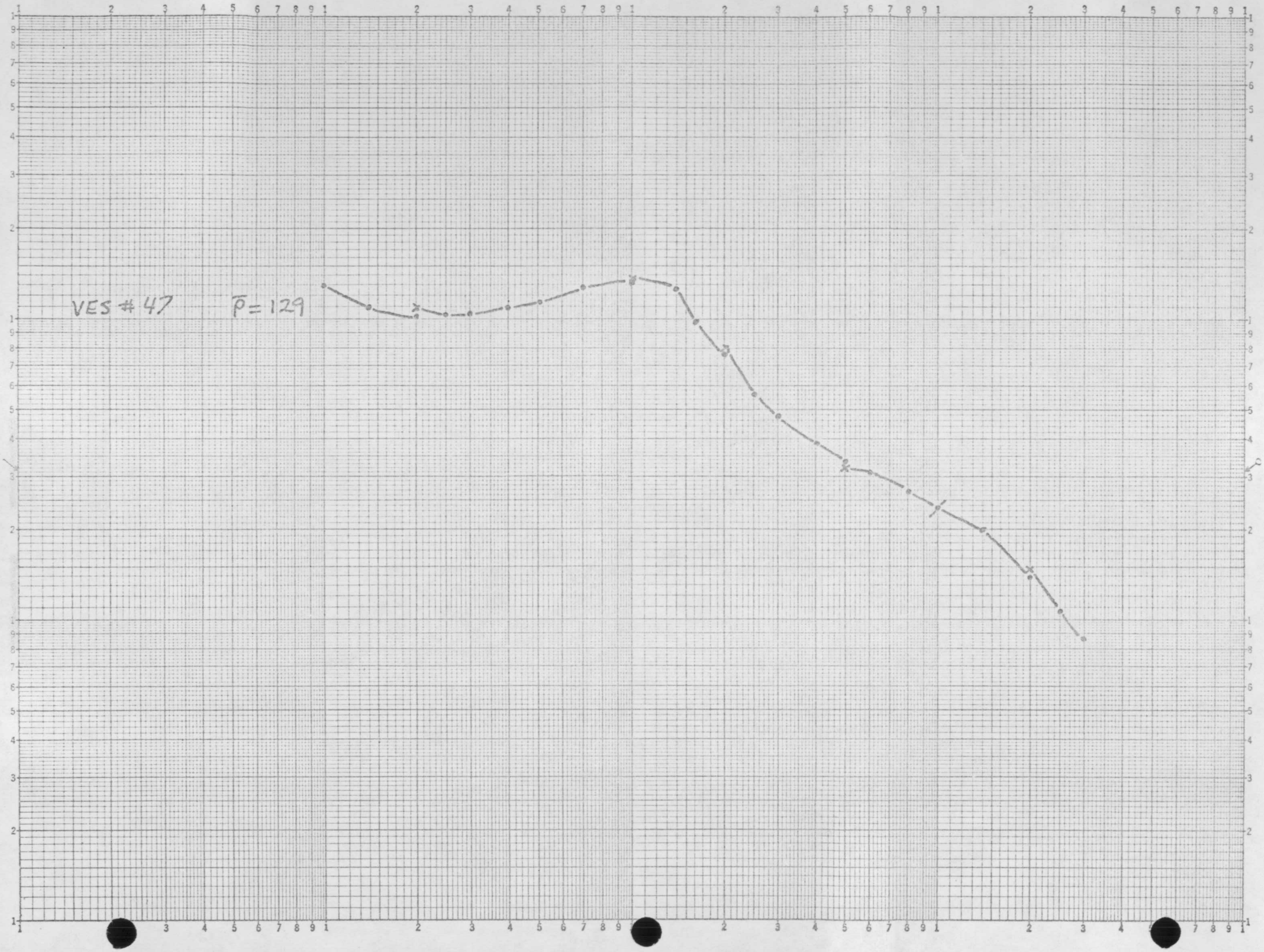

12b

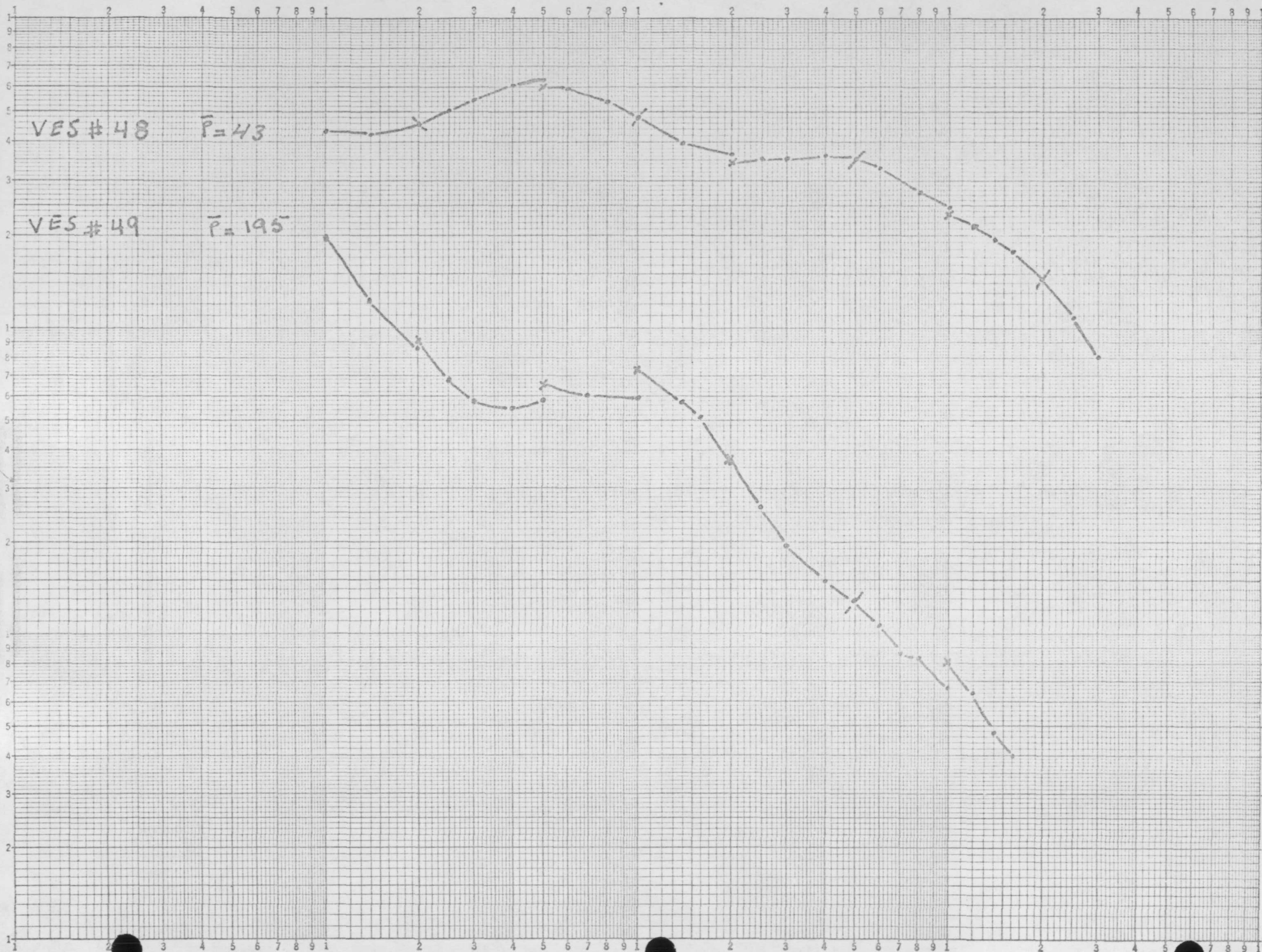

GPO 859-290

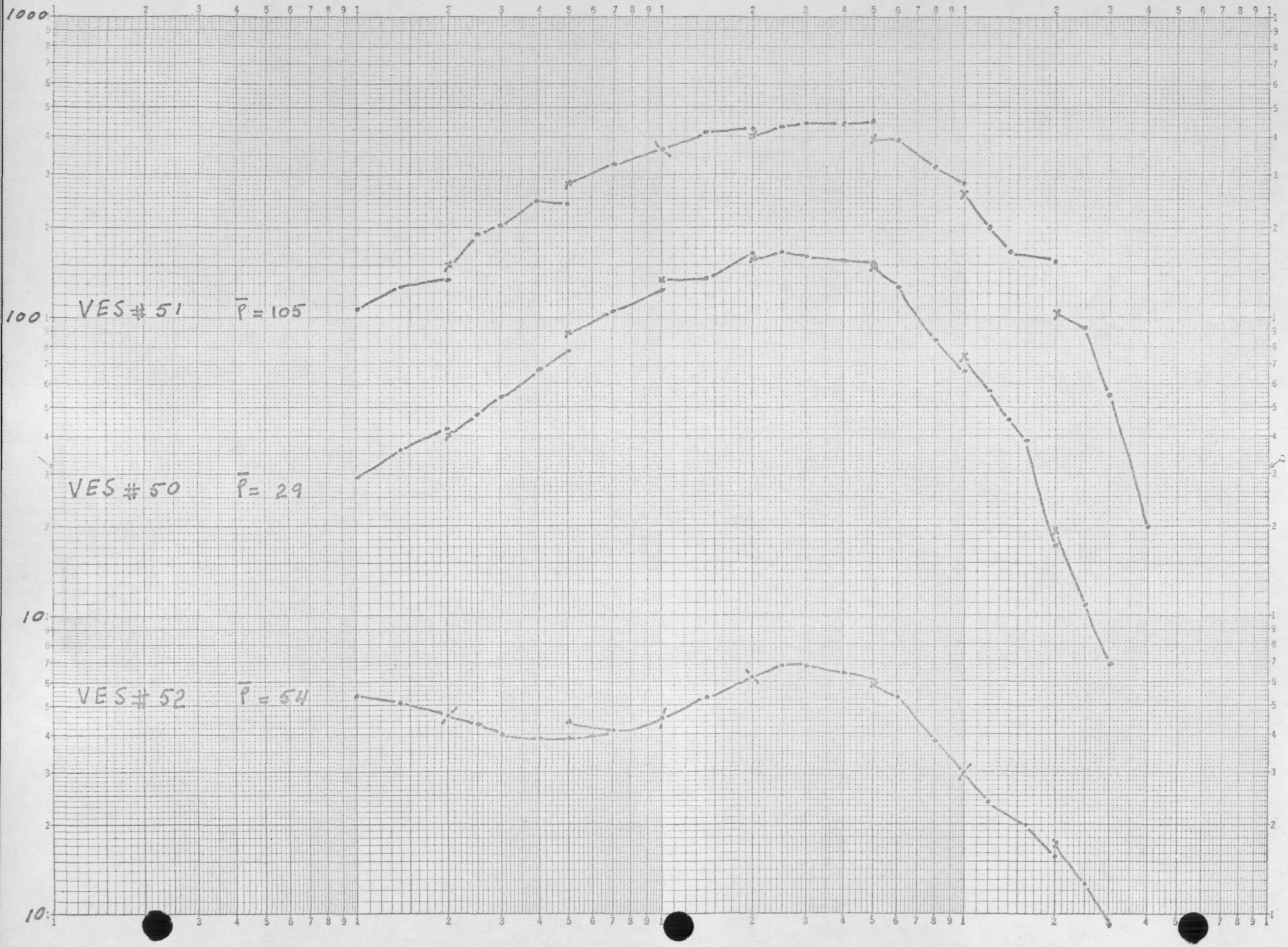
1000
100
10
VES # 51
P̄ = 105
VES # 50
P̄ = 29
VES # 52
P̄ = 54
GPO 859-290

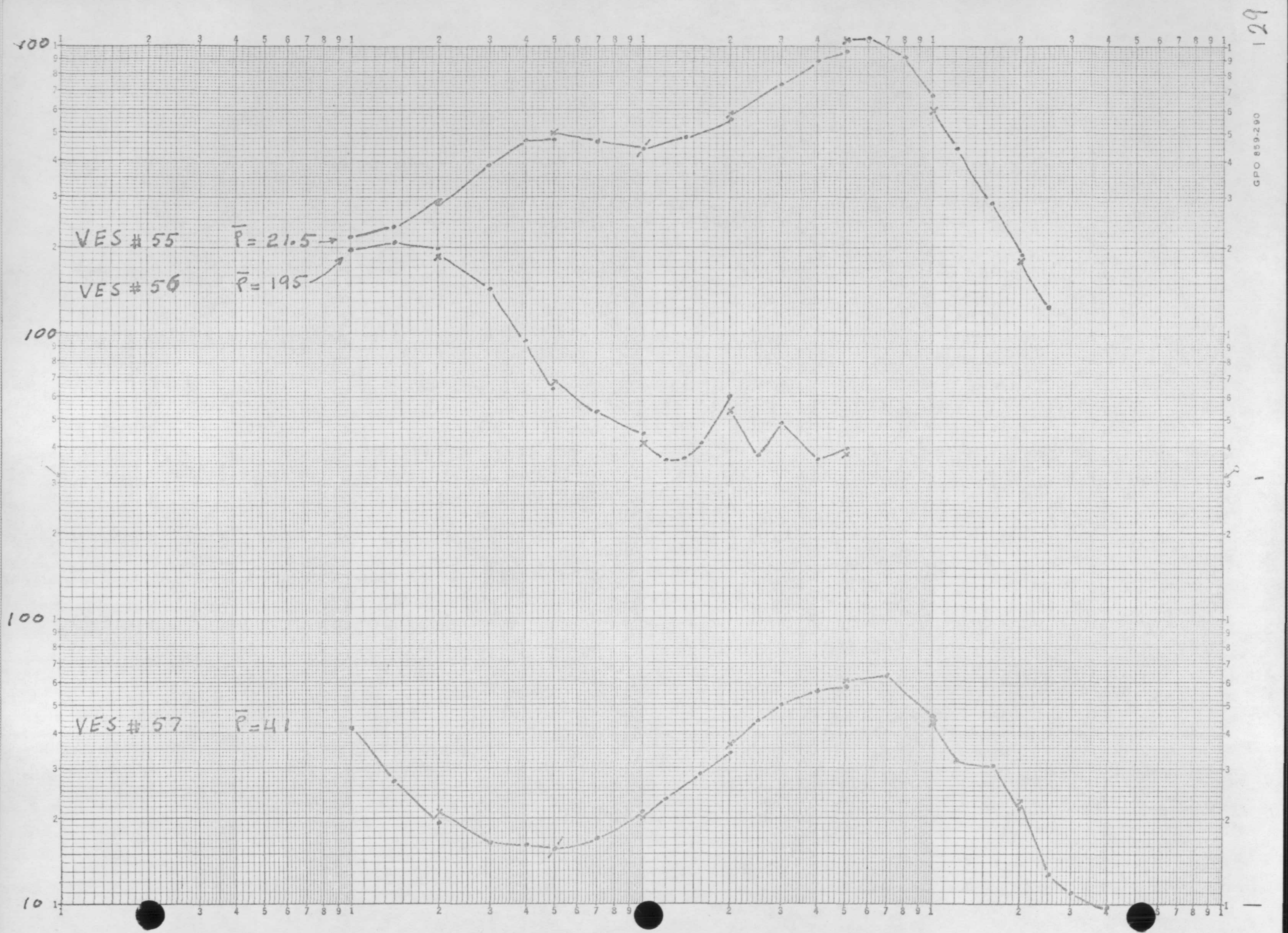

129
VES # 55
$\bar{\rho}$ = 21.5
VES # 56
$\bar{\rho}$ = 195
VES # 57
$\bar{\rho}$ = 41
100
100
100
10
GPO 859-290

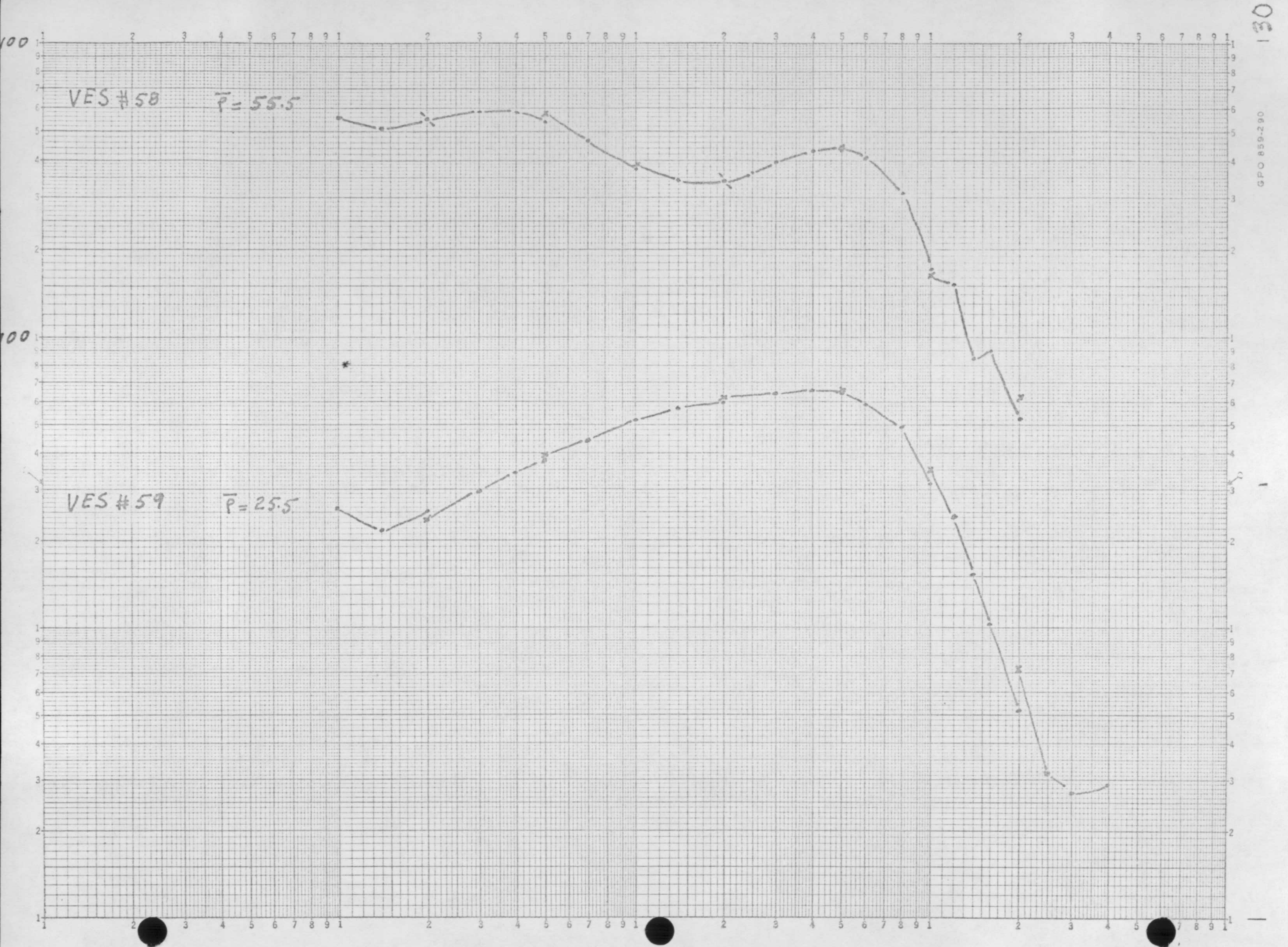

100
VES #58
$\bar{\rho} = 55.5$
100
VES #59
$\bar{\rho} = 25.5$
130
GPO 859-290

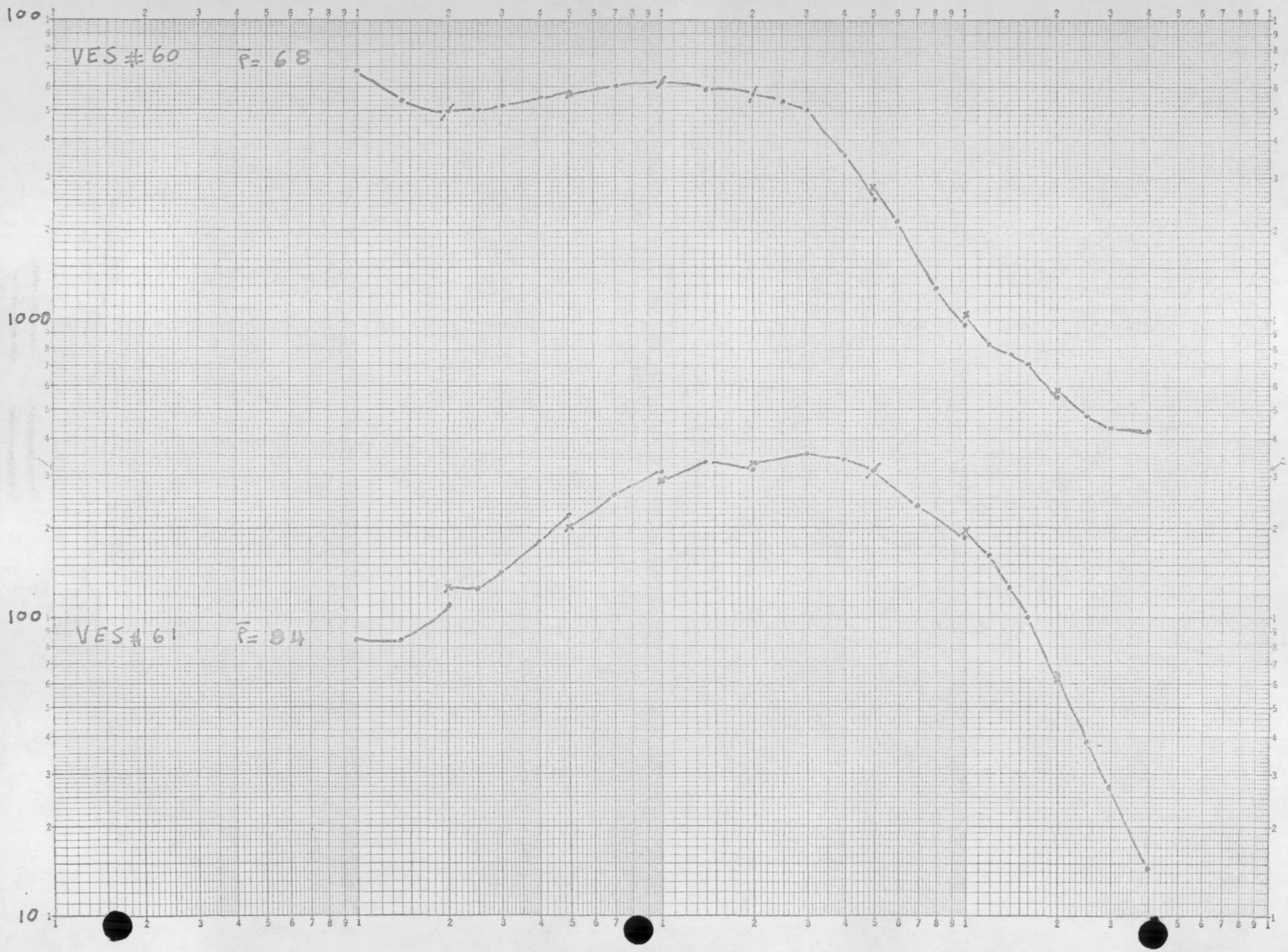

VES #60
ρ̄= 68
VES #61
ρ̄= 84
100
1000
100
10

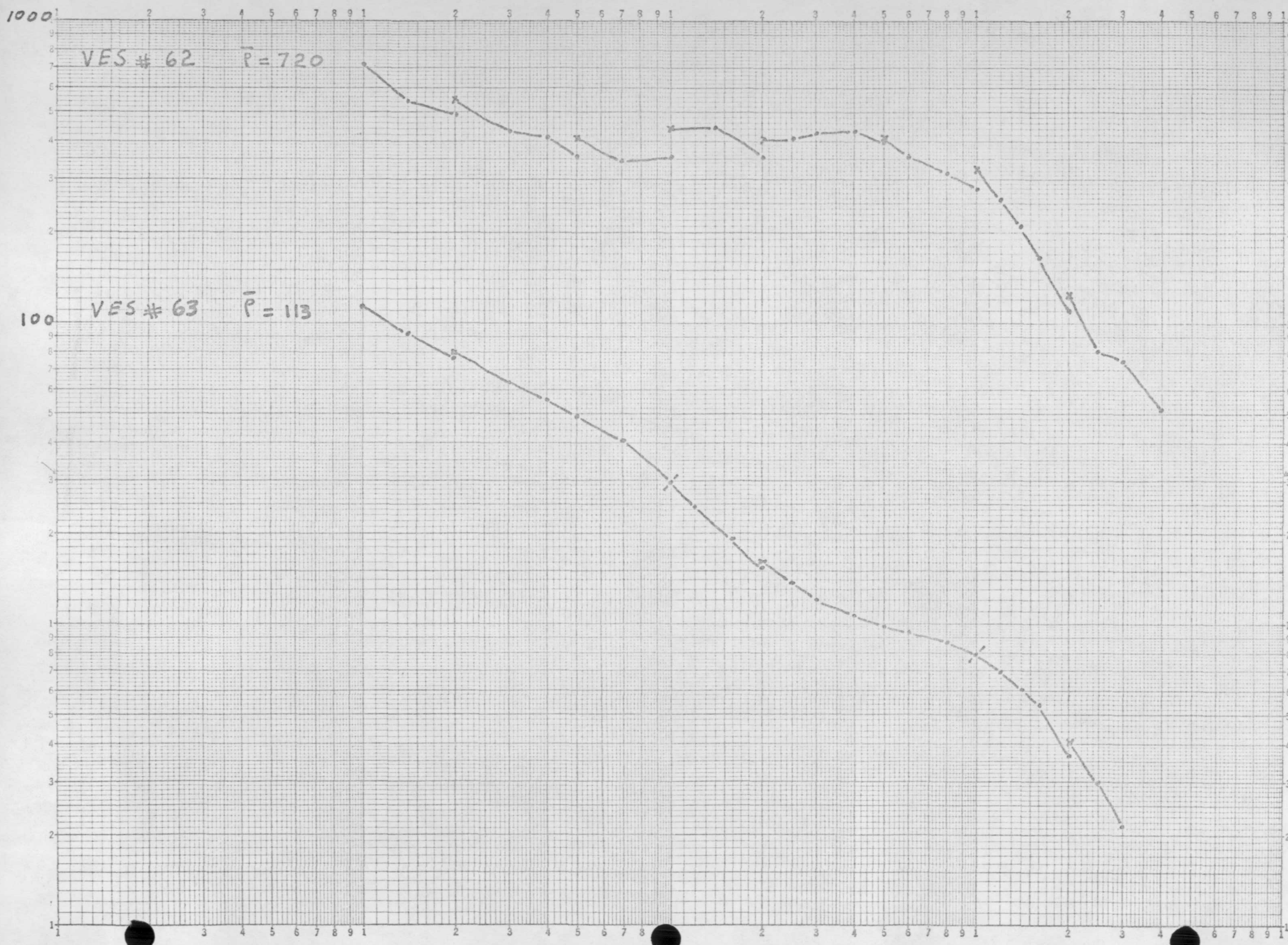

1000
VES # 62 P̄ = 720
100
VES # 63 P̄ = 113
GPO 859-290

133

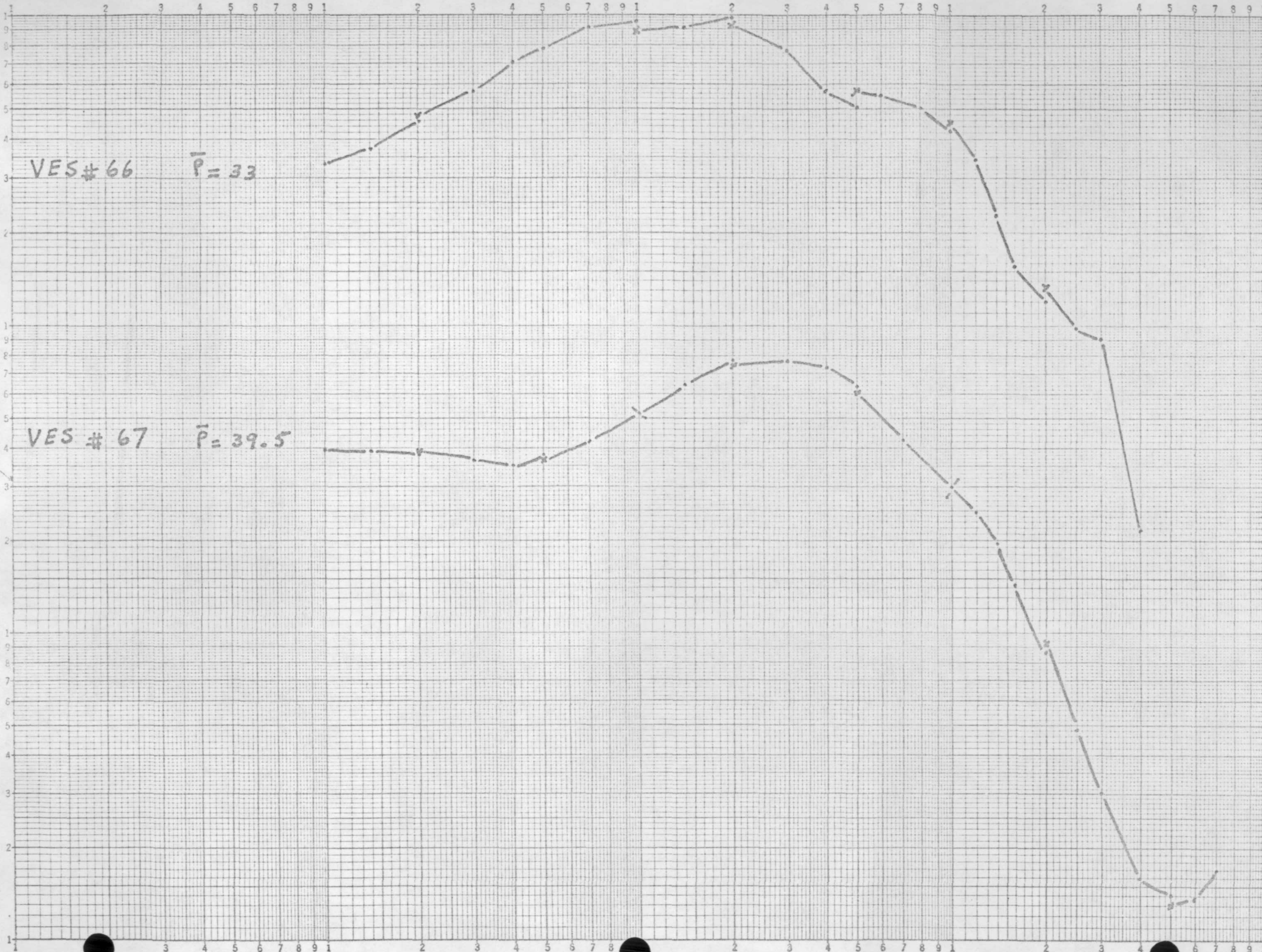

GPO 859-290


VES # 68 $\bar{\rho}$ = 70
VES # 69 $\bar{\rho}$ = 118
VES # 70 $\bar{\rho}$ = 350

135

136


VES #73
ρ̄ = 172
VES #74
ρ̄ = 32
GPO 859-290

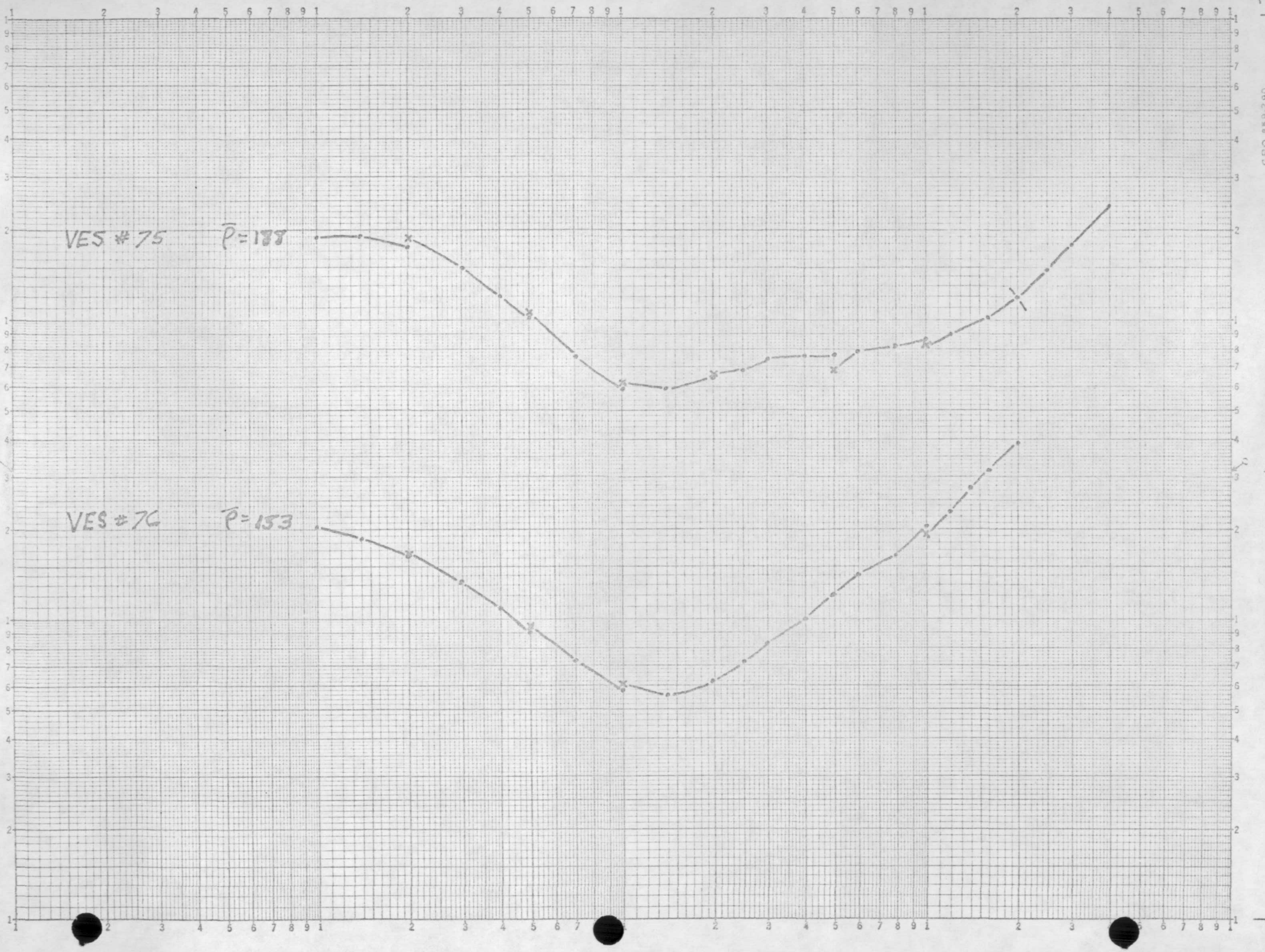
VES #75 ρ̄=188
VES #76 ρ̄=153
GPO 859-290


VES #77 ρ̄ = 137
VES #78 ρ̄ = 39

140

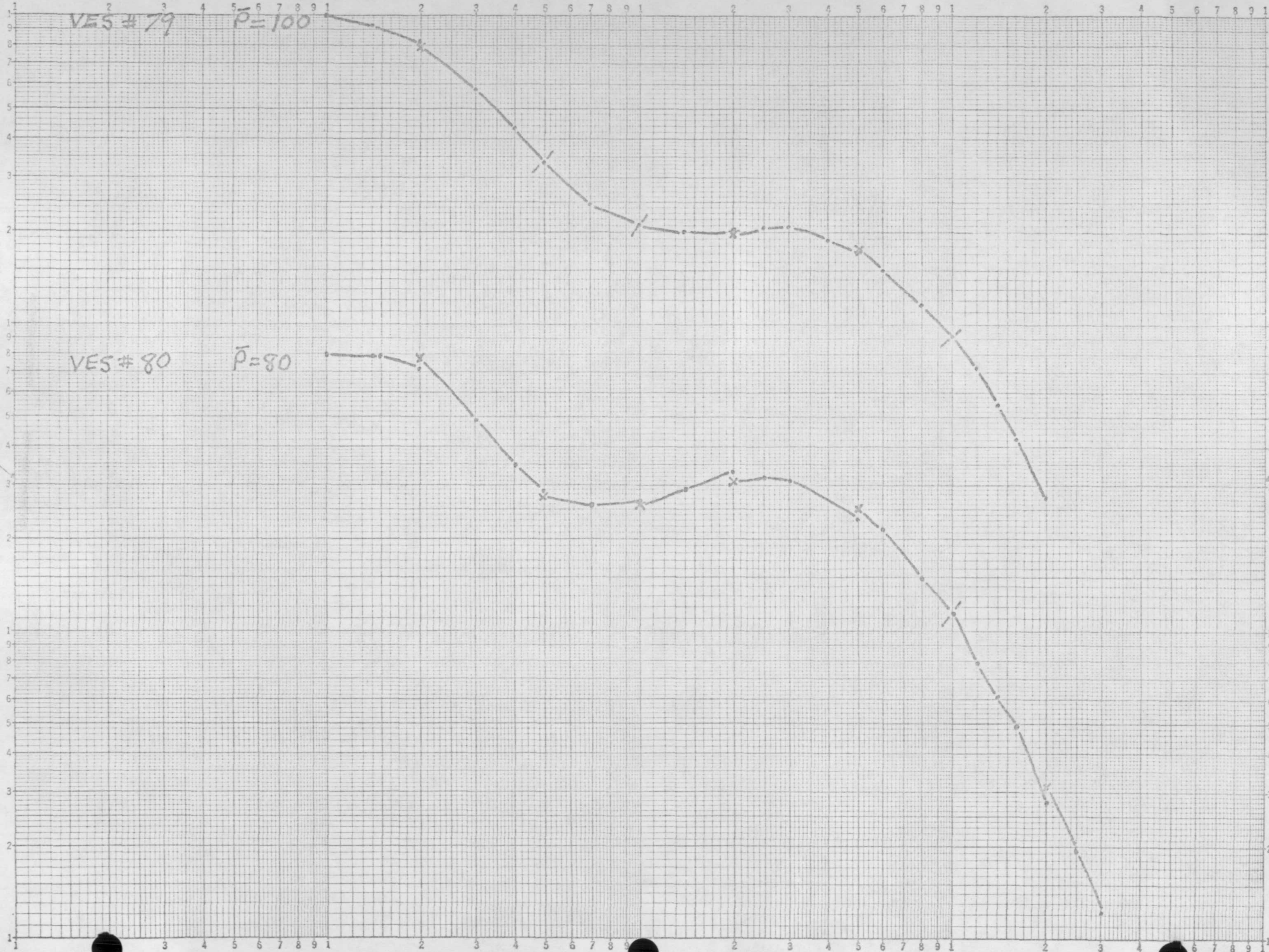

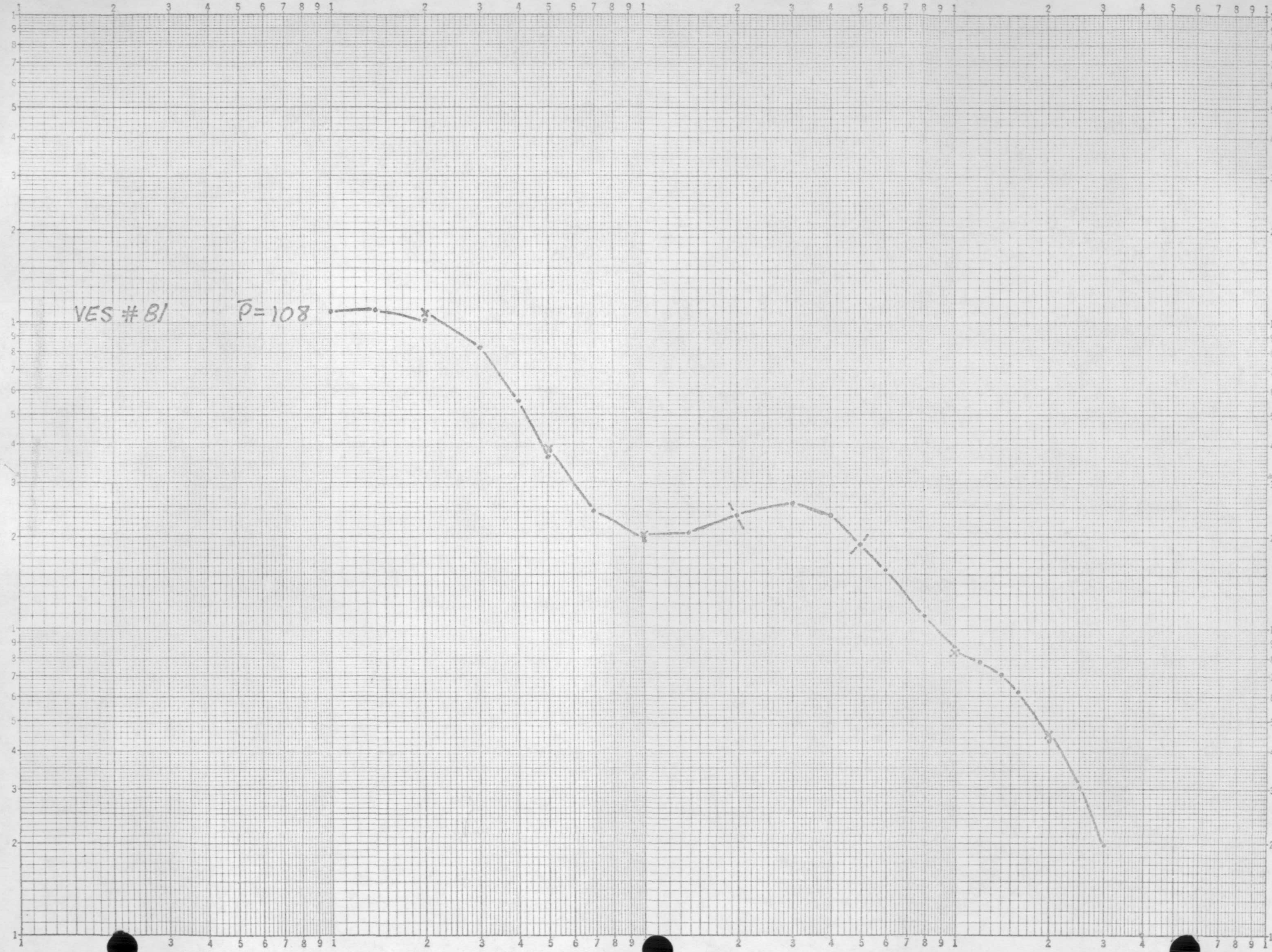
VES #81
$\bar{\rho}=108$

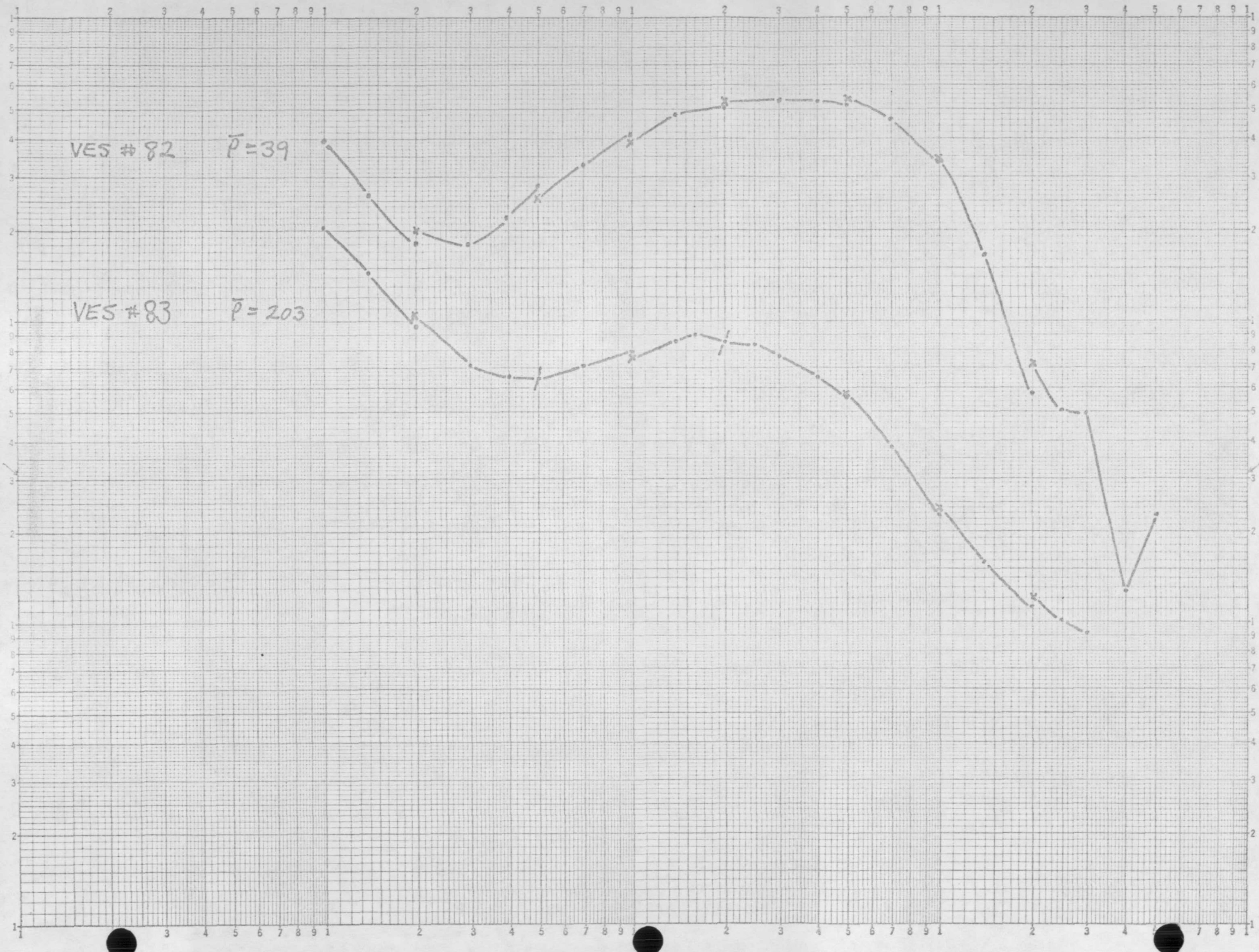
VES #82 ρ̄ = 39
VES #83 ρ̄ = 203
GPO 859-290

143

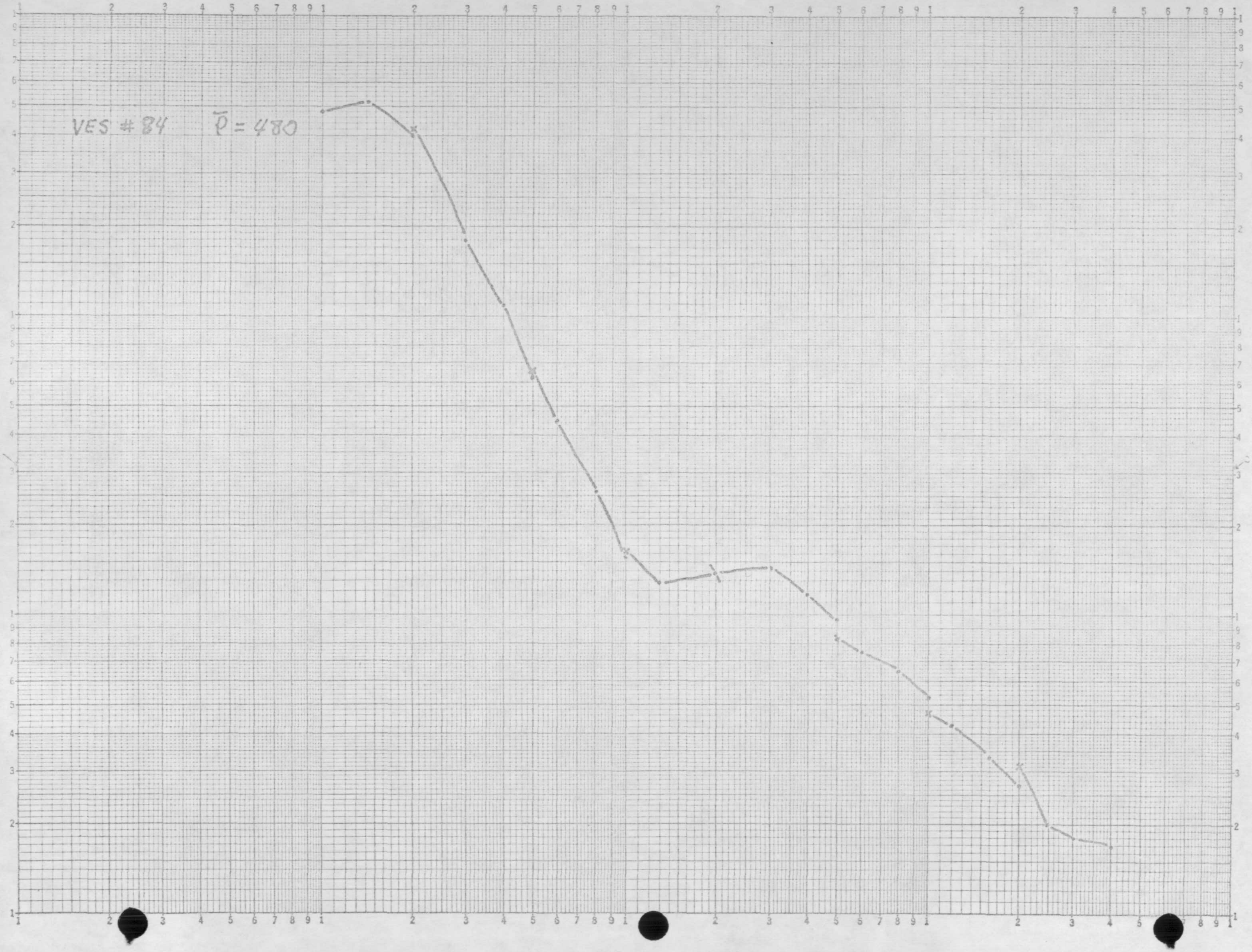

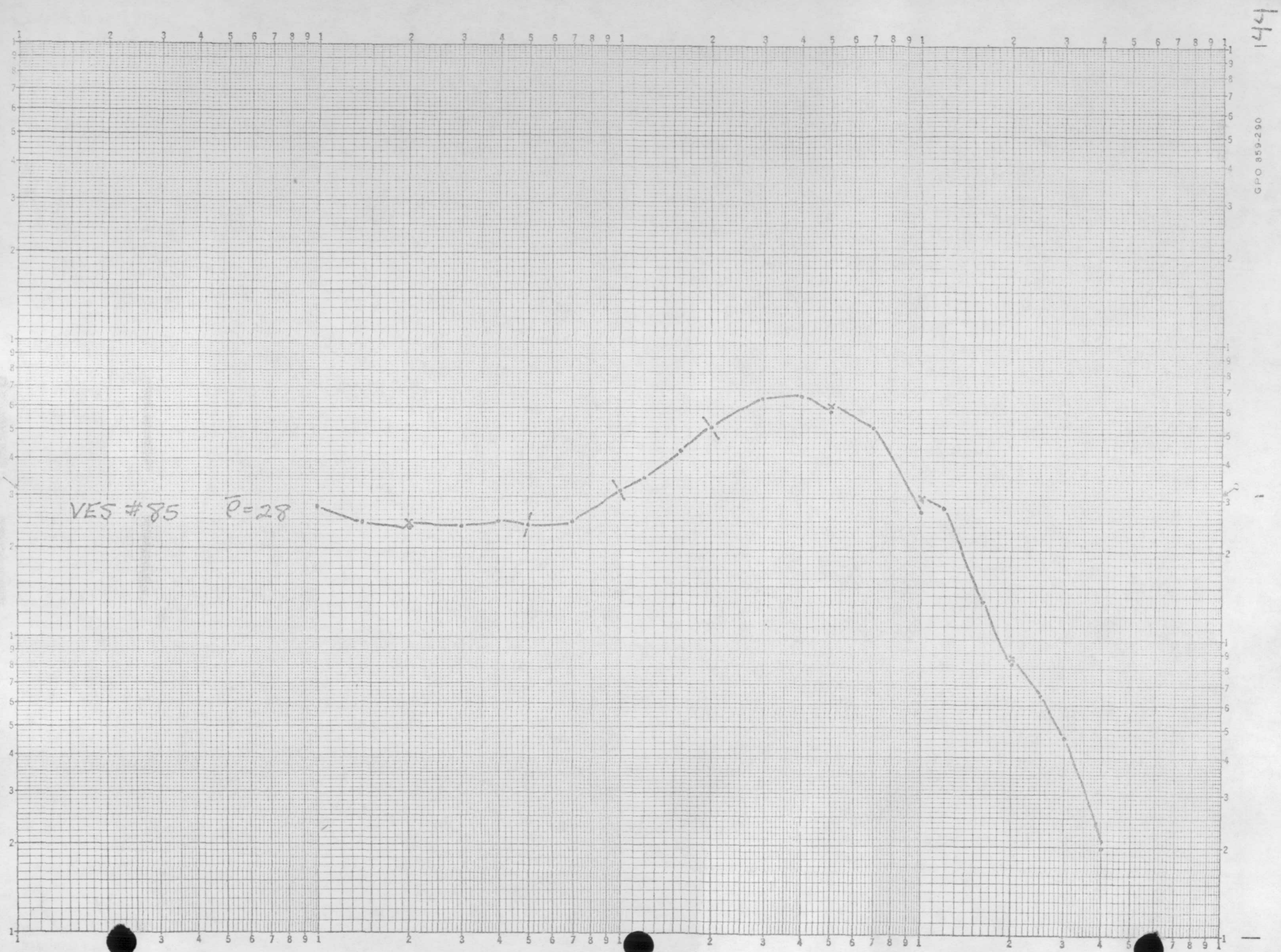

VES #85
ρ̄=28
141
GPO 859-290